THE ROLE OF THE PROTEIN PGR5 IN PHOTOPROTECTION AND PHOTOSYNTHETIC PRODUCTIVITY IN RICE (*Oryza sativa* L.)

Olubukola Omowunmi Ajigboye

B.Agric (Crop Improvement), M.Sc. (Genetics)

Thesis submitted to the University of Nottingham for the degree of Doctor of Philosophy

Division of Plant and Crop Science
School of Biosciences
University of Nottingham
Sutton Bonington Campus
LE12 5RD

JANUARY, 2013

ABSTRACT

The role of the protein PGR5 in photoprotection and photosynthetic productivity in rice (Oryza sativa L.)

In plants, the need to efficiently respond to constant environmental fluctuations has led to the evolution of photoprotective mechanisms to regulate photosynthetic light reactions. One of such mechanism is cyclic electron transport (CET) which generates a pH gradient inducing the nonphotochemical quenching (NPQ) of excess excitation energy, synthesis of ATP and maintenance of balanced redox state of the photosynthetic electron transport (PET) chain. Two major pathways of CET involve the NADH dehydrogenase-like complex (NDH)-dependent pathway, and the Proton Gradient Regulation 5 (PGR5)-dependent pathway. However, the mechanism and function of the PGR5-dependent CET to adapt the photosynthetic process in response to environmental variations and its impact in rice photosynthesis remains unclear. This study aims to determine the role of the photoprotective protein, PGR5 in the regulation of photoprotection and photosynthesis under constant as well as dynamic conditions and its impact on plant growth and development.

Oryza sativa var. Kaybonnet, PGR5 RNA interference (RNAi) and over-expression (OE) transgenic rice plants were characterised based on their physiological and morphological traits in a controlled environment and in glasshouse under constant and fluctuating light intensities.

This study showed that PGR5-dependent CET was actively occurring in rice leaves grown under non saturating light but its rate increased significantly with overexpression of the PGR5 protein in saturating light. Under constant and fluctuating light, elevated NPQ observed in the OE was absent in the RNAi lines indicating that PGR5 is essential for cyclic electron flow in rice both during induction and at steady state photosynthesis. CO_2 assimilation in both OE and RNAi were limited by maximum rate of carboxylation (Vcmax) although the RNAi was also photoinhibited.

Experiments under dynamic condition of low atmospheric moisture indicated that the PGR5-dependent CET plays an important role in photoprotection of PSI and PSII. Results from this experiment further suggest that PGR5 could function efficiently in stress alleviation both in the short- and long term.

Growth and biomass accumulation in the glasshouse and controlled environment showed that the PGR5 protein is important in rice leaf photosynthesis. However, in a biomass experiment, significant photosynthetic advantage attributed to overexpression of PGR5 could not be identified except in photoprotection and regulation of the PET chain.

This study indicates that the ATP/NADPH ratio may modulate PGR5-dependent CET response in rice however, its regulation is likely to depend on the availability of PSI electron acceptors such as ferredoxin. PGR5 may be important in meeting the demand for ATP in rice.

In conclusion, this study has shown that the protein PGR5 plays a very important role in enhancing photoprotection and is required for efficient photosynthesis in rice. However, there may be need for balance between enhancing photoprotection and crop productivity in future improvement programmes.

ACKNOWLEDGEMENTS

I am extremely grateful to my supervisor, Dr Erik Murchie for giving me the opportunity to carry out this work and for your guidance, invaluable suggestions and support throughout the course of this study.

I would like to thank my assessor, Dr R. Ray, for your invaluable advice and support which has allowed me to grow more as a research scientist.

I am also thankful to all the Murchie group lab members, Stanley, Ian, Liang and Mubarak for all their assistance with various experiments. Special thanks to Dr Stella Edwards, for your patience and guidance in teaching me the various protocols used in this work. I gained a lot in science from you.

To Fiona, your administrative prowess of always getting things done, the readiness to help with research supplies is appreciated.

I will also like to thank Professors Sanwo and Ogunmoyela and my friends, Olurin, M Adenekan, M Arisa, Presidor for your support and encouragement. I am very grateful.

Words cannot describe how grateful I am to my family, my mother and father, brothers, sisters and Uncle Wale for all of the sacrifices that you've made on my behalf. Your prayers, encouragement, and patience have strengthened and sustained me throughout the years. I would not have made it without the patience, understanding and encouragement of my loving husband Solomon and daughter odunayo through the years of my absence, I am deeply grateful. *Modupe o. Ayo wa abawa kale. Aye, esu, ese ati ota koni raaye laarin wa ni oruko Jesu Kristi, amin.*

OGO NI FUN OLUWA LOKE ORUN

TABLE OF CONTENTS

LIST OF FIGURES

LIST OF TABLES

ABBREVIATIONS

A	Net carbon dioxide assimilation
ADP	Adenosine diphosphate
ATP	Adenosine triphosphate
CET	cyclic electron transport
Chl	Chlorophyll
Ci	Substomatal carbon dioxide concentration
CO_2	Carbon dioxide
Cyt	Cytochrome
DWT	Dry weight
ETR	Electron transport rate
Fd	Ferredoxin
FNR	Ferredoxin-NADP+ oxidoreductase enzyme
FWT	Fresh weight
gs	Stomatal conductance
h	Hour
H_20	Water
HCl	Hydrochloric acid
IRGA	Infrared gas analyzer
Jmax	Rate of electron transport
LAI	Leaf area index
LAR	Leaf area ratio
LET	Linear electron transport
LHCI	Light-Harvesting Complex I
LHCII	Light-Harvesting Complex II
LI_f	Fractional interception
Max	Maximum
MV	Methyl Viologen
NADP	Nicotinamide adenine dinucleotide phosphate
NADPH	Nicotinamide adenine dinucleotide phosphate (reduced)
NDH	NADH dehydrogenase-like complex
NPQ	Nonphtochemical quenching
OE	Overexpressor
OEC	Oxygen evolving complex
PAR	Photosynthetically active radiation
PGR5	Proton gradient regulation 5
PSI	Photosystem I
PSII	Photosystem II
qE	Thermal dissipation

qP	Photochemical quenching of chlorophyll fluorescence
RNAi	Ribonucleic acid interference
Rubisco	Ribulose-1,5-biphosphate carboxylase/oxygenase
RuBP	Ribulose-1,5-biphosphate
SDS	sodium dodecyl sulfate
SDS-PAGE	sodium dodecyl sulfate polyacrylamide gel electrophoresis
SLA	Specific leaf area
TPU	Triose phosphate utilisation
Vcmax	Maximum rate of carboxylation
WT	Wildtype
ϕ(I)	Quantum yield of PSI
ϕ(II)	Quantum yield of PSII

CHAPTER ONE

GENERAL INTRODUCTION

CHAPTER 1: GENERAL INTRODUCTION

1.1 Introduction

Rice (Oryza sativa L.) is a major source of nutrition in the world especially in Asia and Africa (Hibberd et al, 2008). However, rice yields in the last two decades have stagnated (Mitchell and Sheehy, 2006). While demand for rice in the next 50 years is expected to remain strong as world population rises, climate change may adversely impact rice production through extreme fluctuations in weather such as increased heat and drought leading to loss of arable land, decline in yield and subsequently resulting in price increases (Cassman & Liska, 2007; Long et al, 2006). Thus, a major criterion proposed to meet global food demand and achieve food security is to enhance leaf photosynthetic efficiency and hence total biomass per unit of intercepted radiation (Battisti & Naylor, 2009; Hubbart et al, 2007).

Although predominantly grown in the tropics where rice is exposed to a wide daily variation in light intensity with photosynthetically active photon flux density (PPFD) reaching up to 2000 $\mu molsm^{-2}s^{-1}$ at noon on sunny days, the rate of rice photosynthesis is inefficient, acclimating and saturating at light intensities at and below 1000 $\mu molm^{-2}s^{-1}$ (Murchie *et al.* 1999). This may result in the induction of a series of regulatory processes in the photosynthetic apparatus to harmlessly dissipate the excess energy and/or photodamage, which in turn down-regulate photosynthesis, adversely affecting plant productivity. These processes are collectively referred to as being photoprotective.

Enhancing the rate of recovery of photosynthesis from photoprotection has been suggested as a possible approach to improve photosynthetic efficiency in plants (Long et al. 2006). Recent advances towards understanding mechanisms of photoprotection in plants clearly show the possibility of modifying plants genetically to enhance their capacity for photoprotection (Shikanai, 2007). In particular, gene function can be further studied using a suite of tools and approaches such as gene silencing and overexpression techniques (Miki & Shimamoto, 2004; Hubbart et al, 2012). With a greater understanding of the photoprotective mechanisms and their impact on photosynthesis, growth/development and ultimately grain yield, it may be possible to manipulate photoprotection to generate plants with enhanced leaf photosynthetic efficiency and capacity to fit specific environmental conditions.

This thesis will present results of an investigation aimed at determining the impact of the Proton Gradient Regulation 5 Protein (PGR5) on photoprotection and photosynthetic productivity in rice.

1.2 Photosynthesis

Photosynthesis is the process by which light energy is 'converted' into chemical energy. Plant photosynthesis is driven primarily by visible light (wavelengths from 400 to 700 nm). This process is accomplished through a series of redox reactions beginning with absorption of visible light (wavelengths from 400-700nm) by chlorophyll located mainly in the light harvesting protein complexes (LHCs) of photosystem I (PS I) and photosystem II (PS II) in the thylakoid membrane of chloroplasts. Using

energy from light, plants are able to synthesize carbohydrate (chemical energy) required for growth and metabolism.

1.2.1 Redox reactions: an overview

When chlorophyll in PSI and PSII absorb light energy (in the form of photons), an electron becomes excited causing chlorophyll to enter singlet excited state. Excitation energy is transferred from one chlorophyll molecule to another within the light harvesting complexes by resonance transfer until reaching the reaction centre where charge separation takes place. Electrons are transferred from one molecule to another creating a chain of redox reactions, called a photosynthetic electron transport chain to finally reduce $NADP^+$ (Nicotinamide adenine dinucleotide phosphate) to NADPH. Other protein complexes, cytochrome b_6/f and ATP synthase, using energy of electrons from PSII and in some cases from PSI, work together to create a proton gradient (ΔpH) across the thylakoid membrane used by ATPase to drive ATP synthesis. These reactions collectively known as 'light' reactions supply NADPH and ATP used in the 'dark' reactions (Calvin-Benson cycle) and other assimilatory pathways.

1.3 The Chloroplast

In plants and other photosynthetic organisms, the chloroplast within which photosynthetic membranes are located is the site of photosynthesis (Figure 1.1). The outer membrane of the chloroplast is freely permeable while the inner membrane allows exchange of specific photosynthetic and inorganic phosphate products with the cytosol. The soluble fraction (stroma) of the chloroplast contains enzymes of the Calvin-Benson cycle e.g. Ribulose bis-

phosphate carboxylase-oxygenase (Rubisco) and inorganic ions and molecules such as Pi, O_2, CO_2. Within the stroma are stacks of membrane-bounded disk-like structures called thylakoids, which fold upon themselves into structures, called the grana (Anderson 1986). The grana are connected by stroma lamellae.

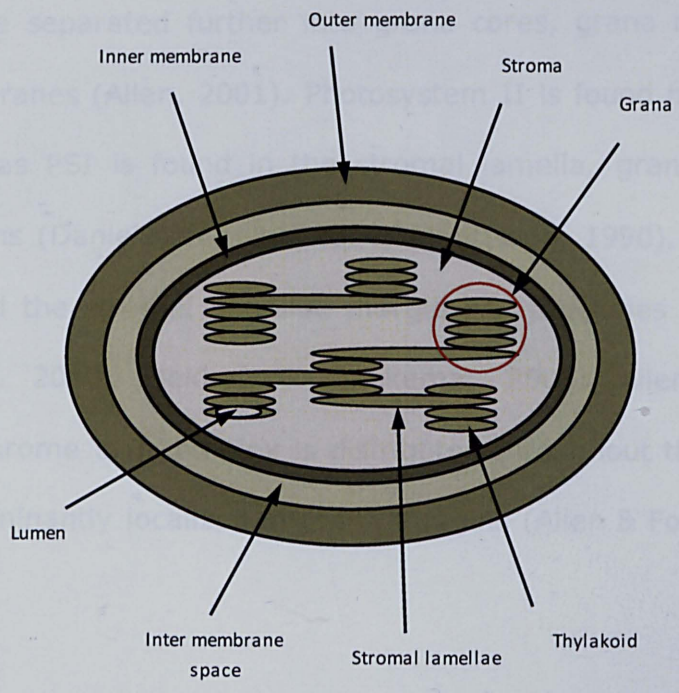

Figure 1. 1 Internal structure of a chloroplast

1.4 The thylakoid membrane

The thylakoid membrane bounds a compartment, the lumen, into which protons are pumped to generate a pH gradient, the ΔpH. The membrane contains protein complexes, electron transport carriers (plastoquinone and plastocyanin), and photosynthetic pigments such as chlorophyll (Chl) and carotenoids. There are four protein complexes in the thylakoid membrane:

PSI & PSII, Cytochrome b_6f complex and ATP synthase enzyme complex (Harbinson & Rosenqvist, 2003), collectively working to convert light energy into chemical energy stored in ATP and NADPH shown in (Figure 1.2). PSI and PSII consist of their respective LHCs and reaction centres (section 1.6). Thylakoid membranes have two regions, the stacked (grana) and unstacked (stromal lamellae) regions (Figure 1.1). The grana stacks can be separated further into grana cores, grana margins and grana end membranes (Allen, 2001). Photosystem II is found mainly in the grana core whereas PSI is found in the stromal lamella, grana end membranes and margins (Danielsson et al. 2004; Albertsson, 1990). ATP synthase is found around the stromal lamellae margin and protrudes into the stroma (Daum et al, 2010; Dekker & Boekema, 2005; Allen & Forsberg, 2001). Cytochrome b_6/f complex is distributed throughout the thylakoid membrane predominantly localized in grana margins (Allen & Forsberg, 2001).

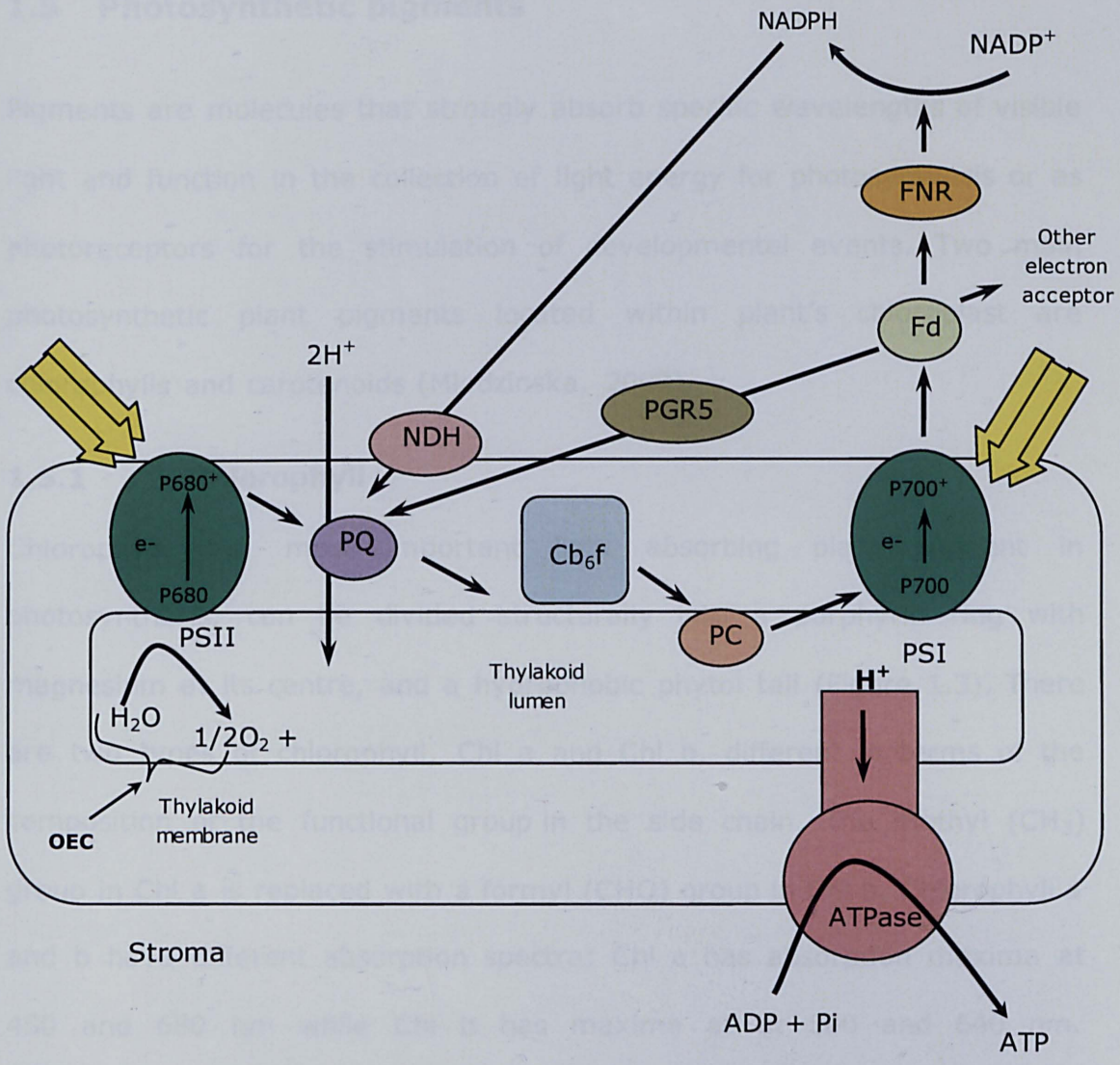

Figure 1. 2 Schematic representation of pathway for photosynthetic linear and cyclic electron flow and proton translocation through the major complexes within
the thylakoid membrane. Absorbed light energy excites photosystem II (PSII) chlorophyll P680 to transfer an electron to cytochrome b6/f (Cb6/f) via plastoquinone (PQ). This transfer via PQ is induced by the Q cycle which pumps protons (H+) into the thylakoid lumen. Electron lost from P680 is replaced through water oxidation in the oxygen evolving complex (OEC) releasing H+ and O2. Photosystem I (PSI) P700 chlorophyll absorbs light energy causing it transfer an electron to ferredoxin (Fd) while accepting electron from Cb6/f via plastocyanin (PC). Fd subsequently reduce other electron acceptors including ferredoxin NADP reductase (FNR) which reduces Nicotinamide adenine dinucleotide phosphate (NADP+) to NADPH. Electrons can also cycle in a loop around PSI, with electrons transferred from Fd or NADPH to PQ pool. NADPH dehydrogenase mediates electron transfer NADPH to PQ pool. Proton Gradient Regulation 5 (PGR5) protein mediates electron transfer from Fd to PQ. Protons translocated into the thylakoid lumen creates a pH gradient to drive ATP synthesis by ATP synthase.

1.5 Photosynthetic pigments

Pigments are molecules that strongly absorb specific wavelengths of visible light and function in the collection of light energy for photosynthesis or as photoreceptors for the stimulation of developmental events. Two main photosynthetic plant pigments located within plant's chloroplast are chlorophylls and carotenoids (Mlodzinska, 2009).

1.5.1 Chlorophyll

Chlorophyll, the most important light absorbing plant pigment in photosynthesis, can be divided structurally into a porphyrin ring with magnesium at its centre, and a hydrophobic phytol tail (Figure 1.3). There are two types of chlorophyll, Chl a and Chl b, different in terms of the composition of the functional group in the side chain. The methyl (CH_3) group in Chl a is replaced with a formyl (CHO) group in Chl b. Chlorophyll a and b have different absorption spectra: Chl a has absorption maxima at 450 and 680 nm while Chl b has maxima at at 500 and 640 nm. Chlorophyll in leaves is bound within proteins complexes of the reaction centres of two photosystems and also within light harvesting complexes which enhance their capability by transfer of energy to reaction centres (Dekker and Boekema, 2005; Lawlor, 2001). Chl a functions as a light harvesting pigment in the antenna complexes of the photosystem and also serves as the primary electron donor in the reaction centres of PSI and PSII and as PSI primary electron acceptor (Lokstein & Grimm, 2007). Chl b is the major light absorbing accessory pigment in plants, mostly found in PSII light harvesting complexes.

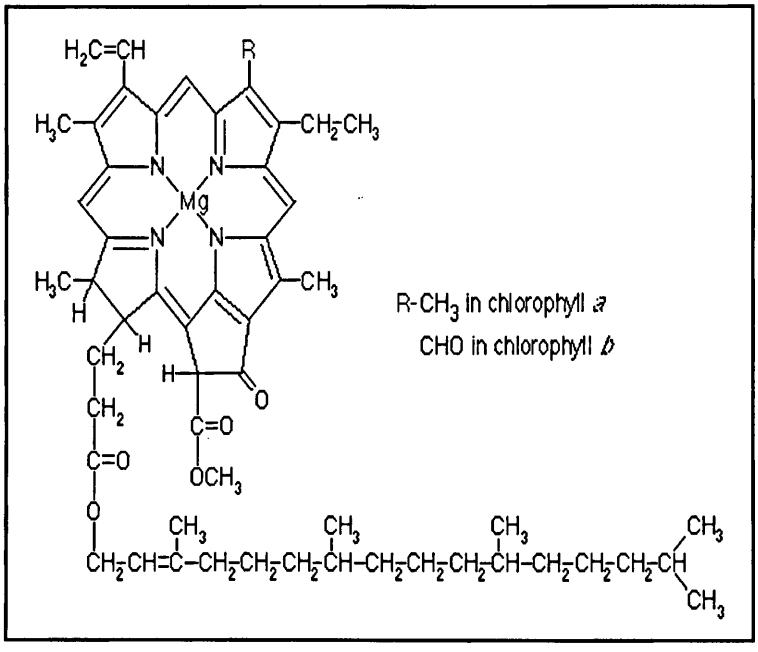

Figure 1. 3 Structure of chlorophyll a and b. R denotes the side group on ring II showing the difference between the two chlorophylls.

1.5.2 Carotenoids

Carotenoids are a large diverse family of hydrophobic molecules found in photosynthetic organism, including plants. They can be divided into two groups, unsaturated hydrocarbons known as carotenes (such as β-carotene) and oxygenated hydrocarbons called xanthophylls which include lutein, zeaxanthin, violaxanthin and neoxanthin. Carotenoids are essential structural components of the photosynthetic antenna and reaction centre of the two photosystems.

In plants, there are several well-documented essential functions of carotenoids. They act as accessory light harvesting pigments, absorbing light at 400-500nm (Lokstein & Grimm, 2007) which they transfer to chlorophyll a for use in photosynthesis. However, perhaps the most important function of carotenoids is photoprotection. First carotenoids can

protect reaction centres of PSII by rapidly quenching triplet excited states of chlorophylls and also singlet oxygen (Blankenship, 2002). Thylakoid membranes are enriched in polyunsaturated fatty acids susceptible to singlet oxygen generation, initiated by lipid peroxidation reactions. Zeaxanthin is an important antioxidant in the thylakoid membrane and is capable of scavenging reactive oxygen species and/or termination of lipid peroxidation chain reactions (Muller et al, 2001). Carotenoids are also involved in regulating energy transfer in photosystem antennae in a process known as non-photochemical quenching (NPQ; section 1.10.3) which involves the xanthophyll cycle (XC) by safely dissipating excess light energy as heat thereby avoiding over-excitation and subsequent photodamage of the photosynthetic systems (Demmig-Adams & Adams 1992; Demmig-Adams 1990). The XC shown in Figure 1.4 involves reversible de-epoxidation of violaxanthin via antheraxanthin to zeaxanthin under excess light and the epoxidation of zeaxanthin to violaxanthin in darkness or under low light (Havaux, 1988). The XC and NPQ limits photodamage in plants under excess light (Demmig-Adams & Adams 1992; Demmig-Adams 1990).

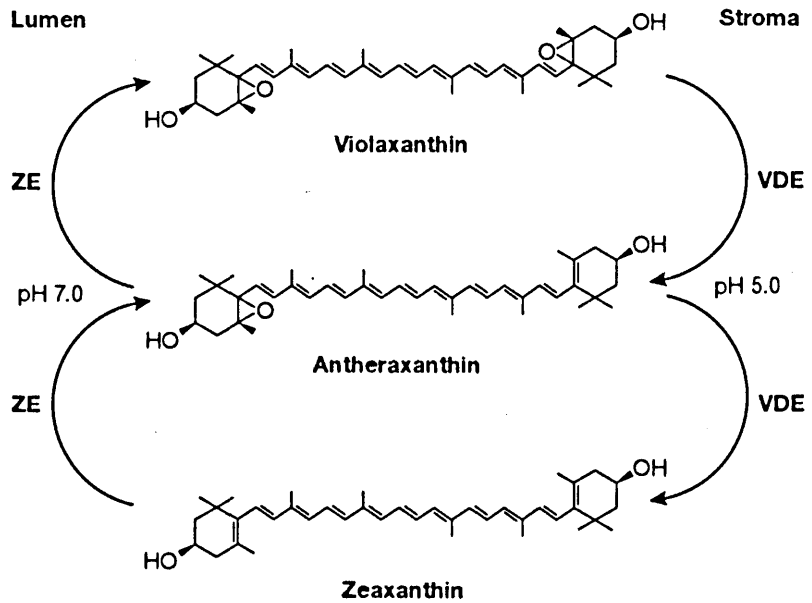

Figure 1. 4 The xanthophyll cycle. Under high-light conditions, violaxanthin de-epoxidase is activated by the ΔpH to convert violaxanthin into zeaxanthin via antheraxanthin. In low light, zeaxanthin is epoxidised. Taken from Szabó et al (2005).

1.6 Thylakoid membrane protein complexes

1.6.1 Photosystems

Light energy required for photosynthesis is absorbed by photosynthetic pigments resulting in the release of electron (charge separation) into the electron transport chain within the thylakoid membrane. A large number of photosynthetic pigments are not involved in charge separation (Croce et al, 1999), instead they are organised into light harvesting pigment-protein complexes (antennas) which collect energy from photons and transfer excitation energy from one pigment molecule to another eventually reaching the reaction centre (RC; Figure 1.5) using an energy 'funnelling' mechanism (Blankenship, 2002). The RC is an integral membrane pigment-protein complexes that traps light energy for use in charge

separation across the membrane. The two photosystems, PSII and PSI consist of a number of light harvesting complexes (LHCs) and a reaction centre containing special chlorophyll, P_{680} in PSII and P_{700} in PSI (Figure 1.5).

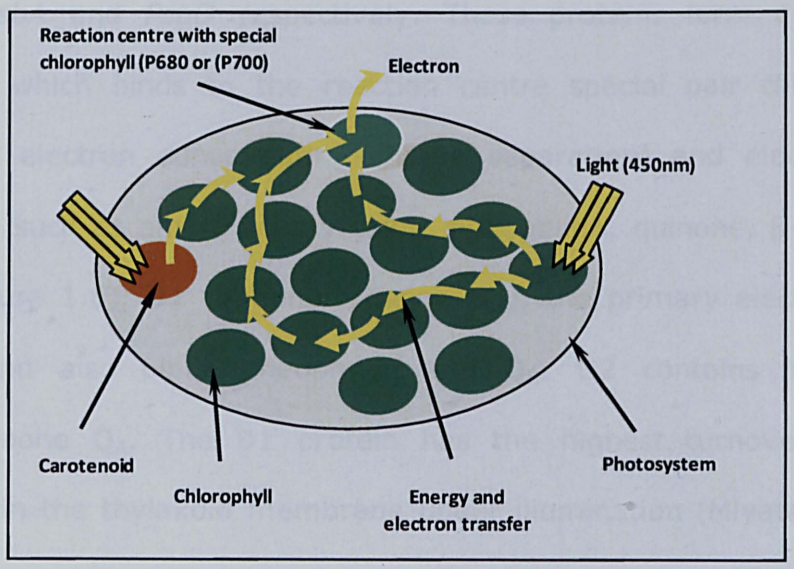

Figure 1. 5 Schematic of excitation energy transfer. Excitation energy moves within the antenna complex to the 'special pair' of chlorophyll molecules (P680 or P700) in the reaction centre, where the energy is captured and used in the transfer of electrons from chlorophyll to other electron acceptors.

1.6.1.1 Photosystem II

Photosystem II is a multi-subunit pigment-protein complex integrated in the grana of the thylakoid membrane that uses light energy to catalyze oxido-reduction of water and plastoquinone. It is most active in its dimeric form (Danielsson et al, 2006) of two similar monomers (Loll et al, 2005). Each monomer consists of several subunits including the peripheral light harvesting antenna, the oxygen evolving complex (the site of water

oxidation) as well as a reaction centre core made up of the reaction centre and inner light harvesting antenna (Figure 1.6).

The reaction centre core complex of PSII is closely bound to several protein subunits such as chlorophyll binding proteins, D1 and D2 encoded by the genes *PsbA* and *PsbD* respectively. These proteins form a heterodimer (D1/D2) which binds to the reaction centre special pair chlorophyll P_{680} (primary electron donor during charge separation) and electron transfer cofactors such as amino acid tyrosine, pheophytin, quinone, β-carotene and iron (Figure 1.6). D1 contains tyrosine (Y_Z), the primary electron donor to $P680^+$ and also binds pheophytin and Q_B. D2 contains Y_D and binds plastoquinone Q_A. The D1 protein has the highest turnover rate of all proteins in the thylakoid membrane under illumination (Miyata et al, 2012; Demmig-Adams and Adams, 1992) with physiological conditions inside the chloroplast influencing its transcription and translation (reviewed in Zhang and Aro, 2002).

A number of low molecular weight (<10kDa) strongly hydrophobic peptides involved in PSII assembly, stabilization, dimerization and photoprotection (Shi & Schroder, 2004) are also bound to the reaction centre core complex.

Closely associated to the PSII reaction centre core is the cytochrome b559, a heme-bridged heterodimer with α- and β-subunits (products of *psbE* and *psbF* genes respectively; Pospisil, 2011). It has been suggested that the oxidase and reductase enzymatic activity of cytochrome b559 in conjunction with β-carotene and chlorophyll, plays a role in the protection

of PSII from photoinhibition under conditions in which the primary path of electron transfer leading to water oxidation is inhibited (Shinopoulos & Brudvig, 2012; Pospisil, 2011) and is essential for PSII assembly in green algae (Burda et al, 2003).

Chlorophyll-protein inner antenna complexes CP43 and CP47, which are encoded by the *psbC* and *psbB* genes respectively, are also in close association with reaction centre (Lokstein & Grimm, 2007). CP43 is linked to D1 subunit while CP47 is linked to the D2 subunit (Blankenship, 2002; Barber et al, 1999). CP43-CP47 antenna pigment protein complex binds chlorophyll a and β-carotene. Apart from harvesting light energy and transfer of excitation energy to the PSII reaction centre, CP47 and CP43 are also thought to be involved in some way in the water splitting process catalysed by PSII (Barber et al, 2000).

Another unique component of the PSII reaction centre core is the oxygen-evolving complex (OEC), the active site of water oxidation. The complex located on the lumenal surface of PSII consist of three extrinsic proteins, of OEE1 (PsbO), OEE2 (PsbP) and OEE3 (PsbQ) which assist in binding catalytic tetranuclear manganese (Mn_4) cluster to calcium (Ca^{2+}) and chloride (Ci^-) ions, essential cofactors in water oxidation (Roose et al, 2007; Rivas et al, 2004). In addition, OEE1 is considered critical in preventing Mn destabilization and system perturbation while OEE2 is suggested as a concentrator of Ca^{2+} (reviewed in Hankamer et al, 1997) to maintain a suitable ionic environment at the Mn-cluster. However, OEC subunits are susceptible to oxidative damage and turnover under illumination (Henmi et al, 2004). Water oxidation takes place when Mn^{2+} of OEC goes through five

series of light induced oxidation states (S0 to S4) to become progressively more oxidised (Blankenship, 2002; Kok et al, 1970). Ultimately four electrons are removed (for $P680^+$ re-reduction) from the Mn cluster accompanied with two water molecules splitting to release one oxygen molecule and four protons into the thylakoid lumen for use in ATP synthesis (Figure 1.6).

1.6.1.2 Photosystem II light harvesting complexes (LHCs)

Excitation energy supply to the PSII reaction centre core is enhanced by peripheral antenna systems which are made up mainly of chlorophyll *a/b* binding light-harvesting proteins coded for by nuclear Lhc genes and xanthophylls. Two groups of PSII antenna systems known in plants include the monomeric minor PSII LHCs made up of Lhcb4-6 proteins (CP29, CP26, and CP24 respectively) and the major antenna, LHCII organised in trimers of three proteins (Lhcb1, Lhcb2 and Lhcb3) (Lockstein & Grimm, 2007). The minor complexes are thought to channel excitation energy from LHCII to the reaction centre core (Veeramn et al, 2007) and are putative sites for dissipation of excess excitation energy as heat measured as non photochemical quenching, NPQ (Ahn et al, 2008).

LHCII is the most important/abundant light harvesting antenna system in plants. It plays a major role in the regulation of excitation energy flow in photosynthesis in processes that may prevent damage, scavenge products of damage or repair of damage of photosynthetic apparatus (Asada, 1999). Two of such regulatory processes identified in antennas of plants include state transitions which enhance the flux of excitation energy between PSI

and PSII by lessening imbalance in relative rates of the photosystem's excitation (Damkjær et al, 2009; Allen & Forsberg, 2001; Haldrup et al, 2001) and NPQ, where excess absorbed energy is dissipated as heat within the PSII antenna, preventing damage to the reaction centres (photooxidation) but may lead to photoinhibition, a sustained decline in photosynthetic efficiency and productivity in plants (reviewed in Long et al 1994 and Horton et al, 1996).

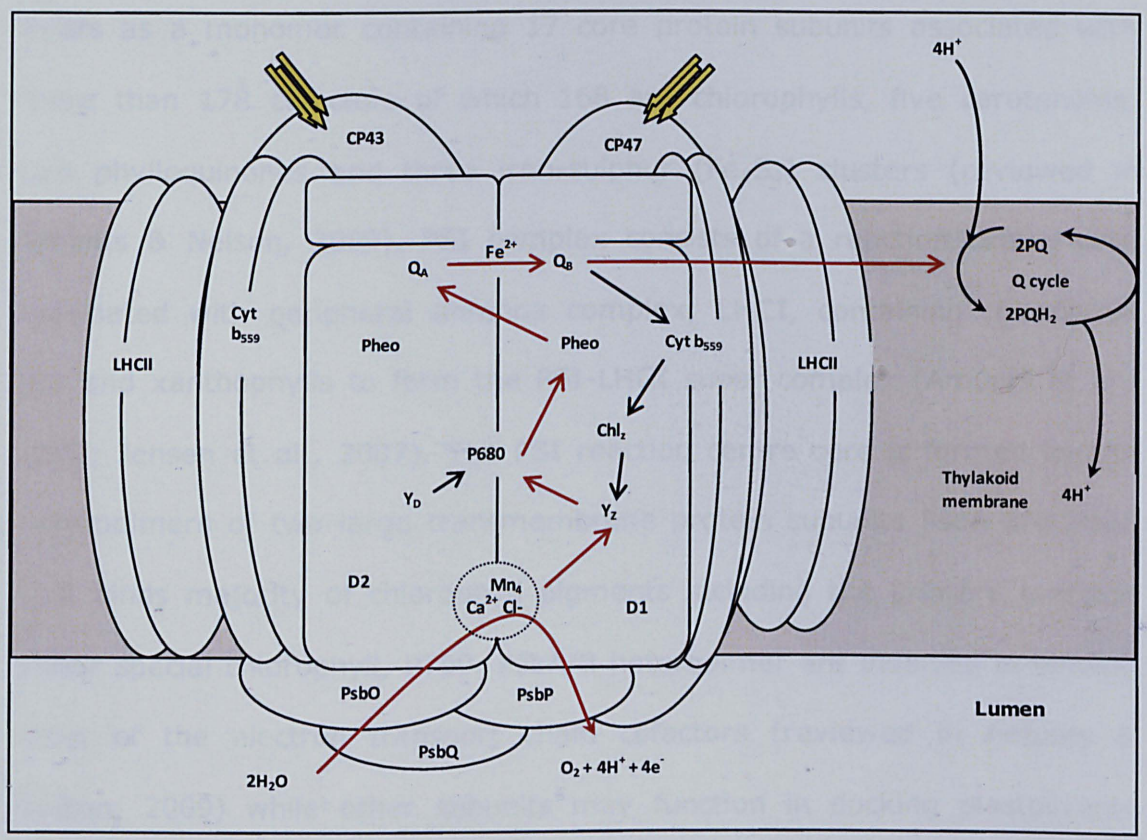

Figure 1. 6 Schematic structure of photosystem II complex embedded in the thylakoid membrane. The red and black arrows indicate primary and secondary pathways of electron transfer, respectively.

1.6.1.3 Photosystem I

The second photosystem involved in light reaction of photosynthesis is the photosystem I (PSI), a multi subunit pigment-protein complex embedded mainly in the stromal regions of the thylakoid membrane. It operates a highly reducing system in contrast to the oxidising system of PSII (Ishikita et al, 2006; Nelson & Yocum, 2006), and uses light energy to catalyse the reduction of ferredoxin (reviewed in Nelson & Ben-Shem, 2004). PSI complex, structurally mapped at 3.4 Å resolutions (Amunts et al, 2007) exists as a monomer containing 17 core protein subunits associated with more than 178 cofactors of which 168 are chlorophylls, five carotenoids, two phylloquinones and three iron-sulphur (Fe_4S_4) clusters (reviewed in Amunts & Nelson, 2009). PSI complex consists of a reaction centre core associated with peripheral antenna complex, LHCI, containing chlorophyll *a/b* and xanthophylls to form the PSI-LHCI super complex (Amunts et al., 2007; Jensen et al., 2007). The PSI reaction centre core is formed by the heterodimers of two large transmembrane protein subunits PsaA and PsaB that binds majority of chlorophyll pigments including the primary electron donor special chlorophyll, P700. PsaA/B heterodimer are involved in binding most of the electron transport chain cofactors (reviewed in Amunts & Nelson, 2009) while other subunits may function in docking plastocyanin and ferredoxin as well as LHCI, LHCII during state transitions and also in PSI stabilization (Jensen et al, 2007; Blankenship, 2002). PSI is highly efficient and almost every photon absorbed results in excitation of the special chlorophyll P700.

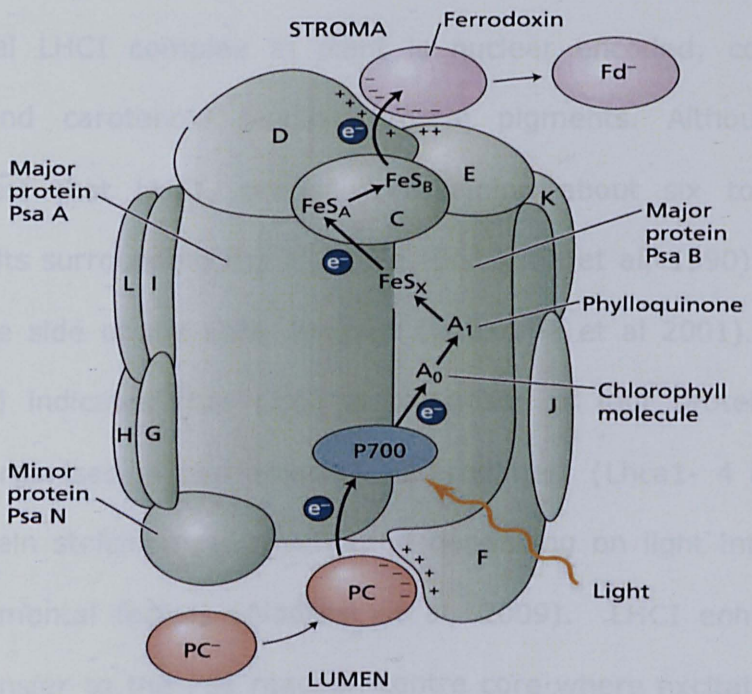

Figure 1. 7 Schematic structure of photosystem I showing electron transfer process. Taken from Taiz and Zeiger (2006).

Excitation energy from antenna pigments is transferred to P700 reaction centre. The electron moves from P700 to reduce chlorophyll molecules A_0 and A_1 (phylloquinone) and then through a set of three iron-sulphur centres (F_X, F_A and F_B) to ferredoxin on the stromal side of the thylakoid membrane. Ferredoxin releases an electron used by ferredoxin – NADP reductase (FNR) to reduce $NADP^+$ to NADPH. Simultaneously, oxidised P700 becomes reduced on receiving an electron from plastocyanin, on the luminal side of PSI.

1.6.1.4 Photosystem I light harvesting complexes (LHCI)

The peripheral LHCI complex in plant is nuclear encoded, consisting of chlorophyll and carotenoid binding protein pigments. Although earlier studies suggest that LHCI, probably containing about six to ten Lhca protein subunits surrounding the PSI core (Boekema et al, 1990) or may be located on the side of the core complex (Boekema et al 2001). Amunts & Nelson (2009) indicated that LHCI is comprised of four protein subunits (Lhca 1- 4) organised in two adjacent heterodimers (Lhca1- 4 and Lhca2-3), their protein stoichiometry fluctuating depending on light intensity and other environmental factors (Alboresi et al, 2009). LHCI enhances light absorption/transfer to the PSI reaction centre core where excitation energy is funnelled toward P700. PSI has been suggested to function in binding LHCII following state transition (Lunde, et al, 2000)

1.6.2 Cytochrome b6/f

The cytochrome b_6f complex (cyt *b6f*) in the thylakoid membrane plays a central role in photosynthetic electron flow transferring electrons one at a time from PSII to PSI. Acting as an oxidoreductase, it catalyzes oxidation of a two-electron donor plastoquinol and reduction of one-electron acceptor protein, plastocyanin in plants which in turn reduces oxidized $P700^+$ in PSI. This transfer is coupled with proton translocation across the thylakoid membrane to generate the proton gradient used by ATP-synthase to synthesise ATP (reviewed in Allen, 2004; Kurisu et al, 2003). The complex functions as a dimer and is composed of four large subunits: cytochrome *f* (*petA*), cytochrome b_6 (*petB*), the Rieske iron-sulphur protein (*petC*), and subunit IV (*petD*) as well as four minor hydrophobic subunits, PetG, PetL,

PetM, and PetN (Breyton et al, 1997). The complex redox-active cofactors: four heme molecules, one chlorophyll a and one β-carotene bind to the first three major units while subunit-IV is the binding site of plastoquinone (Cramer et al, 2006; Kurisu et al, 2003). Cyt *b6f* is an essential player in cyclic electron transport where ferredoxin (Joliot & Joliot, 2002), ferredoxin $NADP^+$ (Zhang et al, 2001) as well as proton gradient regulation 5 protein (Shikannai, 2007) act as intermediates between PSI and Cyt *b6f* complex.

1.6.3 ATP-Synthase

ATP synthase, a large multisubunit enzyme belongs to the family of F-type ATP synthase, and is similar in structure and function to bacteria and mitochondria complexes (Groth and Pohl, 2001). It catalyses ATP synthesis and hydrolysis using proton motive force derived from ΔpH generated across the membrane as energy source. ATP is then released into the stroma for use in the dark reaction of photosynthesis (Calvin-Benson cycle) and other assimilatory pathways.

ATP synthase has two distinct domains, the CFo – a hydrophobic integral membrane multiprotein complex and CF_1, - a hydrophilic peripheral membrane protein complex which protrudes into the stroma, both of which are connected by a 'coupling factor' located in the chloroplast stromal membranes. CF_1 also contains an axle and controls proton movement between CF_0 and CF_1. The CFo domain consists of four subunits, I-IV, and controls proton movement across the thylakoid membrane. The other five subunits (α_3, β_3, γ, δ, and ε) are constituents of CF_1 domain, site of ATP synthesis from ADP and Pi, and hydrolysis (Ackerman & Tzagoloff, 2005; Allen 2002; Groth & Pohl, 2001; Groth and Strotmann, 1999). The

CF_0 domain rotates in response to proton (H^+) flow down a pH gradient across the membrane. This rotation causes the axle to rotate, altering the conformation of components of the CF_1 domain to drive the synthesis of ATP. The synthase can also act as an H^+ pump ATPase when its rotations are reversed by ATP hydrolysis.

1.7 Linear electron transport

Generally accepted as the major mode of electron transport in photosynthetic organisms, linear electron transport (LET) involves the sequential transfer of electrons derived from water oxidation to ultimately reduce $NADP^+$ using light energy (Figure 1.2). This process is initiated when light energy absorbed by LHCII is transferred to special pair chlorophyll molecule, P680 (PSII primary electron donor) to become excited (P680*), subsequently losing an electron to pheophytin (Pheo), the primary electron acceptor in a process called charge separation (Figure 1.6). Electrons from pheophytin are transferred to a permanently bound plastoquinone electron acceptor, Q_A and onwards via an iron atom to loosely bound plastoquinone acceptor, Q_B. Q_B, a two electron acceptor becomes fully reduced after two photochemical turnovers of the reaction centre and binds two protons from the stroma to form plastoquinol (PQH_2). Plastoquinol moves from PSII binding site to enter into the hydrophobic core of the thylakoid membrane where it transfers its electrons through the Q cycle to the Rieske Fe-S centre in the Cyt b_6/f complex. Consequently, the process is repeated as oxidized plastoquinol returns to the Q_B binding. Meanwhile in the Cyt b_6/f, two protons are released into the thylakoid lumen while one electron is transferred to plastocyanin (PC), a soluble electron carrier located in the

thylakoid lumen which serves as an electron donor to oxidized chlorophyll P700 of PSI.

The electron transfer process in PSI shown in Figure 1.7 begins with the transfer of excitation energy from antenna pigments to P700 reaction centre. P700 is oxidized while another chlorophyll molecule A_0 (an electron acceptor) is reduced. The electron moves to A_1 (phylloquinone) and from there through a set of three iron-sulphur centres (F_x, F_A and F_B) to ferredoxin on the stromal side of the thylakoid membrane (Blankenship, 2002). Ferredoxin releases an electron used by ferredoxin – NADP reductase (FNR) to reduce $NADP^+$ to NADPH. Simultaneously, oxidised P700 becomes reduced on receiving an electron from plastocyanin, on the lumenal side of PSI. Protons translocated into the thylakoid lumen from water oxidation in PSII and oxidation of reduced PQ by the Cyt b_6/f complex results in the generation of transthylakoid pH gradient providing the energy to drive ATP synthesis. ATP and NADPH produced are both used in carbon fixation.

At the PSII donor side, light energy allows the cycle of P680 excitation, oxidation and reduction to be repeated which allows oxidised P680 ($P680^+$) to sequentially extract electrons from tyrosine Z (Y_Z). Y_Z in turn extracts electrons from the Mn-cluster in the OEC via the S-state accompanied with water splitting and release of an oxygen molecule and four protons into the thylakoid lumen (Figure 1.6).

1.8 Cyclic electron transport

The ratio of ATP to NADPH produced via LET route has been suggested to be insufficient to meet the requirements of the Calvin-Benson cycle in plants (reviewed in Miyake, 2010, Eberhard et al, 2008). To meet this shortfall, alternative electron transport pathways such as the Mehler reaction and cyclic electron transport (CET) route around PSI has been suggested to supply the extra ATP required to balance chloroplast's ATP: NADPH requirement (Miyake, 2010; Shikanai, 2007). Although first described as cyclic phosphorylation in the early 1950s (Arnon et al, 1954) knowledge concerning details of CET mechanisms and its physiological function is still being unravelled. As shown in Figure 1.2, CET activity is driven solely by PSI with electrons recycled in a loop from PSI to plastoquinone via either reduced ferredoxin or NADPH and onwards to increase flow of electron through Cyt b_6/f complex of the electron transport chain. The Q cycle subsequently transfers protons from the stroma into the thylakoid lumen enhancing its acidification to generate a large pH gradient (ΔpH) which provides energy required for ATP synthesis without accumulating NADPH (Shikanai, 2007). This is crucial for the Calvin-Benson cycle to function efficiently while meeting the requirements of other assimilatory pathways (Shikanai, 2007). Apart from ATP synthesis, high (ΔpH) generated via CEF also functions in photoprotection, controlling light harvesting which enables plants to cope with excess light or fluctuating light flux under natural conditions (reviewed in Johnson, 2011; Munekage et al, 2004). The photoprotective role of CET will be discussed in section 1.12.

1.9 Mehler reaction

The Mehler reaction (water-water cycle) routes electrons from water oxidation in PSII to PSI where reduced ferredoxin or one of the Fe-S clusters bound to PSI is oxidized by molecular oxygen (O_2) instead of $NADP^+$. This process results in the formation of superoxide radicals (O_2^-) which are rapidly converted to hydrogen peroxide (H_2O_2) and oxygen (O_2) by copper/zinc superoxide dismutase (Cu/ZnSOD). H_2O_2 may accumulate in the stroma, oxidizing thiol groups while inactivating irreversibly the Calvin cycle enzymes, namely, NADP-glyceraldehyde-3-phosphate dehydrogenase, fructose-1,6-bisphosphatase and phosphoribulokinase (Kaiser 1979). In addition, H_2O_2 generates a hydroxyl radical through the Fenton reaction if transition metal ions, irons and copper are present (Asada 1996; Halliwell & Gutteridge, 1992). The hydroxyl radical oxidatively damages RuBisCO (Ishida et al 1997, 1998) and glutamine synthetase (Palatnik et al 1999).

To prevent such damages, H_2O_2 must be scavenged as rapidly as it is produced. The water-water cycle scavenges O_2^- and H_2O_2 (Asada 1999). The H_2O_2 is rapidly converted back into water by membrane-bound ascorbate peroxidase (thylakoid-APX) in a series of complex reactions also called the water-water cycle. Thus, efficient degradation of superoxide to water helps to avoid/reduce damage to the chloroplast by toxic H_2O_2 and O_2^- (reviewed in Eberhard et al, 2008). The ascorbate used by thylakoid-APX is converted into monodehydroascorbate, an ascorbic acid radical, and subsequently reduced back to ascorbic acid by ferredoxin using PSI electrons (reviewed in Miyake, 2010; Eberhard et al, 2008). Overall, the

cycle passes electron from PSII water molecule to another water molecule produced by peroxidase proximal to PSI.

Apart from scavenging O_2^- and H_2O_2 to prevent photodamage, the water-water cycle also pumps protons into the thylakoid lumen, maintaining pH gradient (ΔpH) across the thylakoid membranes when fewer electron transport acceptors are available in PSI. This ΔpH enhances ATP synthesis as well as dissipation of excess light energy as heat (reviewed in Eberhard et al, 2008). Although physiological and biochemical studies have inferred the role of the water-water cycle, estimates of its contribution to photosynthesis are still under debate. However, Makino et al (2002) showed in rice that the water-water cycle functions at the start of photosynthesis by generating ΔpH across thylakoid membranes required for thermal dissipation of excess excitation energy and supplying ATP for carbon assimilation. This cycle was also implicated in protecting *Arabidopsis thaliana* from photooxidative stress (Rizhsky et al, 2003) while recently, Strizh (2008) suggested that the Mehler reaction plays an important role in stress sensing and redox signalling in a variety of plants.

1.10 Photoprotection and photoinhibition

Photosystem II (PSII) light harvesting antenna system in plants serve to increase the amount of captured light energy transferred to the reaction centre and also plays a key role in the regulation of light harvesting (Horton et al, 1996). However, in high light, plants may absorb excess excitation energy beyond their photosynthetic capacity. Also, adverse environmental conditions such as drought, cold or high temperature could limit carbon

dioxide supply by closing the stomata, reducing rate of photosynthesis and thus predisposing plants to accumulation of excess excitation energy. The build-up of excess energy enhances production rate of triplet chlorophyll (^{3}Chl) e.g by intersystem crossing and toxic reactive oxygen species (ROS) which may induce photodamage to lipids, critical pigment cofactors and PSII protein subunit within the photosynthetic apparatus. Accumulation of ^{3}Chl and ROS in turn leads to sustained lowering of the quantum yield of PSII, which adversely affects photosynthesis, growth and development in plants, a condition known as photoinhibition (Murchie & Niyogi, 2011; Ort et al. 2011).

Although photosynthetic plants possess a complex set of regulatory mechanisms to dissipate toxic species (Asada, 1999), damage to the photosynthetic apparatus may still occur and additional mechanisms are present to repair the system. Part of the core PSII reaction centre complex is the D1 protein, a major target of photoinhibitory damage induced by inefficient electron transfer at the donor or acceptor sides of PSII (Andersson & Aro, 2001). The donor side mechanism occurs when rate of electron donation to PSII surpasses the rate of electron removal to the acceptor side, leading to an increase in the lifetime of $P680^+$ and Y_Z^+ (oxidized form of redox active tyrosine of PSII D1 protein) which then oxidizes PSII reaction centre proteins and pigments (Andersson & Aro, 2001). Photoinhibitory damage induced on the acceptor side involves primary charge separation between the chlorophyll dimer, P680 and pheophytin molecule (Pheo) to form a primary radical pair, $P680^+/Pheo^-$. Recombination of $P680^+/Pheo^-$ enhanced by impairment of Q_A function

gives rise to triplet chlorophyll (^{3}P680) which can readily react with oxygen to form singlet oxygen ($^1O_2$). $^1O_2$ is highly reactive, oxidizing pigments, redox active cofactors and proteins especially D1 causing damage to the reaction centre and subsequently inducing photoinhibition (Andersson & Aro, 2001).

Damage of D1 protein is reversible because plants possess a remarkable damage-repair cycle in which the damaged PSII reaction centre migrates into the stromal lamellae and is disassembled while damaged D1 is degraded. The degraded D1 protein is replaced with a newly synthesized protein molecule and subsequently reassembled into a functional PSII before migrating back to the grana thylakoid (Aro et al, 1993). Thus, the amount of D1 damage, migration rate of PSII reaction centres, the decomposition of damaged D1, as well as the rate of synthesis of new D1 determine the extent of photoinhibition (Long et al., 1994). However, inhibition of the repair of photodamaged PSII at the step of the de novo synthesis of the D1 protein was proposed as a major limitation (Takahashi et al, 2009).

Whenever the PSII rate of damage exceeds its rate of repair, usually in excessive light or other stress conditions, inactive PSII reaction centres accumulate resulting in decreased photosynthetic efficiency. Such plants are said to be photoinhibited as a result of the net loss of functional PSII reaction centres and in extreme conditions of photodamage, may suffer oxidative stress. To limit photoinhibition, plants have developed several protective mechanisms to control light energy absorption, utilization and dissipation under excess light (Horton et al, 1996).

Photoprotective mechanisms include prevention and control of excess light absorption, removal of reactive oxygen species and quenching of chlorophyll excited state (reviewed in Murchie & Niyogi, 2011; Horton et al 2008). The first group of photoprotective mechanisms include adjustments of leaf area and angle, chloroplast movement, changes in antenna size and organization of LHCs (Ort et al. 2011; Jiang et al, 2006; Wada et al, 2003). The second group involves scavenging of reactive oxygen species by carotenoid and components of the antioxidant system especially the reduced ascorbate and glutathione (Foyer & Shigeoka, 2011). The third category involves dissipation of up to 75% excess absorbed light energy as heat (Kiss et al 2008) which involves quenching of singlet excited state chlorophyll (^{1}Chl) measured as nonphotochemical quenching (see 1.10.3) by chlorophyll fluorescence analysis (reviewed in Krause & Weis, 1991).

1.10.1 Chlorophyll fluorescence

As chlorophyll molecules, mostly PSII chlorophyll a, absorb light photons, they move into a higher energy state, releasing their energy (decay) over time as chlorophyll fluorescence. This process is however in competition with other processes:

1. Photochemical reaction (K_P)
2. Thermal deactivation (heat dissipation) (K_D)
3. Excitation energy transfer to nonfluorescent pigments (K_T)

Re-emitted light from decayed chlorophyll in proportion to other competing processes can be measured as fluorescence yield of chlorophyll (ΦF) and it

accounts for around 3% of absorbed light under physiological conditions (reviewed in Krause & Weis, 1991). Because fluorescence is emitted at longer wavelengths than absorbed light, it can therefore be measured as the amount of re-emitted fluorescence by exposing a plant to a light of defined wavelength. Fluorescence yield can be quenched either by an increase in K_P ending up as photochemical quenching (qP) or an increase in K_D or K_T which results in nonphotochemical quenching (NPQ). Energy distribution between these three processes is flexible and constantly changes with environmental conditions (Kramer et al. 2004; Krause & Weis 1991). Because chlorophyll fluorescence yield can be measured, information on the potential yield of qP and NPQ will enable us understand the functional state of the photosynthetic apparatus in terms of photochemical and photoprotective mechanisms utilised by plants under different environmental conditions (reviewed in Krause & Weis, 1991).

1.10.2 Chlorophyll fluorescence analysis

A simple and robust method to measure chlorophyll fluorescence as well as photosynthetic efficiency in plants is via the use of modulated measuring system. This method permits only fluorescence yield stimulated by the measuring light to be recorded as a result of which fluorescence yield in the light can be measured (Schreiber et al, 2004; Quick & Horton 1984) as described.

When a leaf kept in the dark is illuminated with weak measuring light, a minimum level of fluorescence (F_o) is attained, at which point all reaction centres of PSII are said to be 'open', Q_A is fully oxidized and photochemical efficiency is at a maximum rate. If after reaching F_o, a saturating light for a

very short duration (≤1 s) is applied, Q_A becomes maximally reduced closing all reaction centres. At this point photochemistry is at a minimum and maximum fluorescence level (F_m) is attained.

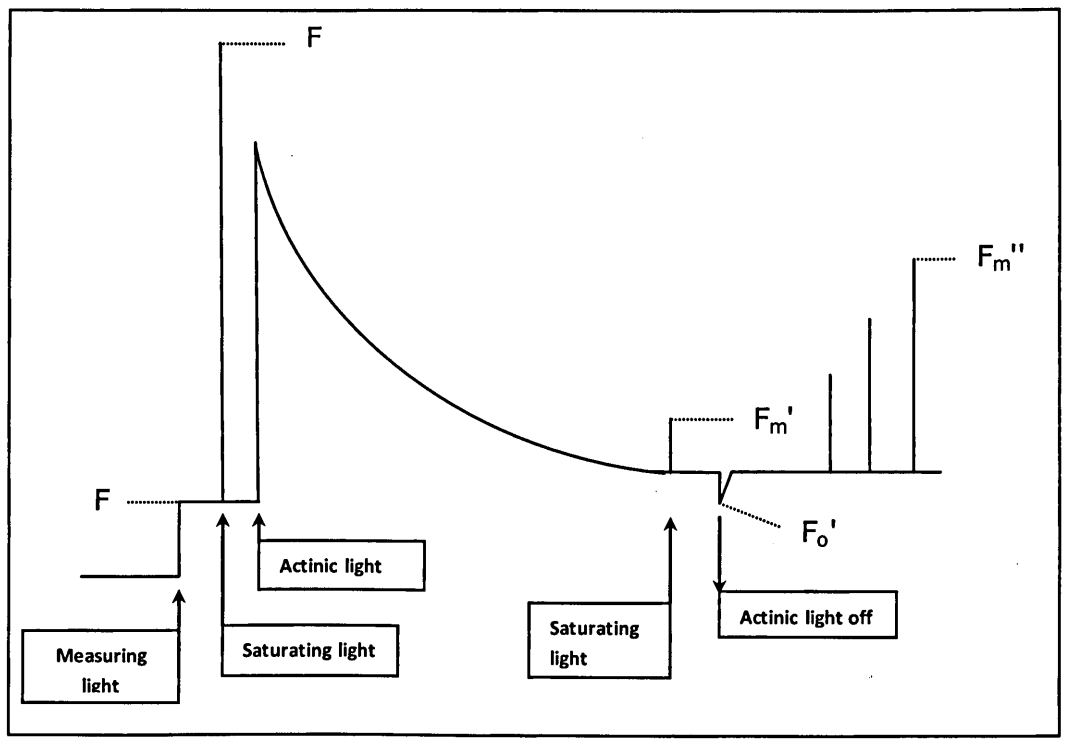

Figure 1. 8 An example of fluorescence trace showing the decrease in fluorescence yield after illumination. F_o is the minimum fluorescence after the measuring light is turned on. F_m and $F_{m'}$ are the maximum fluorescence in the dark and light adapted sate respectively. F_o' is the minimal fluorescence in the light while F_m'' maximum fluorescence during relaxation. F_t is the steady state fluorescence level at any time and it is estimated as the difference between F_m and F_o at that time.

The difference between fluorescence emission between F_m and F_o is described as variable fluorescence (F_v). From these parameters, the potential yield of PSII photochemistry when Q_A is fully oxidized can be calculated as F_v/F_m or $(F_m - F_o)/F_m$ which describes the physiological state

of the photosynthetic apparatus in intact leaves. F_v/F_m value in leaves of most species is around 0.832 decreasing when plants are exposed to stress conditions (Bjorkman & Demmig, 1987). F_t is the steady state fluorescence level at any time and it is estimated as the difference between F_m and F_o at that time (Figure 1.8).

Photochemical quenching of chlorophyll fluorescence occurs when there is a decrease in fluorescence yield as a result of partial oxidation of Q_A with electrons transferred to PSI. qP denotes the proportion of absorbed light energy that is used in photochemistry. A quantitative relationship for the amount of this quenching effect is defined as $(F_m'-F_t)/(F_m'-Fo')$ which is equal to unity when all reaction centres are open and approaches zero as reaction centres close. Other fluorescence parameters can also provide information on the photochemical efficiency of a leaf. Φ(II) estimates the quantum yield of PSII electron transfer and is calculated as (Fm'-Ft)/Fm', reflecting the efficiency of PSII reaction centres under illumination. Φ(II) is used to calculate rate of linear electron transport (J) by Φ(II) x PFDa (absorbed photon flux density measured with an integrating sphere) x (0.5) and therefore photosynthetic rate (Maxwell & Johnson, 2000; Genty et al 1989).

Nonphotochemical quenching decreases fluorescence yield of PSII reaction centres when Q_A is reduced. It can be quantified relative to a dark adapted reference level, Fm, where photochemical efficiency is maximum and heat dissipation is at a minimum (Maxwell & Johnson, 2000). NPQ defined by (Fm-Fm')/(Fm') provides information on processes affecting the antenna system and electron transfer activities in plants (Maxwell & Johnson, 2000).

NPQ can be divided into distinct components described below (Section 1.10.3) with each component quantified from fluorescence yield parameters at steady state under illumination and during dark relaxation. The different components of NPQ relax at different rates and can therefore be distinguished from each other. The fast relaxing component assigned energy-dependent NPQ_F (qE) is calculated as $(F_m/F_m') - (F_m/F_m'')$, where F_m'' is the maximal yield of fluorescence after a period of dark relaxation following the actinic illumination. The slowly relaxing component (NPQ_S or qI) is described as $(F_m - F_m'')/F_m''$ while state transition (NPQ_T or qT) is calculated as $(F_m - F_m')/F_m'$ (Maxwell & Johnson, 2000).

1.10.3 Nonphotochemical quenching

Under high light conditions, plants may absorb light energy in excess of the requirement for photosynthesis resulting in over excitation of chlorophyll molecules over-reduction of the electron transport chain and over-acidification of the thylakoid lumen. Excess excitation energy which potentially can cause photodamage is dissipated as heat. The amount of energy dissipated can be monitored by the nonphotochemical quenching of chlorophyll fluorescence (reviewed in Eberhard et al, 2008 & Horton et al, 1996). There are three major components of NPQ: quenching related to state transition (qT), photoinhibition (qI) and energy-dependent quenching (qE).

1. State transition related quenching, qT

This component involves changes in the relative sizes of PSI and PSII antenna in order to balance flux of excitation energy between the two

photosystems. State transitions depend upon a reversible phosphorylation of antenna proteins e.g. LHCII, by a membrane bound protein kinase which in turn causes migration of the phosphorylated protein from the grana thylakoid to the stromal lamellae to associate with PSI. qT relaxes over minutes and its contribution to quenching in plants is insignificant (reviewed in Eberhard et al, 2008) because plants deficient in qT show normal growth rate under continuous light (Tikkanen et al. 2006). However, under fluctuating light conditions, qT deficient mutants have been shown to exhibit slower growth rate and a more reduced plastoquinone pool (Bellafiore et al. 2005). Finazzi et al. (1999) also suggested that under limiting CO_2 and a highly reduced electron transport chain, qT may be associated with transition from linear to cyclic electron transfer.

2. Photoinhibitory quenching, qI

This type of quenching is linked with stronger level of light stress and reverses slowly over a long period of hours. Part of this quenching portrays photoinhibition of PSII reaction centres described in 1.10, while a major part reflects sustained quenching of the antenna, a protective process thought to operate even when PSII is fully functional (Horton et al, 1996). Although qI incorporates both photodamage and photoprotection which has made it difficult to characterise, chlorophyll fluorescence can be used to differentiate them (Muller et al, 2001). Photoinhibition of damaged reaction centres increases Fo level while decreasing Fm level. Sustained quenching decreases Fo level in direct proportion to Fm (Gilmore et al, 1996). Formation and relaxation of sustained quenching has been associated with zeaxanthin retention even after ΔpH is dissipated (Demmig-Adams et al,

1989). The mechanism operating in qI is thought to be similar to that of qE because energization of the thylakoid membrane persists in the dark. (Horton et al, 1996). qI is measured as NPQ_S, the slow component of NPQ.

3. Energy-dependent quenching, qE.

The major component of NPQ, qE, forms within minutes of exposure to light and is rapidly reversible in the dark. It depends on a change in thylakoid lumen pH below 6 (Munekage et al, 2001) to generate a ΔpH across the thylakoid membrane which results in energy dissipation in PSII antennae under saturating light, thus reducing excitation pressure on the photosynthetic electron transport chain. The ΔpH triggers de-epoxidation of LHCII-bound xanthophyll cycle pigment violaxanthin into zeaxanthin and the protonation of PsbS a protein related to LHCs of PSII (Li et al, 2004). Synergy between these factors produces conformational changes in the antenna of PsbS creating singlet excited state chlorophyll quencher, qE (Johnson & Ruban, 2011; Horton et al, 1996). Strict regulation of qE by the pH in the thylakoid lumen allows PSII antenna to switch between its primary function of light harvesting and energy dissipation in fluctuating light. Joliot & Finazzi (2010) showed that the relationship between qE and ΔpH varies with the state of the xanthophyll cycle de-epoxidation, with maximum qE attained at lumen pH below 6 in the presence of zeaxanthin, suggesting that zeaxanthin modulates qE kinetics (Ruban et al, 2001). The PsbS protein subunit, thought to act as a sensor of the lumen pH (Li et al, 2004) is also postulated to function in concert with minor components of LHCIIs as the site of energy dissipation (Horton et al, 2008).

qE protects via thermal dissipation of energy from singlet excited state chlorophyll in PSII antenna complexes, minimizing the production of triplet excited state chlorophyll molecules that react with ground state oxygen to form toxic singlet oxygen and function in maintaining efficient protein synthesis. Furthermore, qE may down-regulate PSII activity and suppress the production of hydrogen peroxide via superoxide in the Mehler reaction (Asada, 1999).

The nature of qE is controversial and a number of models have been proposed for its mechanism. Holt et al (2004) suggested a direct role for zeaxanthin, involving direct transfer of singlet exciton from chlorophylls to zeaxanthin to form a zeaxanthin cation in PSII antenna by a mechanism that would depend on PsbS and ΔpH. In contrast, a pH/PsbS modulated conformational change was suggested which induce the formation of a dissipative state in the PSII, with zeaxanthin acting as an allosteric effector of qE- implying an indirect role of zeaxanthin in qE formation (Horton et al, 1996). In addition, a third type of quenching was observed independent of the carotenoids of the xanthophyll cycle (Crouchman et al, 2006; Finazzi et al, 2004) but enhanced on zeaxanthin retention (Kalituho et al, 2007).

The zeaxanthin independent quenching could be related to activities at the PSII reaction centre (Finazzi et al, 2004) or PsbS modulation of PSII light harvesting capacity (Crouchman et al, 2006). This type of quenching is transiently induced in dark-adapted leaves when exposed to non-saturating light and disappears once steady state photosynthesis is attained (Kalituho et al, 2007; Finazzi et al, 2004) reflecting changes in the process of the CO_2 fixation by the Calvin-Benson cycle. Stress conditions will modify rate

of CO_2 uptake and utilisation affecting demand for ATP synthesis. The size ΔpH, probably enhanced by CET, will subsequently increase eventually inducing qE.

1.11 Pathways of CET

Whenever plants absorb light energy beyond the capacity of the Calvin-Benson cycle, a pH gradient is generated across the thylakoid membrane by the linear electron transport system. This process is further enhanced by alternative electron transfer system specifically CET (see section 1.8), a major contributor to ΔpH (Munekage et al, 2002) through increased electron transfer from PSI back to plastoquinone.

Two major pathways to link the reducing side of PSI to the plastoquinone (PQ) pool are present in plants. One of such is the chloroplast mediated NAD(P)H dehydrogenase (NDH) complex shown recently to form a supercomplex with PSI (Peng *et al* 2011). NDH activity has been found in a number of plant species (Shikanai, 2007). It is an approximately 550 kDa thylakoid membrane protein complex constituting 0.2% of total thylakoid membrane protein (Sazanov *et al*, 1998). Several studies have shown the involvement of the NDH complex in alleviating oxidative stress (reviewed in: Shikanai, 2007; Wang *et al*, 2006; Munne-Bosch *et al*, 2005; Horvath *et al*, 2000; Endo *et al*, 1999).

Another pathway is mediated by ferredoxin-dependent PQ oxidoreductase (FQR; Shikanai, 2007). This pathway is sensitive to antimycin A, an electron transport inhibitor. The majority of CET-induced ΔpH is associated with the antimycin A-sensitive pathway (Munekaga et al., 2004).

Munekage *et al* (2002) isolated an *Arabidopsis thaliana* mutant defective in qE formation due to a lack of ΔpH and affected in cyclic flow of electrons associated with the antimycin A-sensitive pathway. This mutant was also sensitive to photoinhibition and showed decreased growth under excessive light. The mutant lacks Proton Gradient Regulation 5 (PGR5) protein. PGR5 is a 10kDa nuclear encoded thylakoid membrane protein sensitive to antimycin A (Munekage *et al*, 2002). During the shift from low to high light, a dose-dependent increase in rate of CET was shown in lines overexpressing PGR5 (Okegawa *et al* 2007).

Another *A. thaliana* mutant deficient in a different thylakoid membrane protein, PGR5-like1 (PGRL1) was isolated. This mutant showed CEF inhibition similar to that of *Arabidopsis pgr5* (DalCorso *et al*, 2008). These two proteins have been proposed to interact physically with PSI, ferredoxin and cytochrome b_6f to facilitate CET in plants; Specifically PGRL1 is thought to anchor PGR5 to the thylakoid membrane forming a protein complex (DalCorso *et al*, 2008). While CET was inhibited under stress conditions such as high light in plants lacking PGR5 or PGRL1 they were still able to carry out cyclic flow comparable to the wild type, suggesting that these two proteins may not be essential for CET (DalCorso *et al*, 2008; Nandha *et al*, 2007) and that rate of electron flow to PSI may be inhibited by regulatory processes (Joliot & Johnson, 2011). Early studies have shown that redox poising of electron transport to avoid over-oxidation or reduction of the electron transport chain is essential for efficient CET (Allen, 2002) with Nandha *et al*, 2007 suggesting the involvement of PGR5 in the redox poising of the electron transport chain. Thus, impairment of CET in

Arabidopsis pgr5 and pgrL1 mutants suggests the role of PGR5/PGRL1 protein complexes in regulating redox poising of the electron transport chain.

Regulation of the redox state of several components of the electron transport chain has been shown to occur at the level of the cytochrome bf complex, specifically during plastoquinol oxidation (Joliot & Johnson, 2011; Ott et al, 1999). This regulation is sensitive to the pH of the thylakoid lumen, slowing down the flow of electrons through the cytochrome bf complex, a complex sensitive to redox poising (Johnson 2003). Work from Hald et al (2008) has led to the proposal that the redox state of the NADP/H pool regulates the cytochrome bf complex. The regulation of electron flow before PSI, preventing over reduction of the electron transport chain suggest that cytochrome bf complex plays a significant role in protecting plants from photooxidative stress, a role which may be inefficient in *pgr5* and *pgrl1* mutants (Johnson, 2011).

1.12 Role of CET in photoprotection

Increases in thermal quenching (qE and qI) down-regulate PSII yield measured as decrease in the value of Fv/Fm (Long *et al.* 1994). Dark adapted (Fv/Fm) values been used as an indicator of photoprotection in rice (Tang *et al.* 2002; Murchie *et al.* 1999) and other plants (Ibaraki & Murakemi, 2006). Majority of mechanisms controlling this down regulation are controlled by acidification of the thylakoid lumen (ΔpH) enhanced through CET, which triggers photoprotective qE quenching of excitation

energy and therefore responds rapidly to changes in light intensities under natural conditions (Takahashi *et al.* 2009; Munekage *et al.* 2004).

Takahashi et al (2007) proposed that CET-dependent generation of ΔpH helps to alleviate photoinhibition by at least two contrasting photoprotection mechanisms: one is linked to qE generation and prevents the inhibition of the repair of photodamaged PSII at the step of D1 protein synthesis, and the other is independent of qE and suppresses photodamage to PSII. However, recent studies have shown that CET plays a key role in photoprotection via qE activation in response to varied (adverse) environmental stimuli. In C_3 plants, CET has been reported to regulate ΔpH in order to control light absorption via NPQ (Johnson, 2005) with higher PGR5 level sustaining transient NPQ longer under fluctuating light (Endo *et al.* 2008). Substantial increases in ΔpH activated qE following a transition from prolonged dark acclimation into high light during the induction of photosynthesis from have been reported (Joet *et al.* 2002; Joliot & Joliot, 2002). In a study comparing the water-water cycle and CET in Rubisco deficient transgenic rice, Makino *et al.* (2002) reported CET around photosystem I (PSI) acts to maintain a higher NPQ in the long-term, thus preventing PSI photoinhibition/photodamage, in conditions in which the absorption of light energy for photosynthesis exceeds its rate of utilisation. In such conditions causing over-reduction of LET and the stroma in plants, it is suggested that CET increases flow of electrons from LET and PSI back into the plastoquinone pool accompanied by H^+ intake into the thylakoid lumen from the stroma (Shikanai, 2007). This subsequently increases ΔpH, activating qE and increasing ATP synthesis (Shikanai, 2007). CET was

significantly stimulated under high light and drought stresses to activate NPQ (Golding & Johnson, 2003; Miyake et al. 2005). Takahashi *et al.* (2007) showed that impairment of photosystem I CET by mutation of PGR5 suppressed qE and accelerated photoinhibition.

1.13 Role of CET in photosynthesis

In changing environment, LET generates ATP and NADPH at a fixed ratio insufficient to meet the requirements of the Benson-Calvin cycle and other metabolic processes in the chloroplast (Allen, 2002; Joet *et al*, 2002; Johnson, 2005). The generation of ΔpH dependent CET across thylakoid membranes not only activates qE, alleviating over-reduction of acceptor side of PS I thus preventing photoinhibition, it is also used by ATP synthase to activate ATP production without generating NADPH in order to maintain proper ATP/NADPH ratio in the chloroplast (Shikanai, 2007; Heber & Walker, 1992).

CET is generally known as an important source of ATP synthesis including bundle sheaths of C_4 plants where it is associated with a low amount of PSII (Majeran et al, 2008) and a high amount of PGR5 protein and NDH complex subunits in bundle sheath chloroplast, relative to species in question (Johnson *et al*, 2011; Munekage *et al*, 2010). Although still controversial in terms of its role, CET is thought to play an insignificant role in C_3 plants under steady state photosynthesis except during induction of photosynthesis and under stress conditions (Nandha, et al, 2007; Golding & Johnson, 2003; Golding et al, 2004; Allen, 2002). In contrast, Munekage et al (2008) showed that impairment of PGR5-dependent CET inhibited

photosynthesis and subsequently reduced growth in Arabidopsis suggesting that PSI CET is essential for steady state photosynthesis in C_3 plants. Indeed, the pgr5 defect was also suggested to lead to an imbalance in ATP/NADPH ratio during photosynthesis inhibiting normal growth. When ATP production is inadequate, unused NADPH by the Calvin cycle accumulates in the stroma of the thylakoid membrane resulting in the over reduction of the electron transport chain and photoinhition/photodamage (Munekage et al, 2004). To support this, recent studies showed mutants lacking the PGR5 protein are specifically defective in qE-type of NPQ and CET and as such are more sensitive to photoinhibition whilst showing decreased photosynthesis, growth and fitness under high light/fluctuating light and other stress conditions (Suorsa et al, 2012; Takahashi et al, 2009; Munekage et al, 2008).

Similar reductions in photosynthesis, growth and fitness have been observed in low qE plants deficient in PsbS (Hubbart et al, 2012; Tikkanen et al, 2010; Li et al, 2002). qE has been shown to affect plant productivity when grown under fluctuating light in the growth chamber or field. For example npq4, a qE deficient mutant, declined in fitness which was attributed to a decline in PSII quantum yield (Kulheim et al, 2002). Based on metabolic analysis, Frenkel et al (2009) suggested diversion of carbohydrates towards defence rather than growth may explain the decline in performance observed in plants. However, Hubbart et al (2012) recently showed that qE attributed to PsbS accumulation exerts a direct control over leaf photosynthesis via PSII redox state, suggesting that improvement of photoprotective processes is critical to achieve maximum photosynthetic

productivity even in the absence of photoinhibitory stress. Similarly, Murchie et al (2009) proposed optimization of photoprotective processes is critical in order to increase stress tolerance, biomass and photosynthetic productivity of crop plants. Since many studies have reported the occurrence of CET under stress conditions, the exact effect of qE induced as a result of PGR5-dependent CET activity in rice leaf photosynthesis under varying environmental conditions is yet to be determined. Generally studies on PGR5-dependent CET have mainly been in *Arabidopsis thaliana* (Takahashi et al. 2009; Munekage et al. 2008, Shikanai, 2007). Appreciating the possible function of PGR5-CET in the context of plants species and ecology will enable us gain clear understanding of the function as well as limitations of CET (Johnson, 2011), making it possible to manipulate photoprotection in plants towards enhancing rice leaf photosynthesis.

1.14 AIMS

It is clear that PGR5 is involved in the regulation of photoprotection and photosynthesis although its biochemical function is still unknown. *Arabidopsis thaliana* has been a model crop in elucidating the role of PGR5-dependent CEF in photoprotection and photosynthesis (Takahashi *et al.* 2009; Munekage *et al.* 2008) and as such studies have suggested PGR5-dependent cyclic flow function under stress. However little is known about the function of this protein in more 'physiologically demanding' plants such as rice, particularly how PGR5 affects rice photoprotective responses and its potential impact on rice photosynthesis.

This work aims to determine the role of the photoprotective protein, PGR5 in the regulation of photoprotection and photosynthesis under constant as well as dynamic conditions and its impact on plant growth and development using transgenic rice plants with manipulated levels of the PGR5 protein.

Specific objectives include:

- Characterization of photosynthetic capacity and growth performance of PGR5 transgenic rice plants grown under steady non-photoinhibitory stress conditions.
- Response of transgenic rice plants to dynamic environmental conditions.
- Investigation of the potential impact of the PGR5 protein on photoprotection, photosynthetic efficiency and growth of rice crop at the canopy level.

CHAPTER 2

MATERIALS AND METHODS

CHAPTER 2: MATERIALS AND METHODS

2.1 Gene sequence identification, transformation and plant material

In a previous microarray study performed using chips designed by Syngenta, Murchie et al (2005) measured the effect of high light imposition on global gene expression in rice. Levels of some transcripts involved in photoprotection increased several fold including a sequence with high similarity to Arabidopsis pgr5. A suitable probe sequence annotated as pgr5 was obtained from genomic sequence shown below, equivalent to Os08g0566600. This probe sequence was used to transform the rice cultivar *Oryza sativa var Kaybonnet* at Syngenta, North Carolina using *Agrobacterium* mediated techniques. Transgene expression was driven by the Cestrum yellow leaf curling virus promoter, TATA box and other enhancers. Plants were stably transformed into PGR5 protein RNA interference (RNAi) and overexpression (OE) transformant lines (T_0 generation). Due to the sequence similarity, we refer to this protein as PGR5. Progeny from the various lines were advanced to T_2 generation from which four lines were selected based on their NPQ level for use in this study. The lines include RNAi 151 RNAi 158, OE139 & OE 147. Because of the possibility of segregation, all T_2 plants were screened for their NPQ level before analysis as described in 2.9. Untransformed Kaybonnet rice variety was considered as wild type (WT). The genomic sequence used in transformation process is as follows:

ATGGCAGCAGCTGCAGCATCATCCGTGTCCCTCCCCGGGGCGAGGGCTCTCCCG
ACGTGGTCCAGCTCCGTGTCCGGCGACTCGCACTCGTTGGCGCTGAGCTCGTGG
GCGGCGCGGCCTCGGTCGGCGCGGCCACTGCGGGCGCCGGCGAGGATGGGCA
ACGTGAACGAGGGCAAGGGGATCTTCGCACCGGTGGTGGTGGTGGTGCGCAAC
ATCGTTGGCCGCAAGCGCTTCAACCAGCTCAGGGGAAAGGCCATCGCGCTGCAC
TCGCAGGTGATCACCGAGTTCTGCAAGACCATCGGCGCCGACGCCAAGCAGAGG
CAGGGCTTGATCCGCCTTGCCAAGAAGAACGGCGAGAAGCTCGGTTTCCTTGCC
TGA

2.2 Plant growth room

Plants were grown in a walk-in controlled environment room operating on a 12 hour photoperiod, at day/night temperature of 28°C/24°C respectively. Irradiance was supplied by a bank of 400W metal halide lamps supplemented by domestic incandescent 60W light bulbs to give light intensity of 450 $\mu molm^{-2}s^{-1}$ at plant level. A similar alternate room was used where the conditions were identical with the exception of a higher irradiance (700 $\mu mol\ m^{-2}\ s^{-1}$) supplied by a higher density of 600W metal halide lamps with incandescent lamps and a 1 hour 'ramping' period at the beginning and end of each day where only half the lights were switched on to simulate dawn and dusk. Although plants were clean and did not require chemical spray treatment a previous experiment indicated possible slight risk to plants from red spider mites (*Tetrenychus urticae*). *Phytoseiulus persimilis* (Syngenta, UK) were routinely applied according to manufacturer's instruction to ensure red spider mites were eliminated. Photosynthetic photon flux density (PPFD) in the growth rooms was measured at top of canopy level using a LI-COR (LI-210) photometric sensor attached to a light meter (LI-250A).

2.3 Crop glasshouse

This experiment was carried out in a modern glasshouse under controlled conditions at the University of Nottingham. Plants were grown in plots on irrigated sandy-loam soil in a 5mx5m membrane-lined soil tank with depth of 1m, draining to a sealed 'sump' designed to simulate field conditions and create realistic crop canopies. Temperature and photoperiod were maintained at 30°C and 14hrs respectively. Soil was tested for macro and micro nutrients and nutrient supplement were added to the soil a week prior to transplanting following IRRI's guidelines (IRRI nutrient manager, 2012). Plants were disease and pest free however, *P. persimilis* was routinely applied to prevent red spider mite infestation.

2.4 Hydroponics nutrient solution

For the growth room experiments, hydroponic solution was made with fresh tap water. The water was mixed with the nutrients at appropriate concentrations (Table 2.1) before adjusting the final solution to pH 5.0-6.0 with 2M hydrochloric acid.

Table 2. 1 Nutrient composition of hydroponic solution

Element	Formula	Mr	[Stock] M	Final concentration (mM)
N	NH_4NO_3	80.04	4.2854	1.4
P	$NaH_2PO_4.2H_20$	156	0.8557	0.6
K	K_2SO_4	174.3	0.3838	0.5
Mg, S	$MgSO_4$	246.5	1.205	0.8
Mn	$MnCl_2.4H2_O$	197.9	0.0546	0.009
Mo, N	$(NH_4)6MO_7O_{24}.4H_2O$	1236	0.0004	0.0001
B	H_3BO_3	61.83	0.5564	0.037
Cu, S	$CuSO_4.5H_2O$	249.7	0.0019	0.0003
Zn, S	$ZnSO_4.7H_2O$	287.6	0.009	0.00075
Ca	$CaCl_2.2H_2O$	147	1.5	0.2
Fe	Fe-EDTA	367.1	0.1749	0.07

2.5 Growth room: seed germination and growth

Rice seeds were rinsed thoroughly with deionised water and then germinated on moist filter paper in 5-cm petri dishes sealed with micropore tape (Figure 2.1A). Young seedlings were then transferred into 1.5ml eppendorf™ tubes with the bottom tip of the eppendorf™ cut off. The tubes were placed into a rack floating on hydroponic solution (Figure 2.1B) for approximately one week to ensure root elongation and establishment. They were then transplanted into 20 L plastic light proof container of dimensions of 30cm x 22cm x 12cm filled with hydroponic solutions which were refilled to their 20L capacity throughout growing period of the plants to replace

amount of hydroponic solution lost. Eight holes of 2cm diameter were drilled through a light, lightproof plastic support where each rice seedling was inserted and held in place by a piece of sponge (Figure 2.1C). A randomised block design was adapted where the different lines were evenly distributed throughout each growth room, with each container having at least one representative of each line.

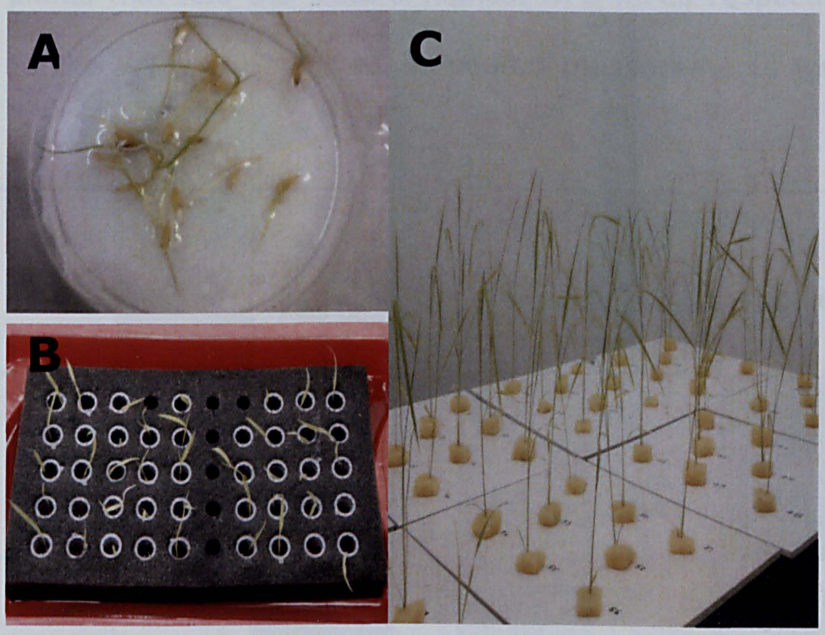

Figure 2. 1 Examples of (A) germinated rice seeds (B) seedlings in eppendorf for root elongation (C) seedlings establishment after transplanting.

2.6 Crop glasshouse: seed germination and growth

RNAi 158, OE 147 and WT were selected because they showed the most divergent NPQ level and ratio of PSII to PSI yield compared to the WT. Seeds were germinated in seed trays filled with Levington 2 compost in the glasshouse during spring 2012. Seedlings of each line were transplanted two weeks after germination into 90- x 90cm plots filled with sandy loamy soil at spacing of 10- x 10cm to achieve a cropping canopy of 64 plants per line per plot in the glasshouse between spring and summer 2012. This was

a fully replicated experiment and involved other types of transgenic rice plants (Figure 2.2). There were altogether 30 plots arranged in a completely randomized design with each transgenic line replicated three times and the wild type replicated nine times. From each plot, twenty plants were randomly selected and screened for NPQ as described in 2.10 using the fifth leaf on the main tiller. Ten RNAi and OE transgenic rice plants that had the least & highest NPQ level, respectively when compared to the WT were selected. Repeated measurements were made on tagged plants.

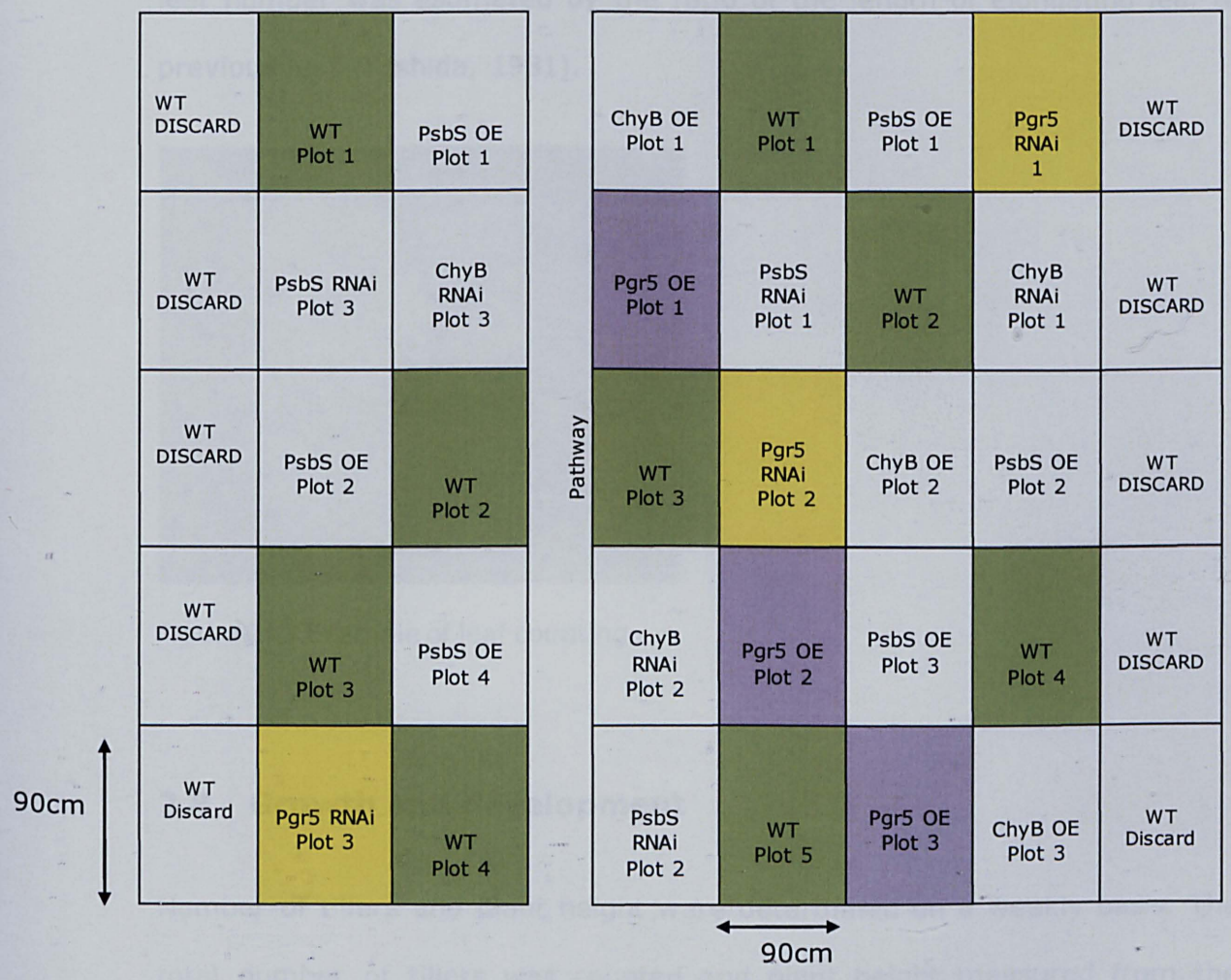

Figure 2. 2 Plot layouts for rice canopy experiment in the crop glasshouse

2.7 Determination of growth stage and leaf number

Leaves were counted on the main stem as shown in Figure 2.3 (Hoshikawa, 1989). This was necessary because of observed variation in the rate of leaf development/physiological age (Yoshida, 1981). The seventh and eighth leaf from emergence on the main stem was used for physiological analysis (Fig. 2.3). When the tip of the next leaf emerged, a leaf was considered fully developed. In most instances in the growth room and glasshouse experiments, observations were made before leaf elongation was complete, leaf number was estimated by the ratio of the length of elongating leaf to previous leaf (Yoshida, 1981).

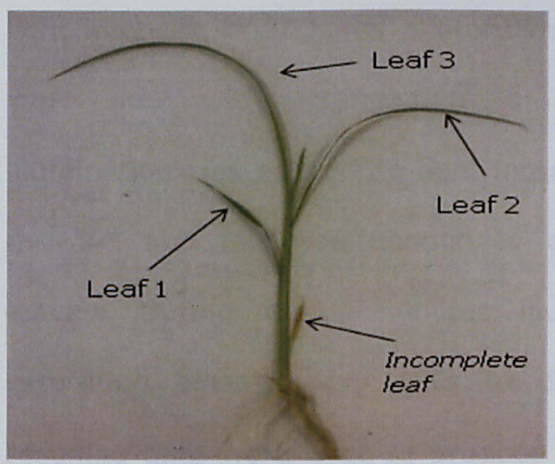

Figure 2. 3 Example of leaf counting

2.8 Growth and development

Number of tillers and plant height were determined on a weekly basis. The total number of tillers was counted and plant height measured from the base of the plant to the tip of longest leaf on main tiller with a ruler.

2.9 FluorCam chlorophyll fluorescence imaging system

Fluorcam (Photon Systems Instruments, Brno, Czech Republic) is an imaging system that measure sequences of chlorophyll fluorescence images with specified light intensity and timing protocols. This system was used to screen all transgenic plants for NPQ level because of the possibility of segregation. At leaf five, leaf segments from plants dark adapted overnight were placed on moist filter paper between glass plates and placed in the fluorcam. Leaf segments were further dark adapted for 30 minutes to ensure PSII reaction centres are maximally oxidized. Fo and Fm were recorded before the fluorcam front panel was opened to apply an actinic light intensity of 300µmol photons m^{-2} s^{-1} from a set of white LEDs. Care was taken with arrangement of the leaf segments to ensure that illumination was even. The light intensity at leaf level was around 250µmol m^{-2} s^{-1} and this was enough to establish differences in NPQ between leaves. During a 15 minutes illumination, Fm' was measured with saturating pulses every 180s to determine NPQ at steady state. The resulting data were used to produce false colour fluorescence image of leaf segments. Red colour represents high NPQ values while blue colour represents low NPQ values (Figure 2.4).

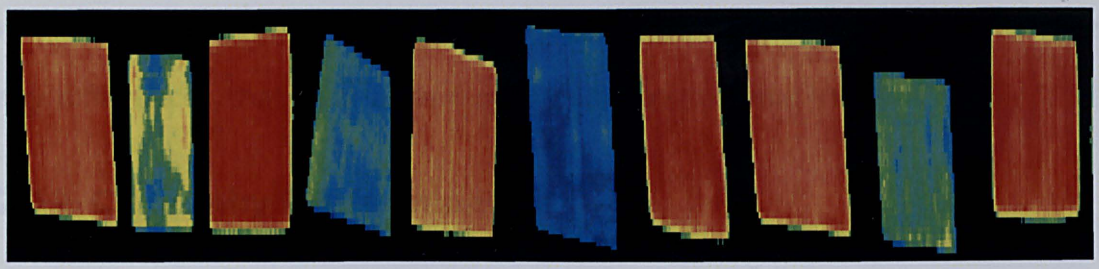

OE147 RNAi 151 OE147 RNAi 158 WT RNAi 158 OE139 OE147 RNAi 151 OE139

Figure 2. 4 Example of a false colour fluorescence image of leaf segment. Red colour represents high NPQ values while blue colour represents low NPQ values.

2.10 MINI-PAM

Chlorophyll fluorescence measurements were carried out on leaves with a portable MINI-PAM photosynthesis yield analyzer (Walz – Effeltrich, Germany). Leaves were dark adapted for 30 minutes using clips (DLC-08; Walz). Fo and Fm, determined by exposing leaves first to weak non actinic measuring light of 0.8 $\mu molm^{-2}s^{-1}$ and then to short pulse of high PPFD density 6000 $\mu molm^{-2}s^{-1}$ for 0.8s respectively, were used to calculate maximum quantum efficiency of PSII photochemistry, Fv/Fm.

2.11 Infiltration with methyl viologen (MV)

Attached leaves of wild type (WT), Overexpressor (OE) (139, 147) and RNAi interference (RNAi) lines (151, 158) were infiltrated with 0.5 mM of Methyl viologen (MV) (Kirchhoff et al, 2004). Uptake was performed by wrapping leaves with laboratory absorbent paper saturated either with MV and immediately incubated in the dark for 1 h. Dark incubation was achieved by wrapping the leaf segment, covered with MV saturated wipes,

with aluminium foil. Distilled water was applied as control to account for any differences that may arise from the infiltration method.

2.12 Chlorophyll determination

Leaf discs were collected with a cork borer of known diameter and were immediately snap frozen in liquid nitrogen. Pigments were extracted by homogenisation in a mortar and pestle with 80% (v/v) acetone and centrifuged at 3000 rpm for 5 minutes to pellet debris. Supernatant absorption was measured at 663nm (A663) and 645nm (A645) using a Cary 50 spectrophotometer. Chlorophyll concentration was estimated using the equation below (Porra et al, 1989).

$$[Chla] = 12.25(A_{663.6}) - 2.55(A_{646.6})$$

$$[Chlb] = 20.31(A_{646.6}) - 4.91(A_{663.6})$$

$$TotalChlorophyll = 17.76(A_{646.6}) - 7.34(A_{663.6})$$

$$Chla : b = \frac{chla}{chlb}$$

2.13 Preparation of rice thylakoid (unstacked)

Thylakoid preparation was the same as in Hubbart et al (2012). Solutions, reagents and materials were kept on ice during extraction process and centrifugations carried out at 4°C. Leaves were harvested fresh, cut and homogenised with 300ml 'slushy' grinding medium (0.33 M sorbitol, 10mM Na4P2O7.10H2O, 2mM D-iso Ascorbate, pH 6.5) in a domestic food blender. The homogenate was filtered through 4 layers of muslin and then through 8 layers of muslin sandwiched with a layer of absorbent cotton

wool. The muslin was gently squeezed to aid filtration. The sample was centrifuged at 5010 rpm for 10 minutes. The pellet was gently resuspended in wash medium (0.33M sorbitol, 10mM MES, pH 6.5) and centrifuged for 10minutes at 5010rpm. The resulting pellet was resuspended in 15 ml resuspension medium (0.33M sorbitol, 1mM EDTA, 50mM HEPES, pH 7.6) and osmotically shocked with 25ml break medium (5mM MgCl2, pH 7.6). After 30 seconds, 25ml osmoticum medium (0.66M sorbitol, 40mM MES, pH 6.5) was added to restore osmotic potential and centrifuged at 5010 rpm. Thylakoids were resuspended in particle wash medium (5mM EDTA, pH 6.3) and stored at -80°C.

2.14 Polyacrylamide gel electrophoresis

2.14.1 Denaturing SDS-polyacrylamide gel electrophoresis

The Biorad mini-protean 3 system was used to produce denatured SDS polyacrylamide gels. The resolving gel contained 15% Acrylamide/bis, 1.5M Tris/HCl pH 8.8, 10% SDS, 10% ammonium persulphate, 0.04% TEMED. The stacking gel contained 6% Acrylamide/Bis, 0.1M Tris/HCl pH 8.8, 0.1% SDS, 0.4% ammonium persulphate and 0.16% TEMED. Samples were mixed with loading buffer (0.625M Tris/HCl pH 6.67, 2% w/v SDS, 5% v/v glycerol. 0.001% bromophenol blue) and denatured by heating at 90%C for 20 minutes. Gels were run at 120V for 60 minutes in running buffer (25mM Tris, 142mM Glycine, 0.1% SDS) before silver staining or immunoblotting.

2.14.2 Staining of polyacrylamide gels

Silver staining of gels was carried out to visualise samples of protein at low concentrations. Gels were stained with freshly prepared solutions. Gels

were twice fixed for 15 minutes (40% MeOH, 10% acetic acid) before they were sensitised in a solution containing 0.2% STS and 68g/L Na acetate for 30 minutes. Gels were subject to three washes (5 minutes) with water before they were impregnated with 2.5g/L AgNO3 for another 20 minutes. Following two quick washes in water, the gels were developed for 5-10 minutes (25g/L Na2CO3, 0.4% HCHO, 0.27% STS), depending on protein concentration and stain intensity. After this, the reaction was stopped using 14.6g/L EDTA for 10 minutes, and the gels washed (5 minutes) in multiple changes of dH20 before drying.

2.14.3 Drying polyacrylamide gels

Gels were dried by enveloping in 2 layers of wet cellophane assembled on the gel air drying system frame clamps (Biorad 165-1780). The gel drying frame was placed in the gel air dryer kept warm until the gel was completely dry.

2.14.4 Immunoblot analyses

For immunoblot analysis, proteins were transferred to Bio-Rad immune-blot PVDF membrane (0.2µm) using a Bio-rad mini trans-blot cell with a current of 80°C for 2h in a transfer buffer (10% Tris/glycine buffer (Bio-rad), 20% MeOH and 70% dH_2O). Blot was probed with antibody against pgr5. The pgr5 antibodies were kindly provided by Toshiharu Shikanai (Fukuoka, Japan). The blot was detected with ECL detection kit (Pierce ECL western blot substrate).

2.15 Growth room-gas exchange and chlorophyll fluorescence

Gas exchange and chlorophyll fluorescence (CF) were measured simultaneously with a portable gas exchange fluorescence system, WALZ GFS-3000 (Walz, Effetrich, Germany), operating with a narrow rectangular leaf adapter 3010-1, a flow rate of 800 μmol air s^{-1}, a cuvette temperature of 30°C and relative humidity of 60±5%. Light was provided by a combination of in-built red (640nm) and blue (470nm) LEDs. Actinic light was provided by 90% red LEDs and 10% blue LEDs. Saturating light pulse of 6,000 μmol $m^{-2}s^{-1}$ was provided via the red LEDs. All measurements were made on the youngest fully expanded leaf 7 or 8 on the main tiller.

2.15.1 NPQ induction and relaxation

For NPQ induction and relaxation experiments, leaves were dark adapted in the growth chamber for two hours prior to measurement by wrapping sections of the leaf in low weight, flexible aluminum foil. Plants were then immediately transferred to a lab adjacent to the growth room for measurement of parameters described in section 1.11. Leaves were placed in the chamber and left for five minutes in darkness prior to Fo measurement. Fo level with all PSII reaction centres open was measured by a blue pulse amplitude modulated light, which was sufficiently low (<0.02 μmol m^{-2} s^{-1}) not to induce any significant variable fluorescence. A saturating pulse was applied to determine Fm with all PSII reaction centres closed. At this point the actinic light was turned on. In the light-adapted state Fm' was measured by applying a saturating pulse of 6000 $\mu molm^{-2}$ s^{-1} (0.8s). Fo' was measured by switching off the actinic light for 2s after the saturating pulse and applying far-red light (dark pulse period).

Fluorescence parameters were calculated as described in 1.11.2. Application of a train of saturating pulses every 120s allowed determination of series of Fm' and Fo' from which the time dependent changes of fluorescence yield are determined. Simultaneously, the infrared gas analyser monitored CO_2 and H_2O exchange every 30 s under conditions described in 2.16.

2.15.2 Light and CO_2 response curves

For light response measurements, the following protocol was used. Plants were dark adapted and Fo and Fm were determined as described above. Actinic light of 1000 μmol $m^{-2}s^{-1}$ was switched on for 600s to fully activate carbon metabolism in the leaves before starting series of actinic light from 0 to 2000 μmol $m^{-2}s^{-1}$, waiting for a set time of 180s at each light intensity to allow the rate of photosynthesis to stabilise before measurements were made. Measurements were made between 10am to 3pm.

For CO_2 response measurements, light adapted leaves were exposed to actinic light intensity of 1000 μmol$m^{-2}s^{-1}$ throughout. Leaves were placed in the cuvette for 5 minutes to adapt to cuvette conditions at ambient CO_2 of 400 μmols CO_2 $m^{-2}s^{-1}$ before a step by step decrease of CO_2 concentration first to 20 μmols CO_2 $m^{-2}s^{-1}$ and back up to 1200 μmols CO_2 $m^{-2}s^{-1}$ in order to minimise stomatal responses during measurement. Leaves were exposed to each CO_2 concentration for 3 minutes to allow the rate of photosynthesis to stabilise prior to saturating light application. The experiment was carried out as rapidly as possible to avoid changes in activation state and stomatal opening.

2.16 Growth room - Chlorophyll fluorescence and P700 absorbance change

All measurements were carried out with Dual-PAM-100 measuring system (Walz, Effeltrich, Germany) as described by Pfündel et al (2008). Weak modulated measuring light from a 620nm LED and blue actinic light of 250 µmol $m^{-2}s^{-1}$ from 460nm LED arrays were applied to the upper leaf surface by a DUAL-DR measuring head. Saturating light pulses (SP) of 10,000 µmol $m^{-2}s^{-1}$ intensity from 620nm LED arrays were given simultaneously for duration of 300ms to the upper and lower leaf side by the DUAL-DR and a DUAL-E emitter unit, respectively. Absorbance changes in PSI was measured by sample (830 nm) and reference beams (875 nm), emitted by the DUAL-E unit, which allows us to follow the oxidation or reduction state of PSI reaction centres (Schreiber et al, 1988). The beams pass through the leaf and were received by a photodiode situated in the DUAL-DR measuring head. Both the DUAL-DR and the DUAL E units were brought into line using a leaf holder (DUAL-B, Walz) in which perspex rods guided light between the leaf and measuring units (Pfündel et al, 2008).

2.16.1 NPQ induction

Measurements were carried out using the automated induction and recovery curve program provided by the Dual PAM software (Pfündel et al, 2008; Klughammer & Schreiber, 1994) involving repetitive application of saturation pulses (SP) for assessment of fluorescence and P700 parameters in order to compute the quantum yields of PS I and PS II. Using dark adapted leaves in the presence of a fluorescence measuring light (126 µmol $m^{-2}s^{-1}$), Fo was determined followed immediately by the application of

saturation light pulse to measure the Fm. After a dark period of 1 min, during which leaves were preilluminated with far red light (128 µmol $m^{-2}s^{-1}$), maximum P700 (Pm) signal was determined by application of a second SP to fully oxidize P700. The Pm is considered as analogous to Fm described in section 1.11. Cessation of far-red light and SP ensures full reduction of P700 for minimal P700 (Po) measurement. Actinic light was turned on for 600s during which SP was applied every 30s for fluorescence and P700 analysis to determine maximum fluorescence and P700 in the light (Fm' and Pm', respectively). A dark-period of 1s followed each SP to determine the minimal P700 signal level Po. Chlorophyll fluorescence parameters were calculated as described in section 1.11. Effective quantum yield of PSI [$\phi(I)$] was calculated as [$\phi(I) = (Pm' - P)/Pm$] (Pfündel et al, 2008). The photosynthetic electron transport rates of PSI (ETRI) was calculated as

$J = \phi(I) \times PFDa \times (0.5)$, where PFDa is absorbed light and 0.5 is a factor which accounts for the partitioning of energy between PSI and PSII.

2.17 Crop glasshouse experiments - gas exchange and chlorophyll fluorescence

Gas exchange and chlorophyll fluorescence (CF) measurements were performed simultaneously with infra-red gas analyzer LI-COR 6400XT (LI-COR Lincoln, Nebraska) portable photosystem with a fluorometer attachment (6400-40 LCF) which provided actinic light by means of blue (10%) and red (90%) LEDs. Saturating light pulse of >7,000 $\mu molm^{-2}s^{-1}$ was provided via the red LEDs for a duration of 0.8s. The IRGA operated

using a flow rate of 500 μmol air s^{-1}, ambient relative humidity of 50±5%, cuvette CO_2 set at 400 μmols CO_2 $m^{-2}s^{-1}$ and block temperature of 30°C. All measurements were made on the youngest fully expanded leaf from the main tiller.

2.17.1 NPQ induction experiment

NPQ induction and relaxation kinetics at light intensity of 1500 $\mu molm^{-2}s^{-1}$ was measured on leaves dark adapted for 2hr. Leaves were placed in the chamber and left for eight minutes in darkness before Fo measurement with modulated red light. Fluorescence parameters were determined as described in 2.16.1.

2.17.2 CO_2 response curves

CO_2 response measurements were as described in 2.16.2.

2.18 Crop glasshouse light environment

Photosynthetic active radiation (PAR) was measured using a lightweight, portable Ceptometer (AccuPAR LP-80 Pullman, Washington). A series of 80 individual light sensors are located on a 99cm rod, integrating measurements of PAR across a wide area. A spirit level is attached to the base of the rod to enable levelling. The ceptometer takes an average reading of these 80 light sensors and all measurements were made at midday when solar penetration was at its peak. The ceptometer is levelled above the crop canopy and PAR measurement is taken. Similarly, PAR interception is measured below the canopy by placing the ceptometer below all of the leaves. For a reliable measurement under fluctuating light, since light can be very variable particularly below the canopy, five readings

above and below the canopy at different locations within crop plots were taken. The amount of photosynthetically useful radiation intercepted by the canopy measured as fractional interception is calculated as:

$$f \cong 1 - t$$

Where t is the fraction of incident radiation transmitted by the canopy, calculated as t=T/S. S is the PAR reading from an upward-facing ceptometer above the plant canopy and T is the upward-facing ceptometer below the plant canopy.

Leaf area index (LAI) of plot provides information for assessment of canopy density and biomass based on the above and below-canopy PAR measurements along with other variables. Following Norman (1979), LAI is calculated by:

$$LAI = \frac{\left[\left(1 - \frac{1}{2K}\right) f_b - 1\right] \ln \tau}{A(1 - 0.47 f_b)}$$

where τ is the ratio of below canopy PAR measurements to the above canopy PAR measurements, f_b is the fraction beam of incident PAR, K is the extinction coefficient for the canopy (Campbell 1986) and A = 0.283 + 0.785a - $0.159a^2$ where a is the leaf absorptivity in the PAR band. Calculations were made automatically by the ceptometer.

2.19 Biomass analysis

For the growth room experiment, growth analysis was performed at 74 days after germination. Leaf area was determined with Li-COR (Lincoln, Nebraska) laboratory leaf area meter (LI-3100C). Plants were removed from the container and Leaf and stem fresh weight was analysed by separating from root and weighing each individually. Samples were oven-dried immediately at 80°C for 72hrs to a constant weight for dry weight analysis. Total fresh weight was calculated as the collective sum of leaf and stem fresh weight. Dry weight of leaves and stems were altogether regarded as total dry weight. Other growth indices such as leaf area ratio (LAR) and specific leaf area (SLA) were calculated as described below.

LAR = Total leaf area per plant / Total dry weight per plant (cm^2/g)

SLA = Total leaf area per plant / Total leaf dry weight per plant (cm^2/g)

Tagged plants (see section 2.6) in the crop glasshouse experiment were harvested for growth analysis 92 days after germination and processed as described for the growth room experiment except that roots were not included.

2.20 Sequence alignment and construction of a phylogenetic tree

Sequences of the PGR5 protein from diverse photosynthetic species were searched with Blast programs using databases at the National Centre for Biotechnology Information (NCBI). Sequences were aligned using T-coffee multiple sequence alignment program default settings on EMBL-EBI server.

A phylogenetic tree was generated with MEGA 5.10 using the default settings - Neighbour joining (NJ) method (Saitou and Nei, 1987).

2.21 Statistical analysis

One-way analysis of variance was performed using SigmaPlot version 11.0 (Systat Software Inc.) followed by Bonferroni's *t*-test for *post hoc* test. Differences were considered significant at the $p<0.05$ level.

CHAPTER 3

CHARACTERIZATION OF PGR5 TRANSGENIC PLANTS

CHAPTER 3: CHARACTERIZATION OF PGR5 TRANSGENIC PLANTS

3.1 Introduction

Light energy is essential for photosynthesis. Plants are sedentary in nature and are exposed to changing light intensity & quality which could be harmful. The need for plasticity to efficiently respond to constant environmental fluctuations has led to the development of series of photoprotective mechanisms to regulate photosynthetic light reactions. Light reactions result in photosynthetic electron transport (PET) across thylakoid membrane of the chloroplast. The PET chain operates via two major pathways: the linear electron transport (LET) and cyclic electron transport (CET) pathways Despite CET being discovered over 50 years ago (Arnon et al, 1954), research to improve plant photosynthetic efficiency has focused mainly on LET. Because ATP: NADPH must meet plants metabolic and photoprotective requirements to achieve photosynthetic efficiency, understanding the mechanism of CET, particularly how electron transport between CET and LET is regulated to meet cellular demand is essential.

Recent studies have suggested a role for CET in redox poise within the chloroplast (reviewed in Johnson, 2011). Competition between CET and LET for reduced ferredoxin (Fd) modulates CET: LET, with the relative rates of the two processes being determined by the balance between PSI donor and acceptor redox states (Breyton et al, 2006). Since many studies have reported the occurrence of CET under stress conditions, the exact effect of photoprotection induced as a result of PGR5-dependent CET activity on leaf

photosynthesis in the absence of photoinhibitory stress is yet to be determined. In addition, Munekage et al (2008) suggested that PGR5 deficiency may induce other effects leading to growth reductions which are yet to be clarified.

Whilst mechanism and function of PGR5-dependent CET to adapt the photosynthetic process in response to environmental variations and its impact on photosynthesis remains unclear, our current understanding so far has mainly been in *Arabidopsis thaliana*. The *A. thaliana* phenotype is quite distinct from rice in terms of its slow growth rate, low capacity for NPQ, photosynthesis and environmental light intensity (Bailey et al, 2001) and would therefore not be an ideal model for investigating mechanism of photoprotection in crop productivity.

Taken into account that rice is a resource demanding crop, it can be argued that CET may be functional in rice plants in the absence of stress in order to meet the required ATP: NADPH essential to achieve photosynthetic efficiency. As a step towards understanding the function of PGR5 CET in rice leaf photosynthesis and growth performance under non-photoinhibitory conditions, gas exchange and chlorophyll fluorescence methods were used to assess rate of electron flow, photosynthetic capacity, biomass accumulation in PGR5 RNA interference (RNAi) and overexpression (OE) transgenic rice plants.

3.2 Results

3.3 Screening and selection of transgenic lines

Because of the possibility of segregation, all plants used in this study were screened with the FluorCam imaging system. This system provides a rapid analysis of fluorescence characteristics from which corresponding NPQ levels are computed (see section 2.10). Transgenic rice plants showed wide range of NPQ levels for all plants screened. This can be seen in a box plot showing range of NPQ levels in the different transgenic lines from five independent screens (Figure 3.1A). In the RNAi lines, NPQ levels ranged from 0.3 to 1.5 ($P<0.05$). NPQ levels in the WT ranged from 1.0 to 1.66. OE139 showed NPQ within the range of 1.12 to 1.63, while NPQ level was between 0.62 to 1.93 in OE147.

From NPQ of plants shown in Figure 3.1A, plants were selected for further analysis (Figure 3.1B). Selection was based on most divergent NPQ from the WT. In the case of the RNAi lines, NPQ below 1.0 were selected which constitutes about 50% and 72% of total number of screened plant in RNAi 151 and RNAi 158, respectively. In the OE lines, plants with NPQ above 1.38 (i.e. WT mean NPQ) were selected constituting approximately 50% and 60% of total number of plants screened in OE139 and OE147, respectively. When NPQ of selected plants were solely considered, as shown in Figure 3.1B, RNAi transgenic plants as well as OE147 were significantly different from the WT.

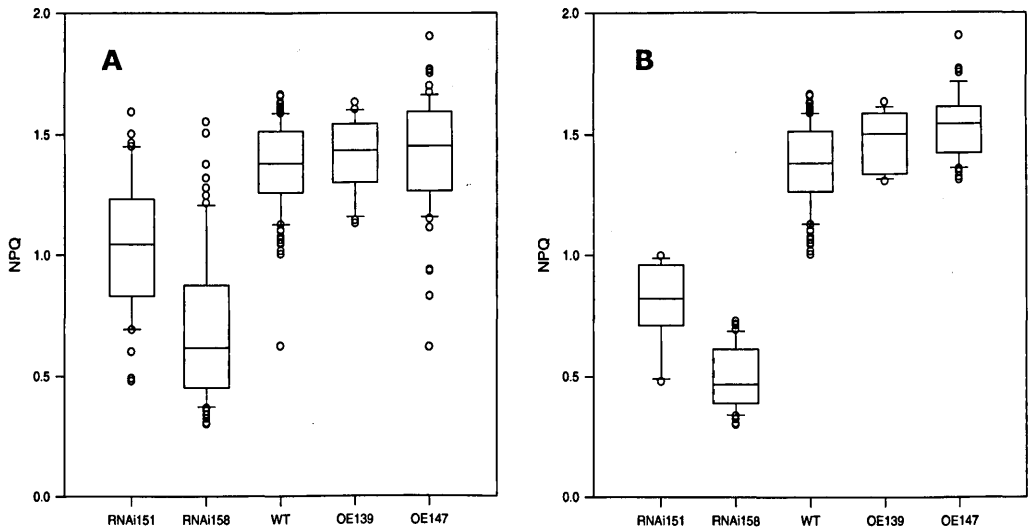

Figure 3. 1 NPQ values for wild type and PGR5 transgenic plants. (A) range of NPQ levels from five independent screens (B) NPQ of selected plants. Excised leaf segments (1cm) were dark adapted and NPQ (average value per segment) was measured after a 15mins illumination in a chlorophyll fluorescence imager as described in section 2.10. NPQ was calculated as (Fm-Fm')/Fm', where Fm is the maximum dark-adapted fluorescence and Fm' is the maximum fluorescence on application of a saturating pulse during actinic illumination. (N=40-100). The box plots summarize the distribution of points for each line. The ends of the box are the 25th and 75th percentiles . The line across the middle of the box is the median value. The lines extending from the ends of the box denote the maximum and minimum values while the circles represent outliers.

3.4 PGR5 homology and content

PGR5 genomic sequence encodes PGR5 protein which consists of 125 amino acids with a predicted molecular mass of 13.2kDa. Blast searches with full-length protein sequence revealed the existence of highly homologous protein sequences in other photosynthetic organisms (Figure 3.2A) including vascular plants, the rose moss (*Portulaca grandiflora*) and green algae (*Volvox carteri* and *Chlamydomonas reinhardtii*).

To further assess relationships between our putative PGR5 protein sequence and other published PGR5 protein sequences, we conducted phylogenetic analyses using the neighbor-joining algorithm (Saitou and Nei, 1987) (Figure 3.2B) based on protein multiple sequence alignments shown in Figure 3.2A, generated using T-coffee (Notredame et al, 2000). The *PGR5* protein showed a high degree of conservation within the monocot group sharing about 75 to 100% amino acid identity. More distantly related *PGR5* proteins were also found including *A. thaliana* as indicated by longer branch length (Figure 3.2B) which confirms the suitability of rice as a model in investigating the influence of photoprotection on crop productivity.

Figure 3.3A shows the western blot analysis of different PGR5 protein levels in the T_2 lines used in this study. Using specific PGR5 antibody, a visual assessment concludes that the protein was completely missing in the RNAi lines while one of the OE lines accumulated more PGR5 than the WT. The SDS PAGE of thylakoid membrane complexes showed that other major thylakoid membrane proteins such as LHCs were not significantly altered (Figure 3.3B).

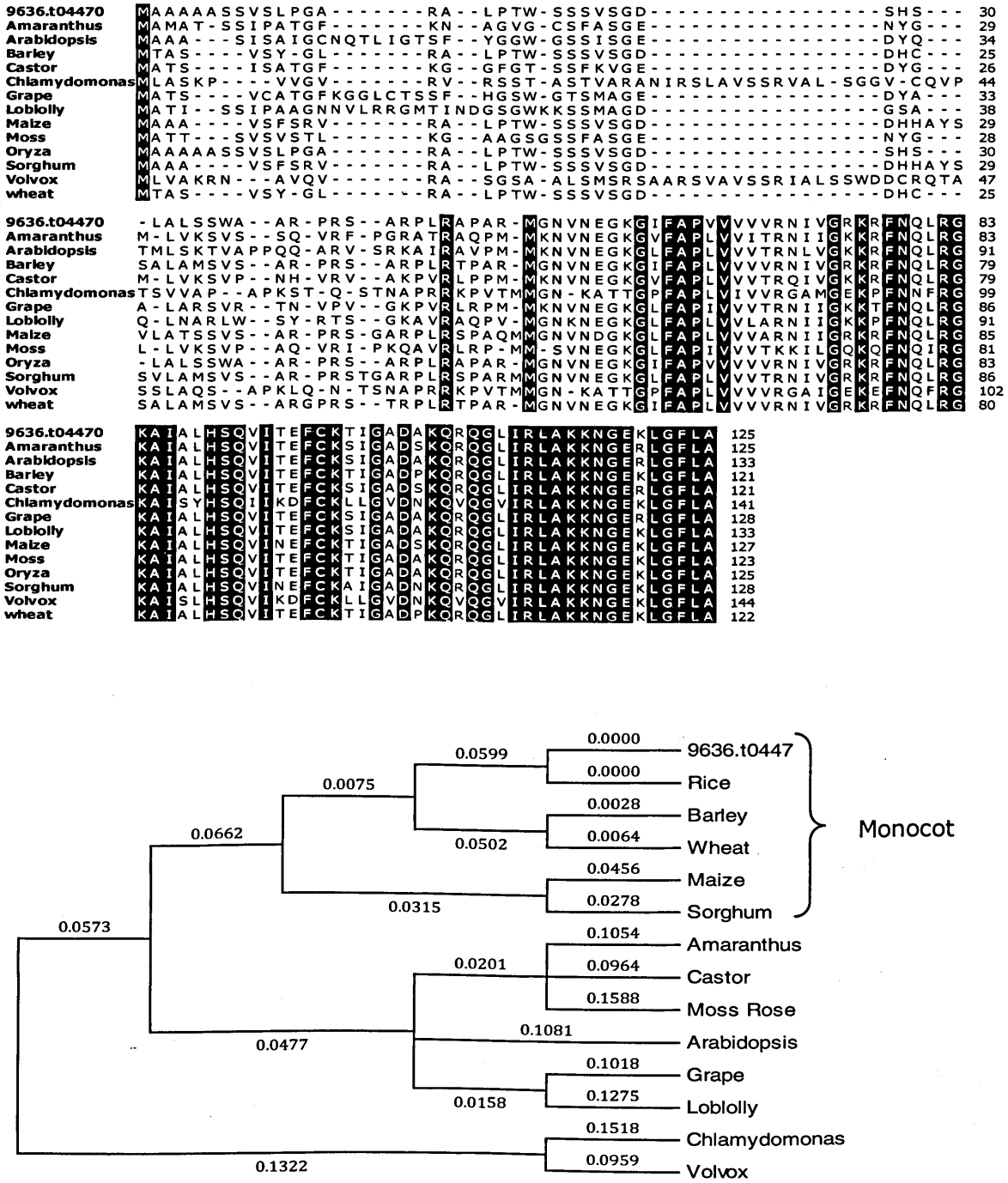

Figure 3. 2 Sequence alignment and phylogenetic tree of the pgr5 proteins in O. sativa, other plants and algal species. The protein sequences of the pgr5 family were obtained from NCBI (http://blast.ncbi.nlm.nih.gov). (A) Pgr5 protein sequences were aligned with T-coffee. Identical residues are shaded in black and similar residues are shaded in grey. Dashes are gaps introduced to maximize the alignment. The figure was generated with Bioedit (Hall, 1999). (B) Phylogenetic tree was generated with MEGA 5.10 (Tamura et al, 2011) using the Neighbor joining (NJ) method (Saitou and Nei, 1987). The branch lengths are proportional to the amount of inferred evolutionary change (Zuckerkandl and Pauling, 1965).

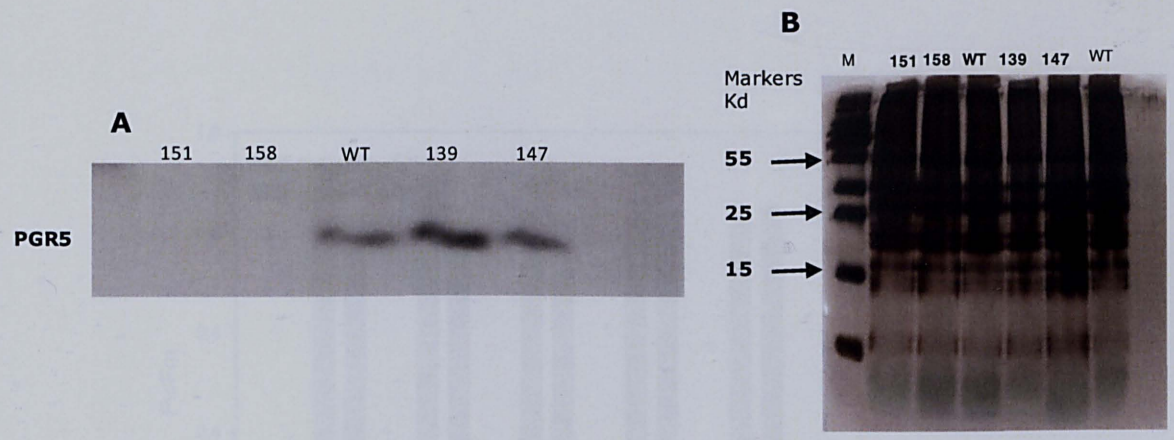

Figure 3. 3 PGR5 protein levels and SDS PAGE in WT and transgenic lines.
(A) Western blot analysis using specific PGR5 antibody. (B) SDS PAGE showing profile of major thylakoid proteins. Lanes were loaded with thylakoid corresponding to 5µg of chlorophyll.

3.4 Growth room acclimation

Plants were grown under light intensities (450 µmols $m^{-2}s^{-1}$ and 700 µmols $m^{-2}s^{-1}$), which in rice were insufficient to saturate the electron transport chain (see Chapter 4). *A. thaliana pgr5* mutants have shown high sensitivity to photoinhibition under strong saturating light (Munekage et al, 2002), while Long et al (2008) observed similar sensitivity in *A. thaliana* over-accumulating PGR5. To determine whether plants were photoinhibited under growth conditions, at the midpoint of the diurnal cycle the maximum quantum yield of PSII (Fv/Fm, ratio of variable to maximum fluorescence in the light) was measured after 20 min in the dark. As clearly shown in Figure 3.4, there was no significant difference between WT and transgenic rice plants grown under the two different light intensities.

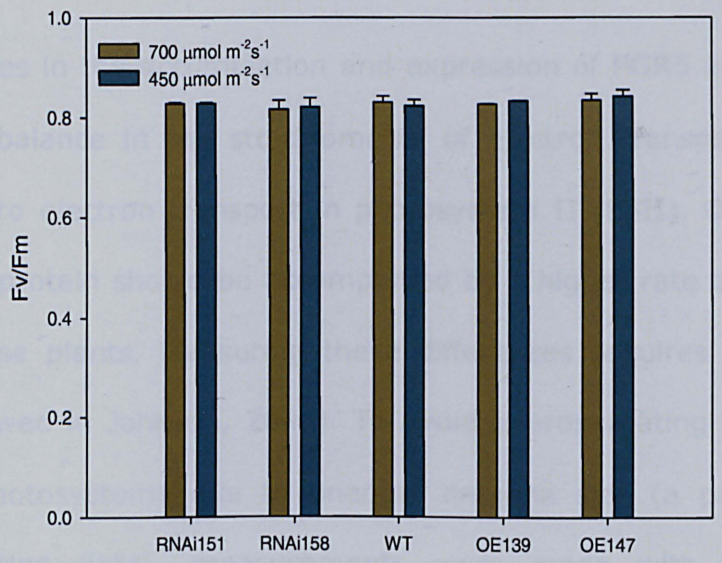

Figure 3. 4 Maximum quantum yield (Fv/Fm) for the WT, OE lines (139, 147) and RNAi lines (151, 158) grown at 450 & 700 µmol $m^{-2}s^{-1}$. Fv/Fm was measured at midpoint of the diurnal cycle in the growth room. Mean values of two independent experiments ± SE (n=8)

3.5 Chlorophyll

Table 3. 1 Total chlorophyll content (µg/cm^2) and chlorophyll (Chl) a/b of WT wild type and PGR5 transgenic plants. Plants were grown at 450 µmols $m^{-2}s^{-1}$. Mean values from one experiment ± SE (n = 4). *P<0.05.

Lines	Total chlorophyll (µg/cm²)	Chlorophyll a/b
RNAi151	44.1688 ± 1.1769*	3.65
RNAi158	36.4326 ± 1.2279*	3.61
WT	46.0083 ± 1.9587	3.51
OE139	39.5695 ± 0.8092*	3.32
OE147	40.4280 ± 1.9902*	3.46

Total chlorophyll content and chlorophyll (Chl) a/b is shown in Table 3.1. Total chlorophyll content was significantly higher in the WT compared with other plants studied. There was no significant difference in Chl a/b of WT and transgenic plants.

3.6 NPQ induction and cyclic electron transport

Changes in the accumulation and expression of PGR5 are expected to cause an imbalance in the stoichiometry of electron transport in photosystem I (PSI) to electron transport in photosystem II (PSII). Overexpression of the PGR5 protein should be accompanied by a higher rate of CET relative to LET in these plants. Measuring these differences requires careful consideration (reviewed in Johnson, 2005). To avoid overestimating the quantum yield of the photosystems due to unequal antenna size (a possibility under non-saturating light), measurements were made with in the presence of saturating actinic light intensity. Actinic light intensity of 1000 µmols $m^{-2}s^{-1}$ has been shown to saturate field grown rice. Therefore, comparing the quantum yield of both photosystems, variations in the ratio of the effective quantum yield of PSII [ϕ(II)] to PSI [ϕ(I)] should give us an indication of the occurrence of CET. We simultaneously measured chlorophyll fluorescence and P700 absorbance by applying actinic light intensity of 1000 µmols $m^{-2}s^{-1}$ to assess electron flow in dark adapted leaves of WT and transgenic plants grown under light intensity of 450 µmols $m^{-2}s^{-1}$. PGR5 dependent CET has been shown to occur under stress conditions such as high light therefore WT and PGR5 transgenic plants were grown under a higher light intensity of 700 µmols $m^{-2}s^{-1}$ (but otherwise identical conditions) to compare their response with those grown under lower light intensity described above. Chlorophyll fluorescence and P700 absorbance changes were measured in the high light grown plants with application of actinic light intensity of 2000 µmols $m^{-2}s^{-1}$ to impose light stress.

Figure 3.5A shows time course of nonphotochemical quenching (NPQ) induction during a 10 min illumination with actinic light intensity of 1000 μmols $m^{-2}s^{-1}$ in the WT and OE lines. A sharp rise in NPQ was observed in the OE lines and WT which relaxed rapidly towards the end of the period of illumination. This coincides with a reported NPQ transient observed in rice within 10 min of induction from dark to light (Hubbart et al, 2012). Within the first few seconds of induction, NPQ in OE139 was rapidly induced ($P<0.05$) compared to the WT. Within 250s of induction in both OE lines, NPQ was about 20% higher ($P<0.05$) than WT. Both RNAi lines showed a low and slower rate of NPQ development throughout the period of illumination. At the end of illumination, NPQ in all lines were almost at the same level (Figure 3.5A). Relaxation of transient NPQ has been attributed to activation of enzymes of Calvin-Benson cycle (Finazzi et al, 2004; Munekage et al, 2002)

Figure 3.5B shows time course of NPQ induction during a 10 min illumination with actinic light intensity of 2000 μmols $m^{-2}s^{-1}$ in the WT and OE lines. The transient was absent at this light intensity in both OE lines and WT. A more rapid rate of NPQ induction was observed in OE line 147 ($P<0.05$) compared to the WT ($P<0.05$). Within 200s of induction when compared to the WT, NPQ was about 30% and 20% higher in OE139 and OE147 respectively. Again, the RNAi lines showed significantly lower NPQ ($P<0.05$) throughout the period of measurement. At the end of illumination, NPQ in OE lines were significantly higher than the WT, possible reasons for this will be highlighted in Chapter 4.

Figure 3.6 shows time course of photochemical quenching (qP) an indicator of the number of open reaction centres capable of receiving light from the antenna. Under growth conditions of 450 µmol m^{-2} s^{-1}, qP in the OE lines was lower than WT (Figure 3.6A), with OE147 showing a more significant reduction ($P<0.05$) which might suggest a down-regulation of PSII activity. This effect is more clearly seen in plants grown under higher light intensity (Figure 3.6B) with the OE lines displaying a significantly lower qP ($P<0.05$) than the WT.

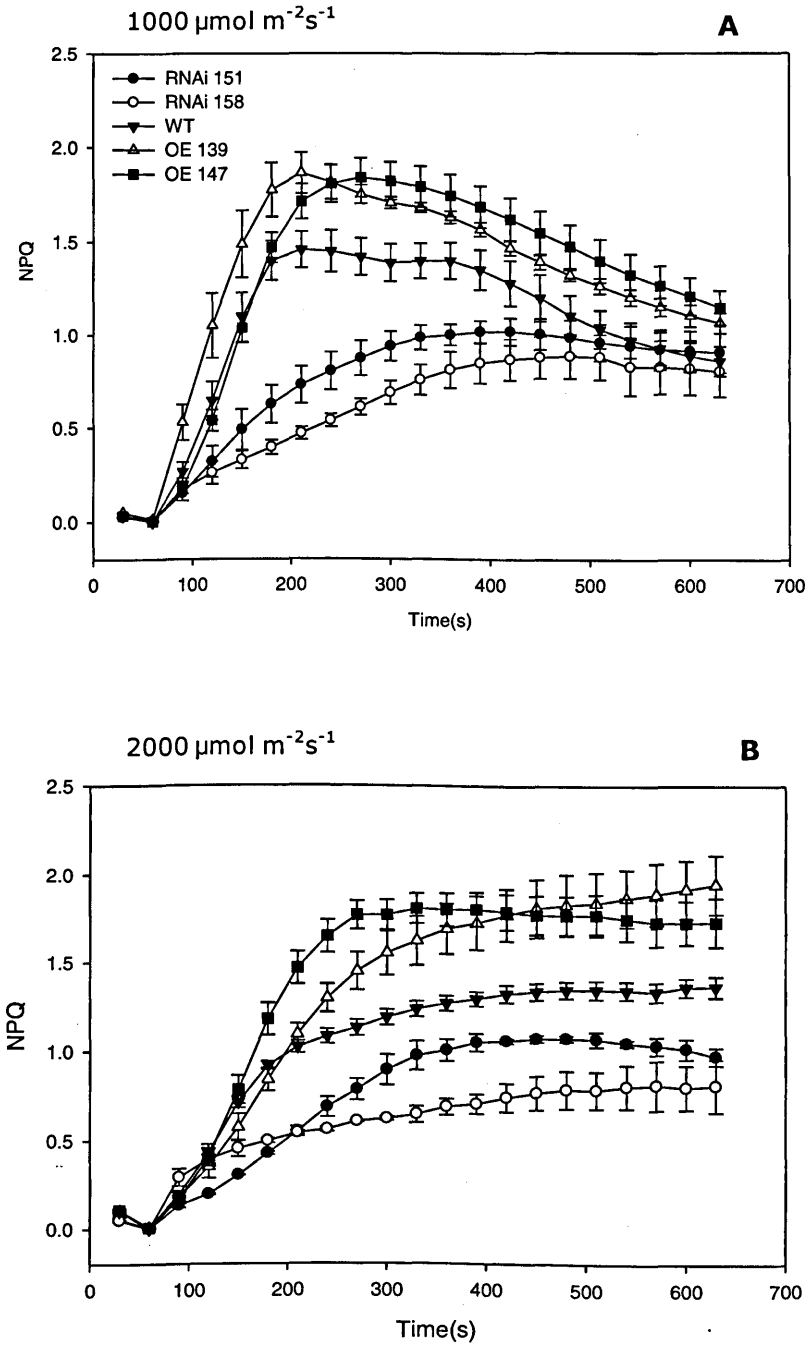

Figure 3. 5 Kinetics of NPQ induction from darkness in wild type (WT), Overexpression (OE) (139, 147) and RNAi interference (RNAi) lines (151, 158). Leaves were dark adapted for 2h before measurement. Mean values of two independent experiments ± SE (n=8) are shown. Actinic intensity is shown on figure. Growth room light intensity, **A** 450 µmol $m^{-2}s^{-1}$, **B** 700 µmol $m^{-2}s^{-1}$.

RNAi plants under the two experimental conditions described in this section displayed significantly lower rate of qP ($P<0.05$) than the WT and OE lines (Figure 3.6). Low qP coupled with low rate of induced NPQ would suggest that the PSII acceptor is reduced (Munekage et al, 2008).

Figure 3.7 shows effective quantum yield of PSI [$\phi(I)$] which gives an indication of electron transport through the photosystem I. In plants grown at 450 µmol m^{-2} s^{-1}, $\phi(I)$ in OE147 was significantly lower than the WT within the first 200s of actinic light application (Figure 3.7A). During this time, its rate of NPQ was comparable to the WT ($P>0.05$) during the same time period (Figure 3.5A). At the end of actinic light application, $\phi(I)$ was not significantly higher in OE lines compared to the WT. In plants grown under higher light intensity (Figure 3.7B), the OE lines showed a significantly higher $\phi(I)$ ($P<0.05$) than the WT. RNAi plants under the two experimental conditions described in this section displayed significantly lower $\phi(I)$ ($P<0.05$) than the WT and OE lines (Figure 3.7) probably due to photoinactivation of PSI (Munekage et al, 2008).

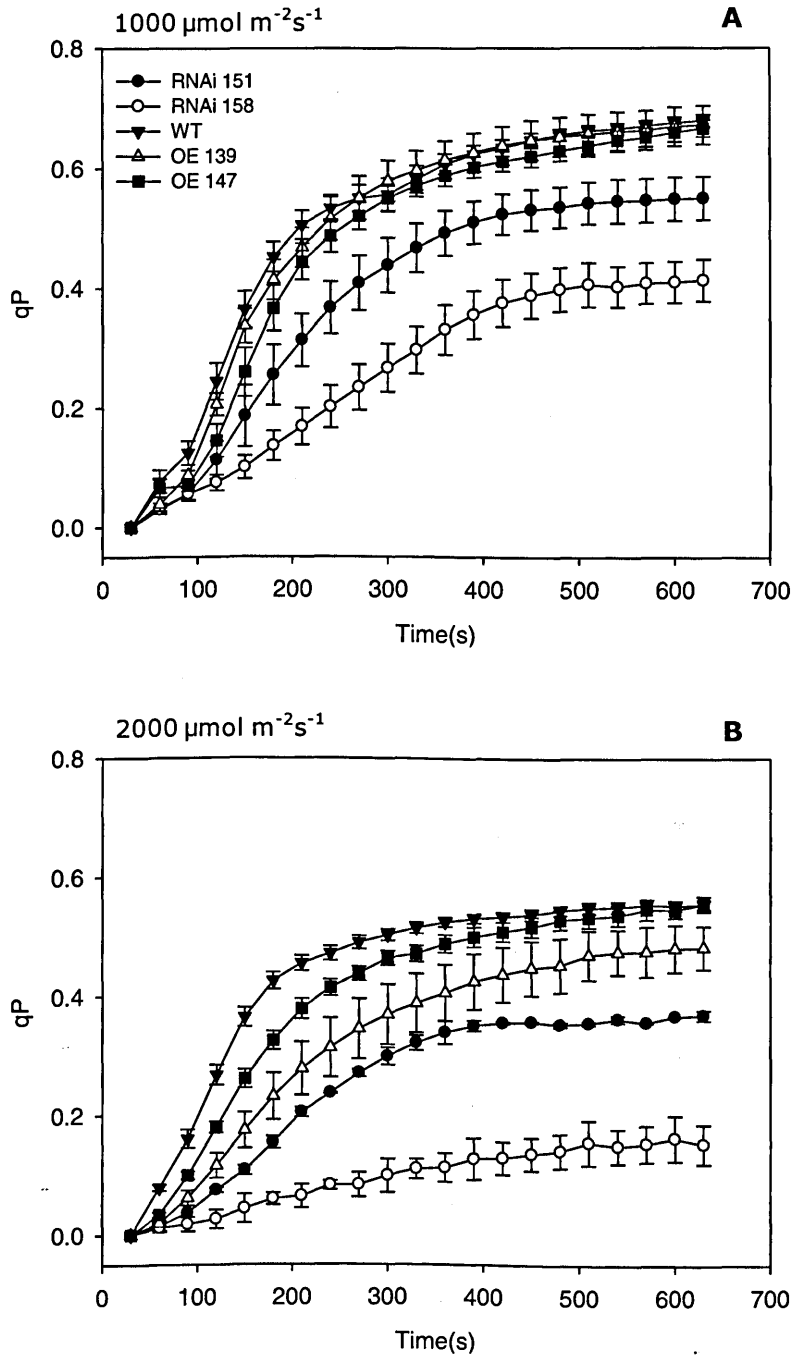

Figure 3. 6 Kinetics of photochemical quenching (qP) in wild type (WT), Overexpressor (OE) (139, 147) and RNAi interference (RNAi) lines (151, 158). Leaves were dark adapted for 2h before measurement. Mean values of two independent experiments ± SE (n=8) are shown. Actinic intensity is shown on figure. Growth room light intensity **A** 450 µmol $m^{-2}s^{-1}$. , **B** 700 µmol $m^{-2}s^{-1}$.

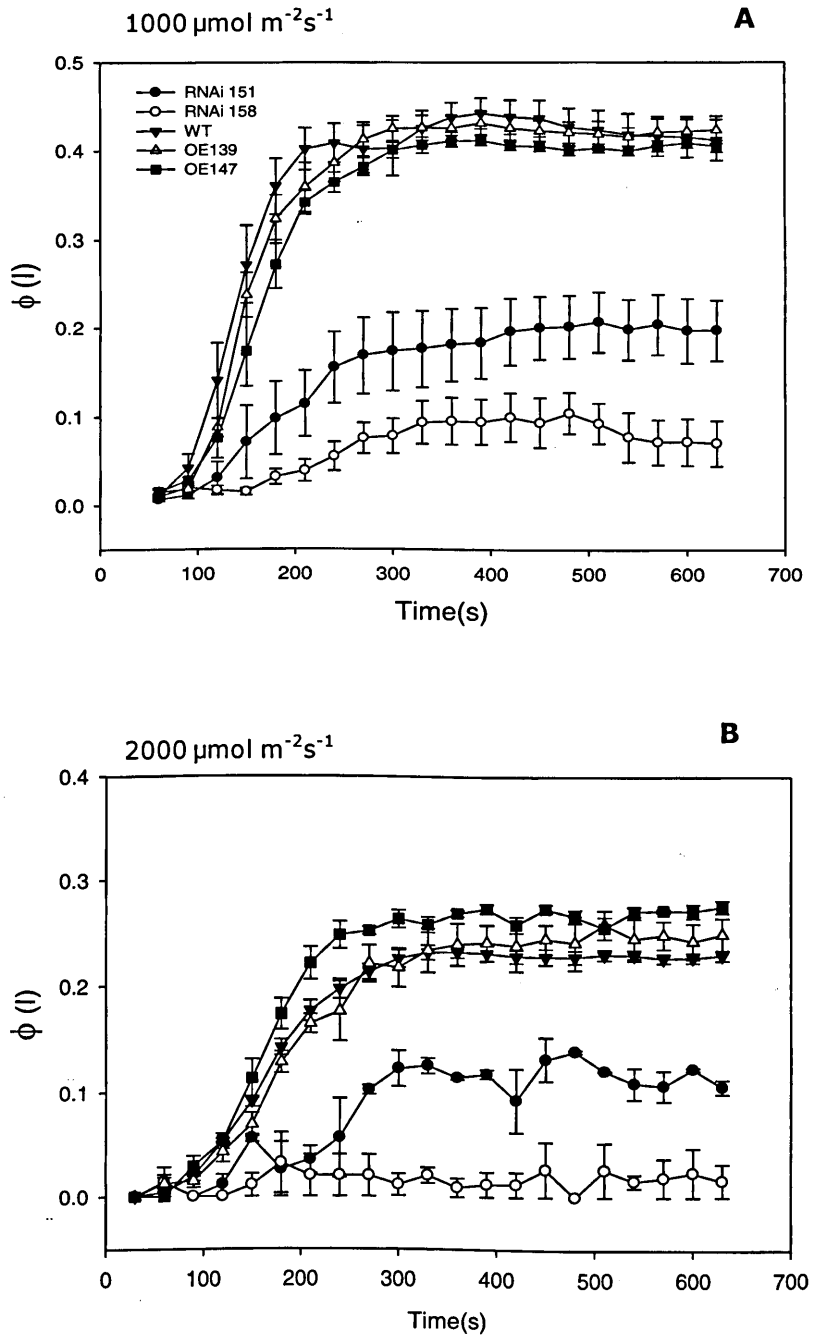

Figure 3. 7 Chlorophyll fluorescence analysis of effective quantum yield of photosystem I [ϕ(I)] in wild type (WT), Overexpressor (OE) (139, 147) and RNAi interference (RNAi) lines (151, 158). Leaves were dark adapted for 2h before measurement. Mean values of two independent experiments ± SE (n=8) are shown. Actinic intensity is shown on figure. Growth room light intensity, A 450 µmol $m^{-2}s^{-1}$ B 700 µmol $m^{-2}s^{-1}$.

Figure 3.8 shows the time course of ratio of quantum yields of Photosystem II to photosystem I [ϕ(II):ϕ(I)] during induction period. If CET is actively occurring, ϕ(II):ϕ(I) in the OE lines should be lower than observed in the WT. For plants grown at 450 µmols $m^{-2}s^{-1}$ and exposed to 1000 µmols $m^{-2}s^{-1}$ OE147 showed a significantly lower ϕ(II):ϕ(I) compared with the WT (Figure 3.8A). In plants grown under high light 700 µmols $m^{-2}s^{-1}$ and exposed to saturating actinic light of 2000 µmols $m^{-2}s^{-1}$, ϕ(II):ϕ(I) was more significantly reduced in the OE lines.

Figure 3.9 shows a strong negative correlation between NPQ and ϕ(II):ϕ(I) in the WT and OE lines, suggesting that ratio of quantum yield of PSII: PSI can give a precise indication of CET occurring under saturating light intensity.

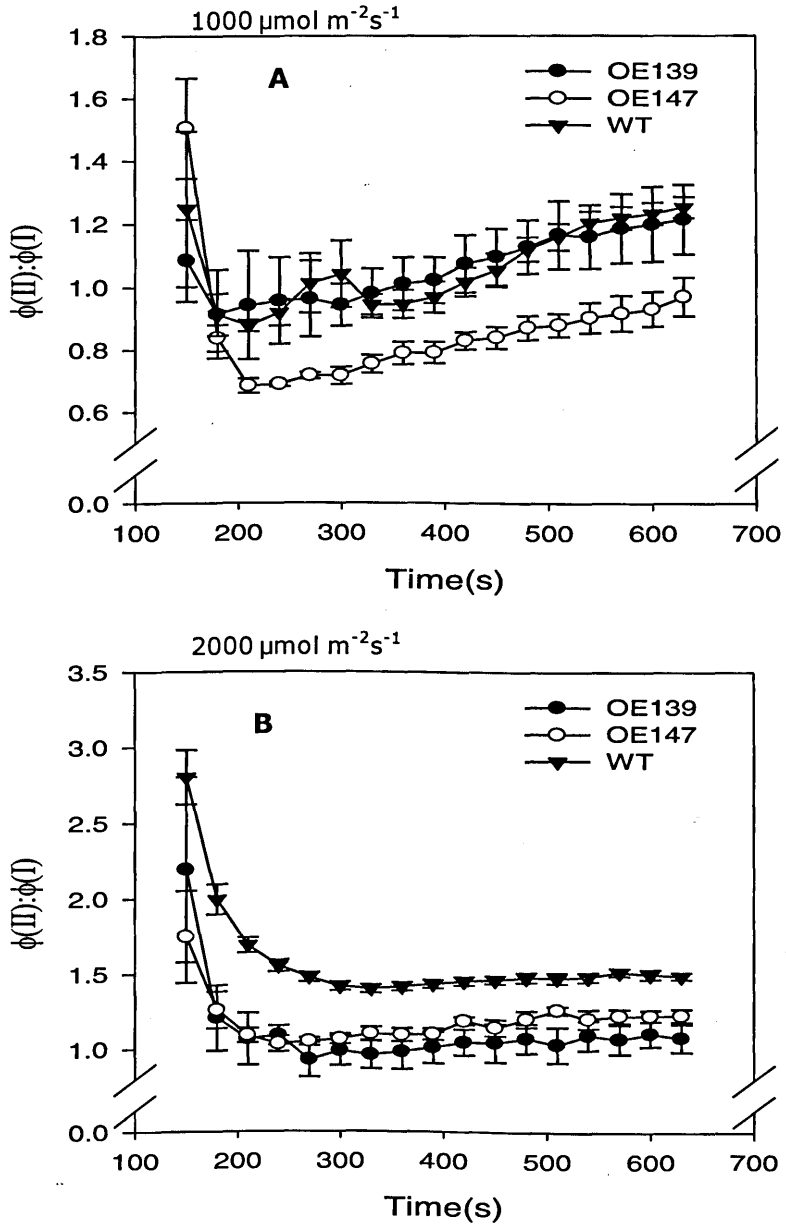

Figure 3. 8 Ratio of quantum yields of Photosystem II to photosystem I [Y(II):Y(I)] in wild type (WT) and Overexpressor (OE) (139, 147). Means ± SE (n = 8). Actinic intensity is shown on figure. Growth room light intensity, **A** 450 µmol $m^{-2}s^{-1}$ **B** 700 µmol $m^{-2}s^{-1}$.

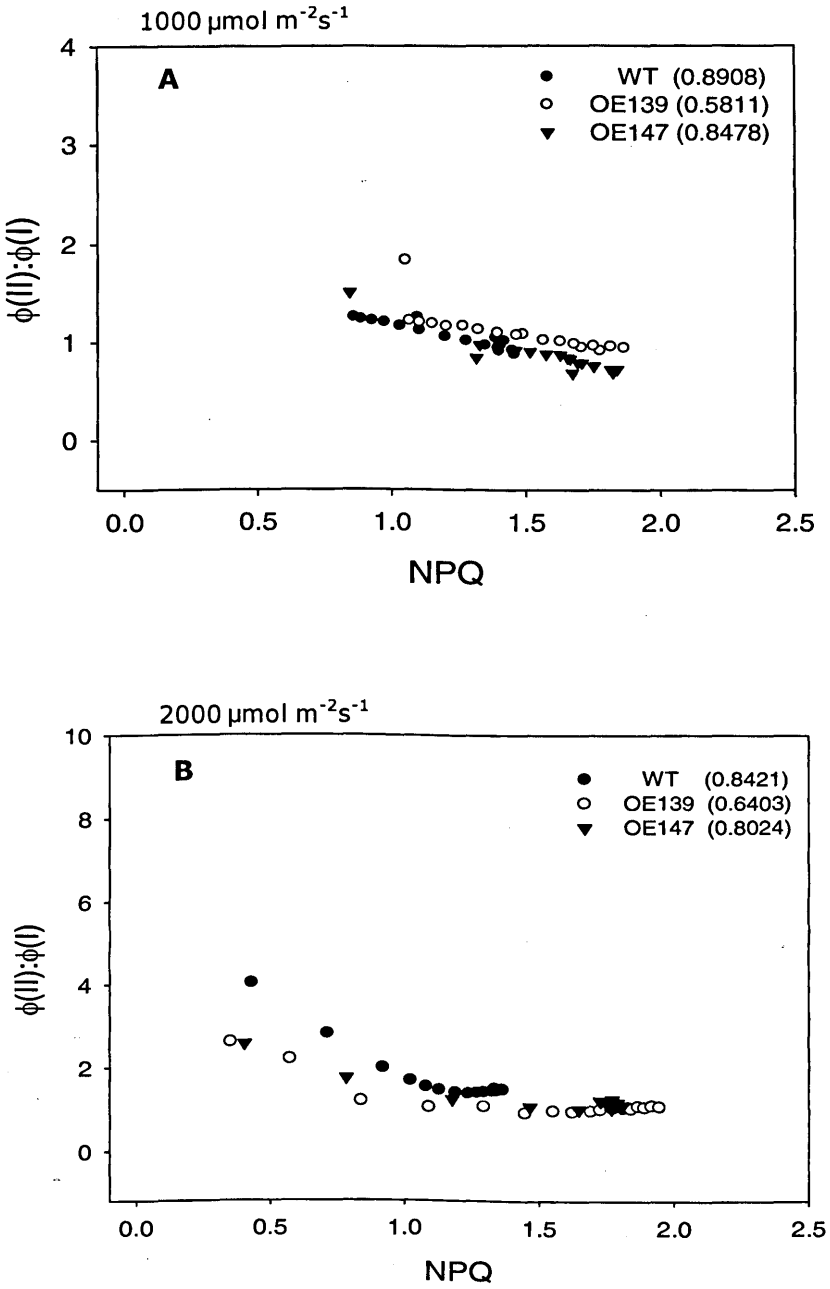

Figure 3. 9 Ratio of quantum yields of Photosystem II to photosystem I [ϕ(II):ϕ(I)] versus Non-photochemical quenching (NPQ). Each point represents single measurement from Figures 3.5 & 3.8. Correlations for wild type (WT), Overexpressor (OE) (139, 147). Actinic intensity is shown on figure. Growth room light intensity A 450 µmol $m^{-2}s^{-1}$ **B** 700 µmol $m^{-2}s^{-1}$.

3.7 PSI acceptor side limitation

Figure 3.10 shows kinetics of NPQ induced in leaves treated with MV. In the RNAi lines NPQ was restored to a level similar to that in the WT and OE lines showing that PSI acceptor chain was not impaired in the RNAi plants but rather observed restrictions in electron transport may be due to limited electron acceptance from PSI attributed to charge recombination of P700 (Munekage et al, 2002).

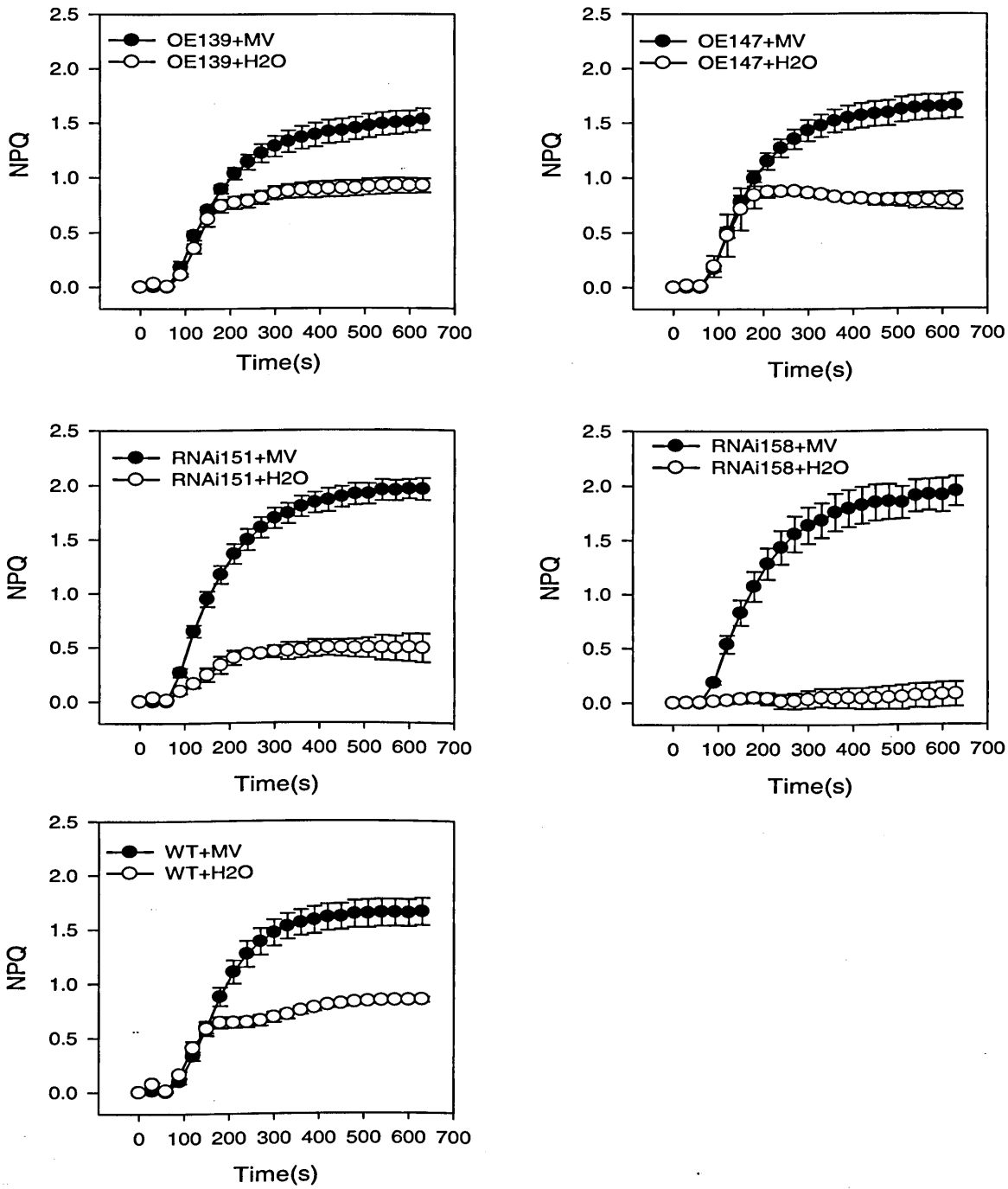

Figure 3. 10 Time course of NPQ induction in the presence of 0.4 mM MV. Uptake was performed by wrapping leaves of wild type (WT), Overexpressor (OE) (139, 147) and RNAi interference (RNAi) lines (151, 158) with laboratory wipes saturated either with distilled water or MV and incubated in the dark for 1h. NPQ was induced by illumination of leaves with actinic light of 1000 µmol m^{-2} s^{-1} for 10 min. Means of one experiment ± SE (n = 7).

3.8 Photosynthesis: dependency on varying CO_2 levels

Dependency of CO_2 assimilation (A) on intercellular leaf CO_2 concentration (Ci) was investigated in the WT and PGR5 transgenic rice grown at 450 µmol $m^{-2}s^{-1}$. Analysis of the assimilation-intercellular CO_2 concentration, Ci (A-Ci curve) at a light intensity of 1000 µmol m^{-2} s^{-1} shown in Figure 3.11A was used to derive information on the maximum rate of carboxylation (Vcmax) by the enzyme ribulose 1,5-bisphosphate carboxylase/oxygenase (Rubisco), maximum rate of electron transport activity (Jmax) and triose phosphate utilization (TPU) (Figure 3.11B) as described by Von Caemmerer & Farquhar (1981).

OE and RNAi rice plants displayed a significant reduction in the maximum rate of carboxylation compared with the WT rice plants ($P<0.05$, Figure 3.11B). Rubisco is a key photosynthetic enzyme involved in catalyzing CO_2 fixation. The decrease in Vcmax could be attributed to several factors such as inhibition in Rubisco activity, reduction in the amount of Rubisco present in the leaf, reduction in Rubisco specificity for CO_2 or an increased affinity of this enzyme for O_2 (Tissue et al, 1999; Cook et al, 1998; Sage et al, 1989). Jordan & Ogren (1984) showed that very minimal variations exist in Rubisco specificity among species. In addition, plants were grown under controlled conditions in this study, thus it's unlikely that Rubisco activity is inhibited by adverse environmental factors (Jordan & Ogren, 1984). However, reductions in the total chlorophyll content observed in the transgenic plants when compared to the WT (Table 3.1) suggest reductions in Rubisco leaf content (Quick et al, 1991).

Jmax was significantly lower ($P<0.05$) in the RNAi lines indicating a lower capacity for electron transport. In the OE lines, Jmax was also lower in OE147 ($P<0.05$) while OE139 showed no significant change ($P>0.05$, Figure 3.11B).

TPU in RNAi 158 were slightly, but significantly, lower ($P<0.05$) than either WT or OE, indicating an inability to increase rate of photosynthesis even in the presence of excess CO_2 (Figure 3.11B)

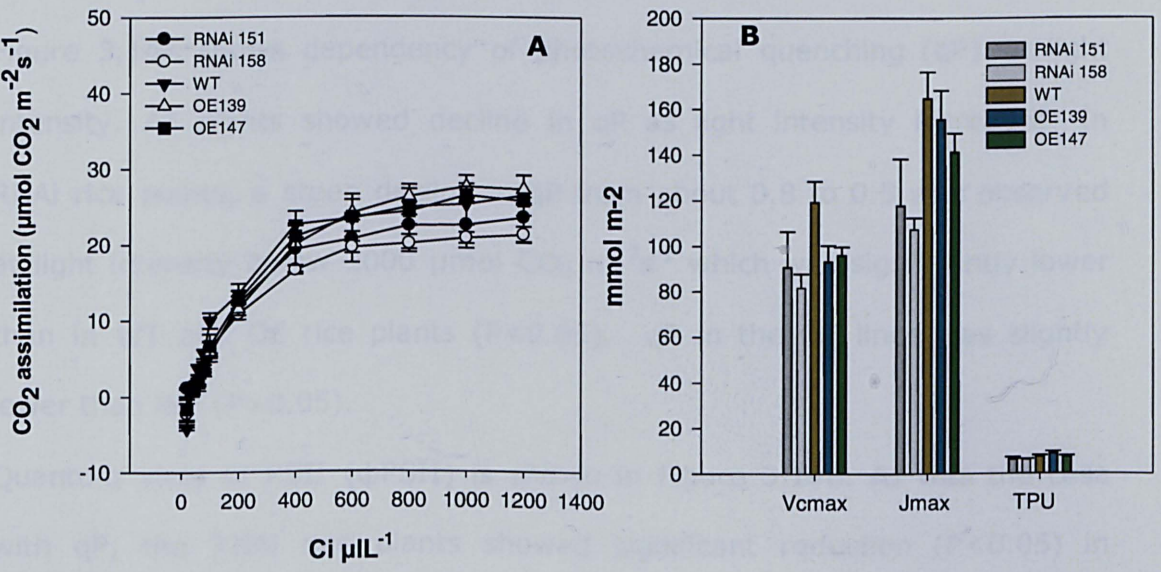

Figure 3. 11 Photosynthetic traits in the wild type (WT), Overexpressor (OE) lines (139, 147) and RNA interference (RNAi) lines (151, 158). (A) Intercellular CO_2 concentration (Ci) response of net CO_2 assimilation (B) Calculated values from A-Ci analysis for the lines studied using the tool in Sharkey et al (2007) to compute values for maximum catalytic activity of Rubisco (Vcmax), maximum electron transport activity (Jmax) and triose phosphate utilization (TPU). Mean values of two independent experiments ± SE (n = 5-6) are shown. $P<0.05$.

3.9 Photosynthesis: dependency on light intensity

In order to investigate the effect of PGR5 on leaf photosynthetic capacity, the dependency of net CO_2 assimilation on light was determined. Figure 3.12 shows the response of WT and transgenic rice plants to changing light intensity. RNAi plants showed significantly lower rates of light-saturated photosynthesis Amax when compared with the WT (13-34%, $P<0.05$) as shown in Figure 3.13. OE147 was also significantly lower (15%, $P<0.05$) than the WT while OE139 was not significantly different. (Figure 3.13).

Figure 3.14A shows dependency of photochemical quenching (qP) on light intensity. All plants showed decline in qP as light intensity increased. In RNAi rice plants, a steep decline in qP from about 0.8 to 0.5 was observed at light intensity below 1000 µmol CO_2 $m^{-2}s^{-1}$ which was significantly lower than in WT and OE rice plants ($P<0.05$). qP in the OE lines was slightly lower than WT ($P>0.05$).

Quantum yield of PSII (ϕPSII) is shown in Figure 3.14B. As was the case with qP, the RNAi rice plants showed significant reduction ($P<0.05$) in ϕPSII compared with WT and OE at all light intensity. Furthermore, the lower capacity for Amax in the RNAi lines further enhances the significantly low ϕPSII and qP, OE147 also displayed lower rate of ϕPSII even at non saturating light intensity below 500 µmol $m^{-2}s^{-1}$.

Figure 3.14C shows stomatal response to increase in light intensity in the WT and transgenic plants. Stomatal conductance in the RNAi 158 was significantly higher $P<0.05$) than the wild type. OE147 had the lowest stomatal conductance ($P>0.05$). Several factors may be responsible for

these variations including changes in stomatal density as well as hormonal control by abscisic acid.

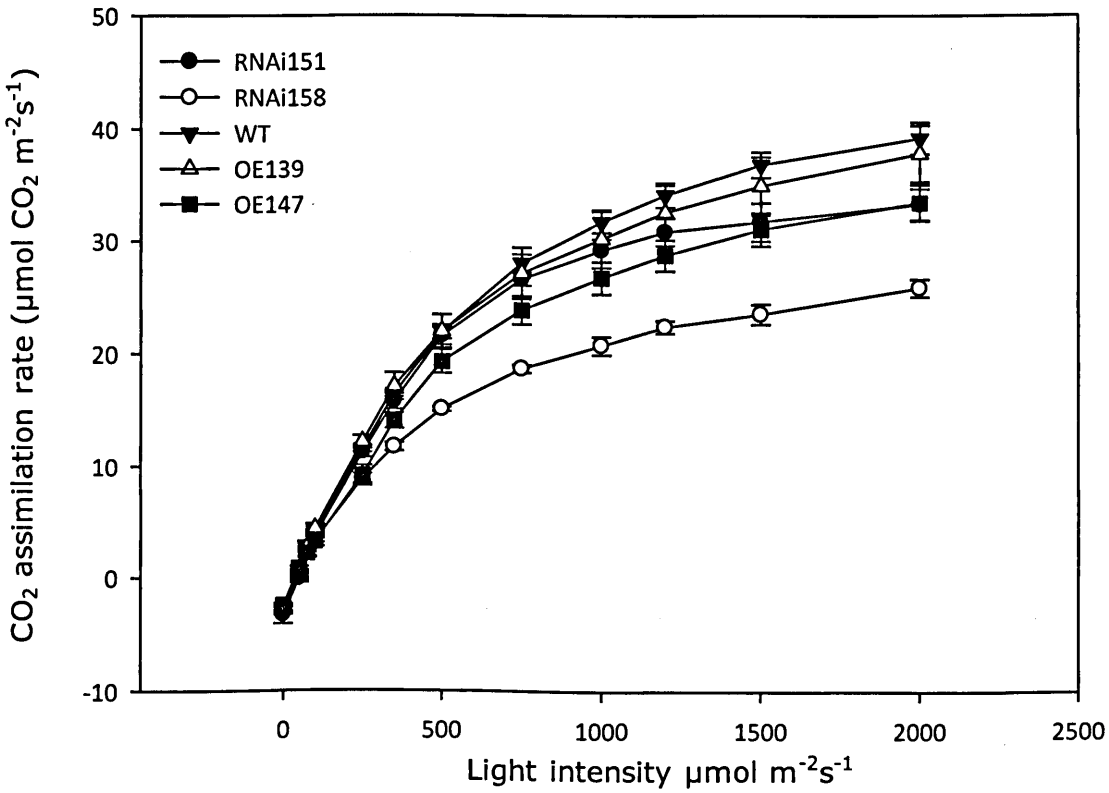

Figure 3. 12 Light-dependent assimilation rate in the wild type (WT), Overexpressor (OE) lines (139, 147) and RNA interference (RNAi) lines (151, 158). Mean values of three independent experiments ± SE (n = 5-9) are shown. $P<0.05$.

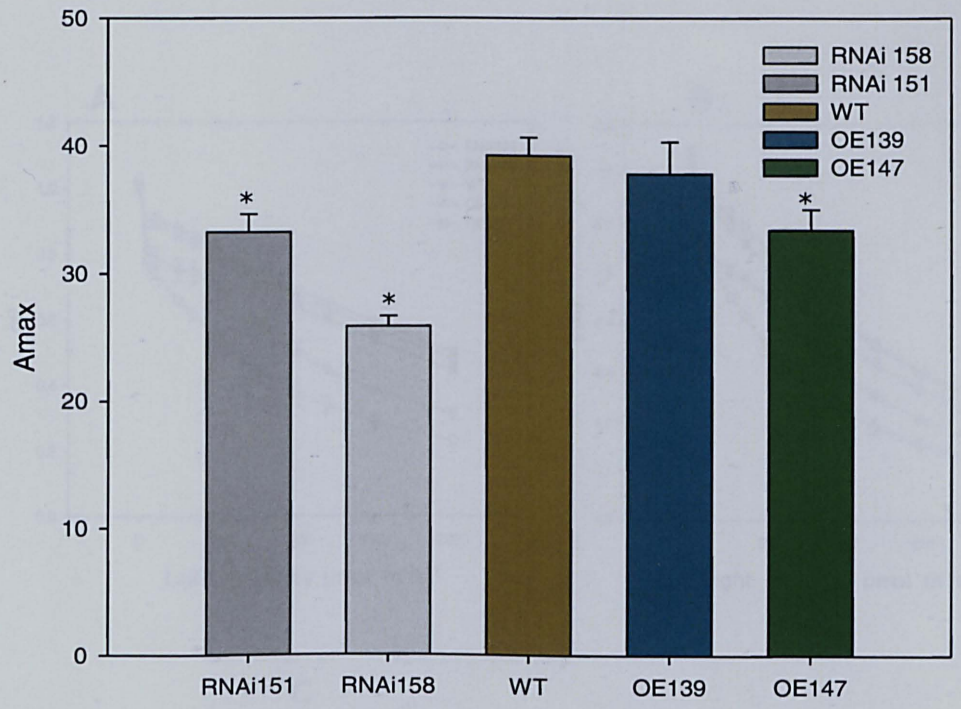

Figure 3. 13 Maximum CO_2 assimilation rate at light intensity of 2000 µmol $m^{-2}s^{-1}$. Mean values of three independent experiments ± SE (n = 5-9) are shown. *P<0.05.

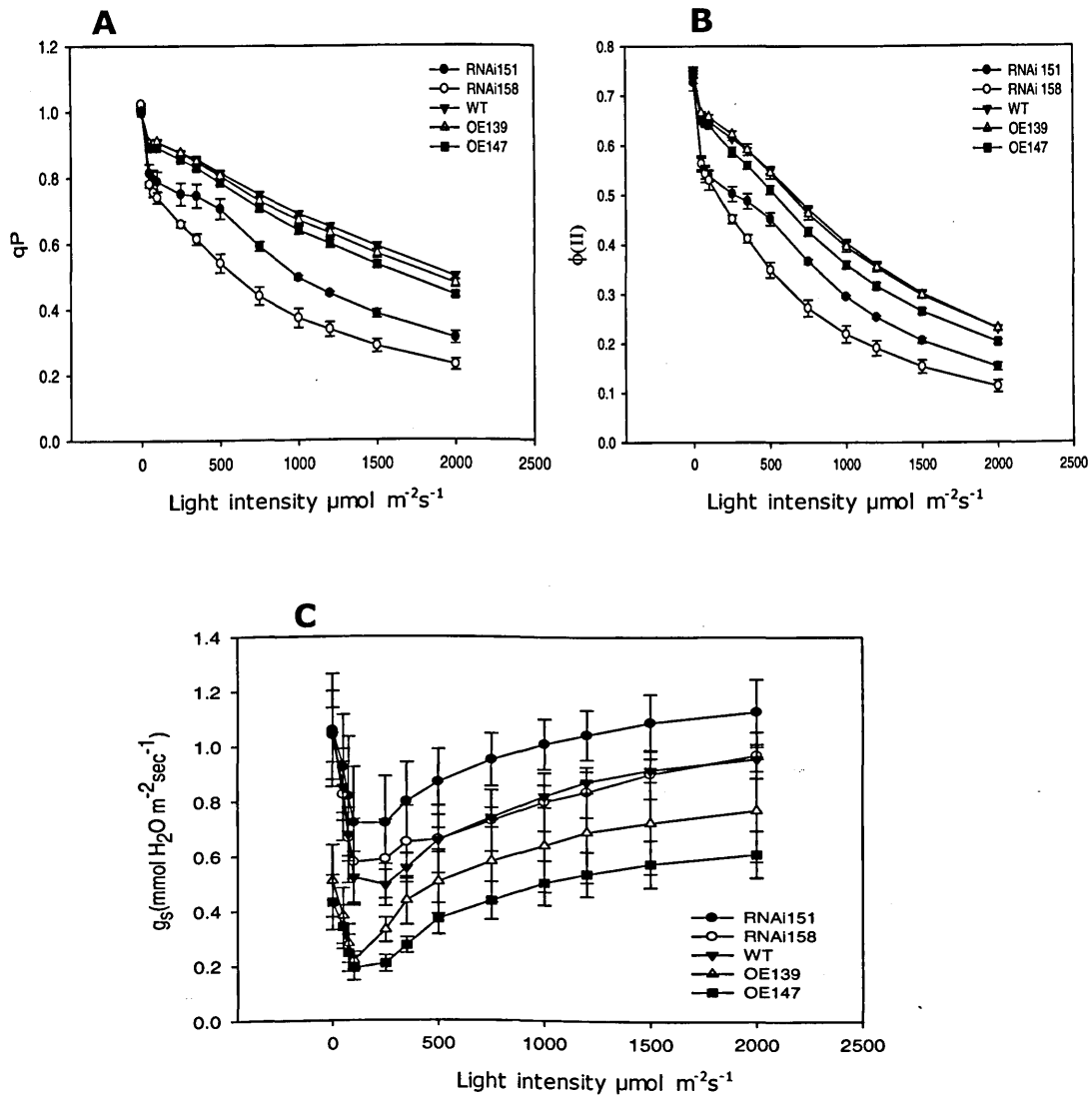

Figure 3. 14 Light intensity dependence of photosynthetic traits in light adapted leaves of the wild type (WT), Overexpressor (OE) lines (139, 147) and RNA interference (RNAi) lines (151, 158). (A) photochemical quenching (qP) (B) quantum yield of PSII [ϕ(II)] (C) stomatal conductance (g_s). Mean values of two independent experiments ± SE (n = 5-9) are shown. $P<0.05$.

Figure 3. 15 A representative picture of the wild type (WT), Overexpression (OE and RNA interference (RNAi) lines grown at 450 µmol $m^{-2}s^{-1}$.

3.10 Growth and biomass

Plant growth analyses were carried out at 77 days after germination in WT and transgenic plants grown at light intensities of 450 and 700 µmol $m^{-2}s^{-1}$. Figure 3.16A shows differences in average number of tillers in the WT and transgenic rice plants. The OE and RNAi lines produced significantly lower number of tillers ($P<0.05$) when compared to the WT at both light intensities. Except in RNAi 158, there was significant increase ($P<0.05$) in

tiller number in all lines studied when grown under high light. The greatest difference was in the WT which increased its tiller number from 9 tillers to 16 tillers under high light intensity. RNAi 158 produced the least number, only two tillers at both light intensities.

Figure 3.16B shows plant height determined by measuring with a ruler from the base of the plant to the tip of the longest leaf on the main tiller. With the exception of RNAi 158, all plants showed significant reduction in height under high light 700 µmol $m^{-2}s^{-1}$ ($P<0.05$). WT and OE139 showed the most increase in plant height ($P<0.05$) of approximately 90cm at this light intensity. At 450 µmol $m^{-2}s^{-1}$, again WT and OE139 where significantly higher than the other lines studied. RNAi 158 did not show any increase in height at both light intensities.

Figure 3.16C shows total leaf area in the WT and transgenic rice plants. At the two light intensities studied, total leaf area in the WT was significantly higher at about 750 cm^2 ($P<0.05$) than in the transgenic plants, with RNAi 158 showing the least total leaf area of 120cm^2. This increase in total leaf area in the WT may be due to increased tiller number.

Figure 3.16D shows variations in leaf width in the WT and transgenic plants grown at light intensities of 450 and 700 µmol $m^{-2}s^{-1}$. Leaf width increased significantly under low light when compared with high light grown plants, atypical shade response. At high light intensity of 700 µmol $m^{-2}s^{-1}$, WT and OE139 showed the widest leaf of about 1.22cm ($P<0.05$) compared with the other transgenic plants. A similar trend was observed in plants grown at lower light intensity of 450 µmol $m^{-2}s^{-1}$.

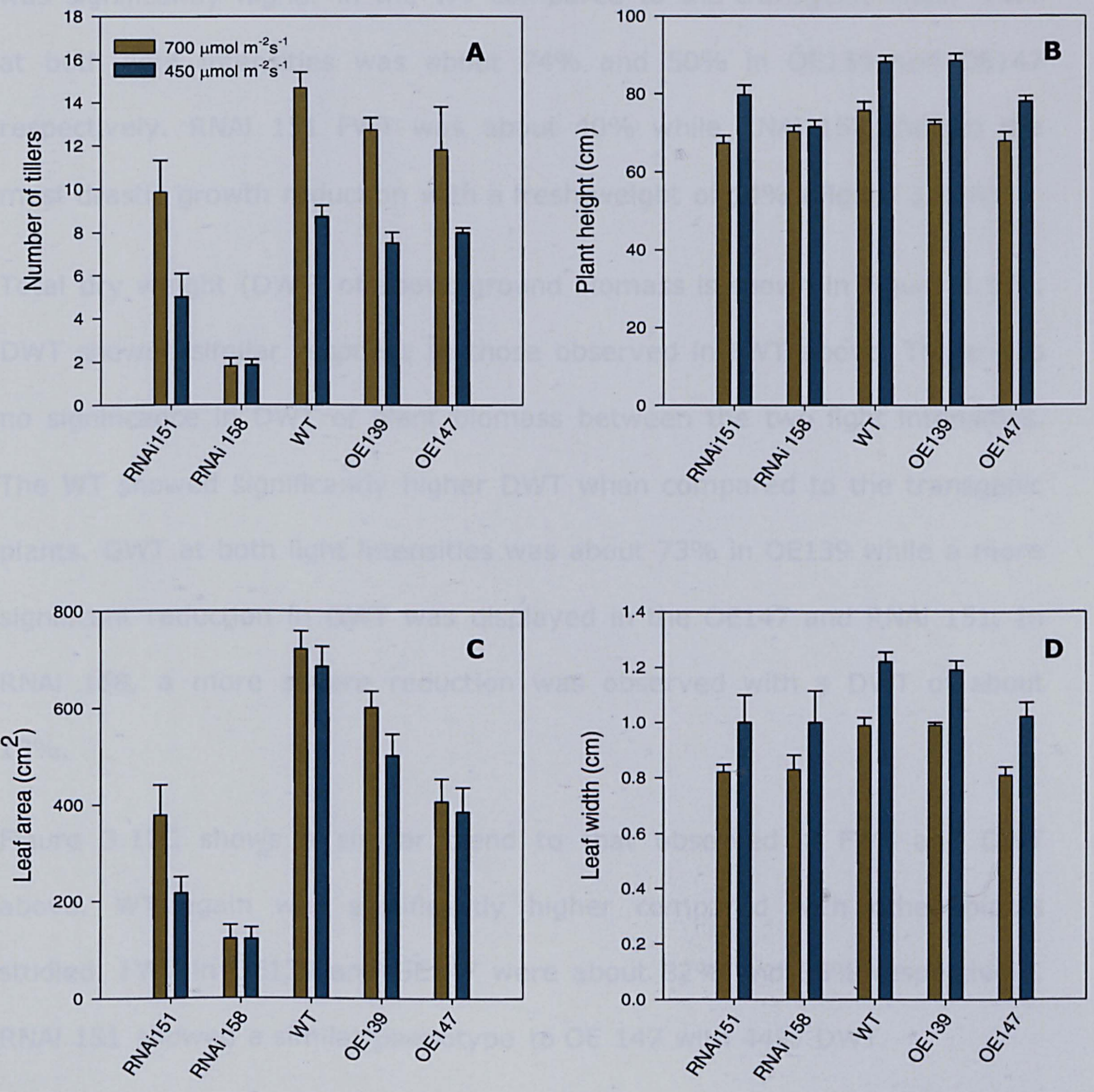

Figure 3. 16 Effect of PGR5-dependent CEF on plant growth parameters. (A) average number of tillers (B) plant height (cm) (C) total leaf area and (D) final leaf width (cm) were analysed in the wild type (WT), Overexpressor (OE) lines (139, 147) and RNA interference (RNAi) lines (151, 158) plants grown at indicated light intensities 77 days after germination. Mean values of two independent experiments ± SE (n = 7) are shown. $P<0.05$.

Figure 3.17 shows some biomass characteristics of WT and PGR5 transgenic rice plants grown under two different light intensities. The total fresh weight (FWT) of above ground biomass which constitutes leaves and stem

was significantly higher in the WT compared to the transgenic lines. FWT at both light intensities was about 74% and 50% in OE139 and OE147 respectively. RNAi 151 FWT was about 40% while RNAi 158 showed the most drastic growth reduction with a fresh weight of 14% (Figure 3.17A).

Total dry weight (DWT) of above ground biomass is shown in Figure 3.17B. DWT showed similar response to those observed in FWT above. There was no significance in DWT of plant biomass between the two light intensities. The WT showed significantly higher DWT when compared to the transgenic plants. DWT at both light intensities was about 73% in OE139 while a more significant reduction in DWT was displayed in the OE147 and RNAi 151. In RNAi 158, a more severe reduction was observed with a DWT of about 13%.

Figure 3.17C shows a similar trend to that observed in FWT and DWT above. WT again was significantly higher compared with other plants studied. FWT in OE139 and OE147 were about 82% and 55% respectively. RNAi 151 showed a similar phenotype to OE 147 with 44% DWT.

Figure 3.17D shows variations in total dry weight (DWT) of roots under light intensities of 450 and 700 µmol $m^{-2}s^{-1}$. A significant increase in root dry weight at light intensity of 700 µmol $m^{-2}s^{-1}$ was observed in all the plants except RNAi 158. Inactivation of PSI has been suggested to be partly responsible for the severe reductions in biomass in pgr5 mutants (Munekage et al, 2008). Results so far suggest a severe reduction in photosynthetic capability of the RNAi attributable to down-regulation of the PGR5 protein.

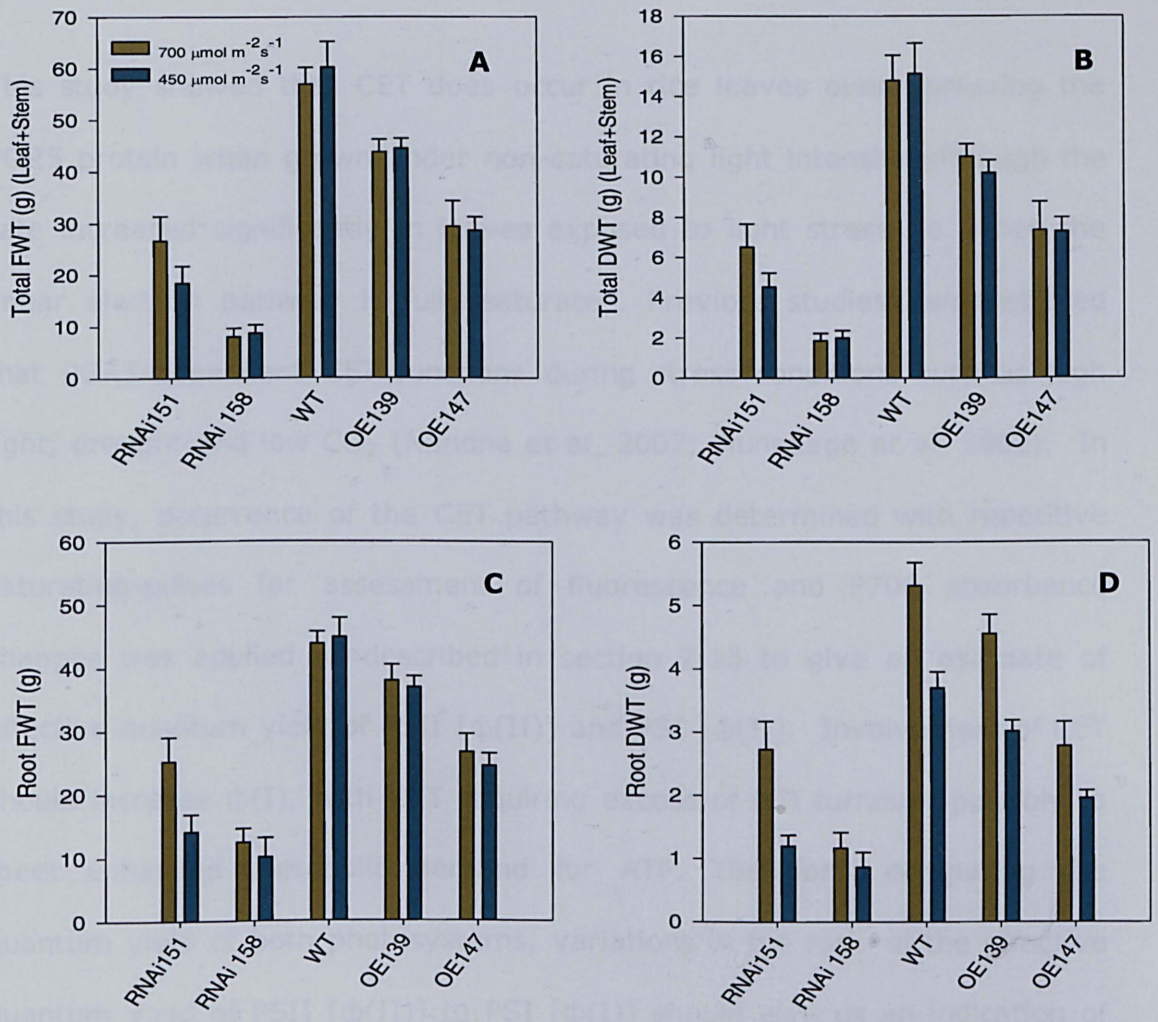

Figure 3. 17 Effect of PGR5-dependent CEF on plant biomass. (A) fresh weight of leaf and stem (g) (B) dry weight of leaf and stem (g) (C) root fresh weight (g) and (D) root dry weight (g) were analysed in the wild type (WT), Overexpressor (OE) lines (139, 147) and RNA interference (RNAi) lines (151, 158) plants grown at indicated light intensities, 77 days after germination. Mean values of two independent experiments ± SE (n = 7) are shown. $P<0.05$.

3.11 Discussion

This study showed that CET does occur in rice leaves overexpressing the PGR5 protein when grown under non-saturating light intensity although the rate increased significantly in leaves exposed to light stress i.e. when the linear electron pathway is fully saturated. Previous studies demonstrated that PGR5-dependent CET functions during stress conditions such as high light, drought and low CO_2 (Nandha et al, 2007; Munekage et al, 2002). In this study, occurrence of the CET pathway was determined with repetitive saturating-pulses for assessment of fluorescence and P700 absorbance changes was applied as described in section 2.16 to give an estimate of effective quantum yield of PSII [ϕ(II)] and PSI [ϕ(I)]. Involvement of CET should increase ϕ(I), with CET requiring excess of PSI turnover possibly to meet enhanced metabolic demand for ATP. Therefore, comparing the quantum yield of both photosystems, variations in the ratio of the effective quantum yield of PSII [ϕ(II)] to PSI [ϕ(I)] should give us an indication of the occurrence of CET. This study showed that PGR5-dependent CET, manifested as the decrease in ϕ(II):ϕ(I) in the OE lines compared to the WT.

A close correlation was observed between ϕ(II):ϕ(I) and NPQ in the WT and OE lines, indicating that PGR5-dependent CET produced a pH gradient across the thylakoid membrane sufficient to drive NPQ (Johnson, 2004). Thus, the size of NPQ induced was dependent on the level of the PGR5 protein, as shown by western blotting, and that PGR5 accumulated in the OE but was absent in the RNAi lines. Since the duration of induction in this experiment was 10 min, the time frame within which transient NPQ is

formed in rice leaves (Hubbart et al, 2012), this result suggests a role for PGR5 dependent CEF during induction of photosynthesis. In addition, the high NPQ sustained throughout the induction period in high light grown plants (Figure 3.5B) may suggest a role for PGR5-dependent CET during steady state photosynthesis, possibly in sustaining NPQ. This will be investigated further in Chapter 4.

The RNAi lines showed significantly low NPQ. However, infiltration with MV, a PSI electron acceptor, restored NPQ to a level similar to that in the WT and OE lines. This observation suggests that PSI acceptor chain was inhibited and not impaired in the RNAi plants in agreement with Munekage el al (2002), which may lead to over reduction of the stroma and photodamage/photoinhibition of PSI (Shikanai, 2007) and subsequently reducing LET (Figure 3.7).

Decrease in the maximum catalytic activity of Rubisco (Vcmax) as well as in the total chlorophyll content suggest lower Rubisco content and/or decreased Rubisco activity in PGR5 overexpression and RNAi rice plants and may partly explain the low rate of PSII electron transport capacity in these plants. It has been reported that Rubisco is capable of limiting photosynthesis (Portis, 1992; Seeman et al, 1988) particularly in rice leaves (Hubbart et al, 2012; Makino et al, 2002). In addition, rate of RUBP regeneration (Jmax) in the OE lines was not different from the WT clearly suggesting that Rubisco-associated limitations significantly influenced rate of CO_2 assimilation in rice plants overexpressing the PGR5 protein. In contrast similar rate of CO_2 assimilation in pgr5 and wildtype A. *thaliana* under conditions where carboxylation efficiency limits net CO_2 assimilation

was reported by Munekage et al (2008). However, significantly low Jmax and CO_2 assimilation in the RNAi lines suggests that limitations associated with Rubisco is not the sole factor limiting photosynthesis but rather limitation partly lies in electron transport as suggested above.

Leaf photosynthesis is important for plant growth and biomass allocation (Stitt & Schultz, 1994). Under non-saturating and saturating light, biomass accumulation in the transgenic lines was consistent with observed rate of CO_2 assimilation. Since CET is an important source of ATP required to maintain proper ATP/NADPH ratio in the chloroplast (Heber, 1992), inhibition of electron transport in the RNAi lines decreases ΔpH and subsequently ATP production required for optimum photosynthesis.

In conclusion, the PGR5 protein plays an essential role in growth and photosynthesis in rice plants in the absence of photoinhibitory stress, potentially limiting growth and photosynthesis by three factors; (i) reduction in Rubisco content and/or decreased Rubisco activity and/or increased rate of Rubisco oxygenation (ii) inhibition of linear electron transport (iii) decreased rate of ATP production limiting optimal rate of photosynthesis.

CHAPTER 4

RESPONSE OF PGR5 TRANSGENIC RICE TO DYNAMIC CONDITIONS

CHAPTER 4: RESPONSE OF PGR5 TRANSGENIC LINES TO DYNAMIC CONDITIONS

4.1 Introduction

Plants do not exist in a static environmental rather they are exposed to rapid and/or irregular changes in light intensity which may be saturating for photosynthesis. This variation may be accompanied by fluctuations in temperature and moisture availability, which predispose plants to stress with impact on metabolic capacity (Demmig-Adams and Adams, 1992). Photosynthetic processes in plants are continuously adjusting photosynthetic capacity to match these complex changes in other to minimise stress/photodamage which may increase/decrease plants fitness. Understanding and exploiting these dynamic changes is crucial in attempts to achieve efficient resource utilization in crops.

The PGR5 protein has been implicated in stress tolerance in several studies. However its regulation and function in photosynthesis is not yet clear. In Chapter 3, photosynthetic responses and growth parameters were characterized in PGR5 RNA interference (RNAi) and overexpression (OE) transgenic rice plants under steady state conditions. In this chapter, responses of PGR5 transgenic lines, grown in low light (450 µmol $m^{-2}s^{-1}$), to dynamic environmental conditions were characterized. Specifically this study aims to determine the role of PGR5 protein in the regulation of rice leaf photosynthesis in RNA interference and over-expression transgenic rice plants under dynamic conditions.

4.2 Results

4.3 NPQ Induction and photosynthesis at ambient CO_2

Figure 4.1 shows the time course of NPQ induction in dark-adapted leaves of WT and transgenic rice using an infra-red gas analyser for simultaneous measurement of CO_2 assimilation and chlorophyll fluorescence. On transition from dark adaptation to actinic light of 500 μmol m^{-2} s^{-1}, in the WT and OE (Figure 4.1A), a large transient was observed within the first 10 min of illumination, a similar timing to that seen in Figure 3.5. This transient was approximately two times higher than NPQ level at steady state following 30 min of illumination. Similar types of NPQ transient has been reported recently in leaves of rice overexpressing PsbS protein when grown at light intensity of 600 μmol m^{-2} s^{-1} (Hubbart et al, 2012) and at very low PAR levels (less than 50 μmol m^{-2} s^{-1}) in both WT *Arabidopsis thaliana* and *A. thaliana* overexpressing the PGR5 protein, although it was enhanced in the overexpressor (Okegawa et al, 2007). The transient was completely absent in RNAi of either rice or *A. thaliana*. The appearance of transient NPQ can be explained by the rapid generation of transthylakoid pH gradient (ΔpH) upon sudden dark to light transition, probably related to a restriction of the electron transport chain, and its subsequent breakdown as reactions of the Calvin-Benson cycle and other assimilatory processes become fully active (Horton, 1983). Throughout the period of illumination, NPQ level was reduced in the RNAi plants. There was no significant difference in the NPQ at steady state in WT and OE.

To increase degree of saturation of the photosynthetic electron transport chain, a higher light intensity (1000 µmol m^{-2} s^{-1}) was applied to induce NPQ (Figure 4.1B). The induction pattern observed at this light intensity was similar but the differences between plant types were more pronounced than at 500 µmol m^{-2} s^{-1}. Under this condition in the WT, NPQ transient induced during the first 5 min of illumination was ~30% higher than at steady state following 30 min of illumination. Again the transient was completely absent in RNAi and the NPQ level reached at the end of illumination was consistently lower in RNAi. In the OE, NPQ was rapidly induced at onset of illumination but only relaxed very slightly throughout the course of illumination. Consistently high NPQ observed at steady state in OE may be due to high rate of CET activity releasing a higher amount of protons into the thylakoid lumen to generate a ΔpH which may out-compete proton utilization for ATP synthesis thus playing a role in regulating the redox poise of the PET chain during induction of photosynthesis and at steady state (Cardol et al, 2010). Furthermore, the degree of NPQ observed in the lines studied implies that the level of pgr5 protein influences the extent of NPQ expression in rice grown under non-saturating light intensity following transition from dark to light and at steady state.

Figure 4.2 shows the time course of qP. At 500 µmol m^{-2} s^{-1} (Figure 4.2A), qP values of around 0.8 were observed in both WT and OE indicating limited closure of PSII centres and a low degree of saturation of photosynthesis. At 1000 µmol m^{-2} s^{-1}, qP in the OE was lower than WT (Figure 4.2B), which might suggest a relative down-regulation of PSII

activity and closure of more PSII centres. Indeed the ϕPSII (Figures 4.2D) during the initial transient supports the suggestion that PSII is more reduced during this time.

qP was consistently lower in the RNAi compared to the WT and OE ($P<0.05$) throughout the period of illumination (500 µmol m^{-2} s^{-1}). Prior to switching off actinic light, qP in RNAi was about 37% lower respectively than in the WT (Figure 4.2A). At 1000 µmol m^{-2} s^{-1}, qP further decreased by about 40% in the RNAi (Figure 4.2B). As was the case with qP, ϕPSII in the RNAi was significantly lower throughout the period of illumination at both light intensities (Figure 4.2C&D). Furthermore, the lower capacity for Amax in the RNAi lines further enhances the significantly low ϕPSII and qP, Since the RNAi leaves are impaired in the PGR5-dependent cyclic flow, these reductions may be attributed to over-reduction of the chloroplast stroma due to PSI acceptor side limitation (section 3.6).

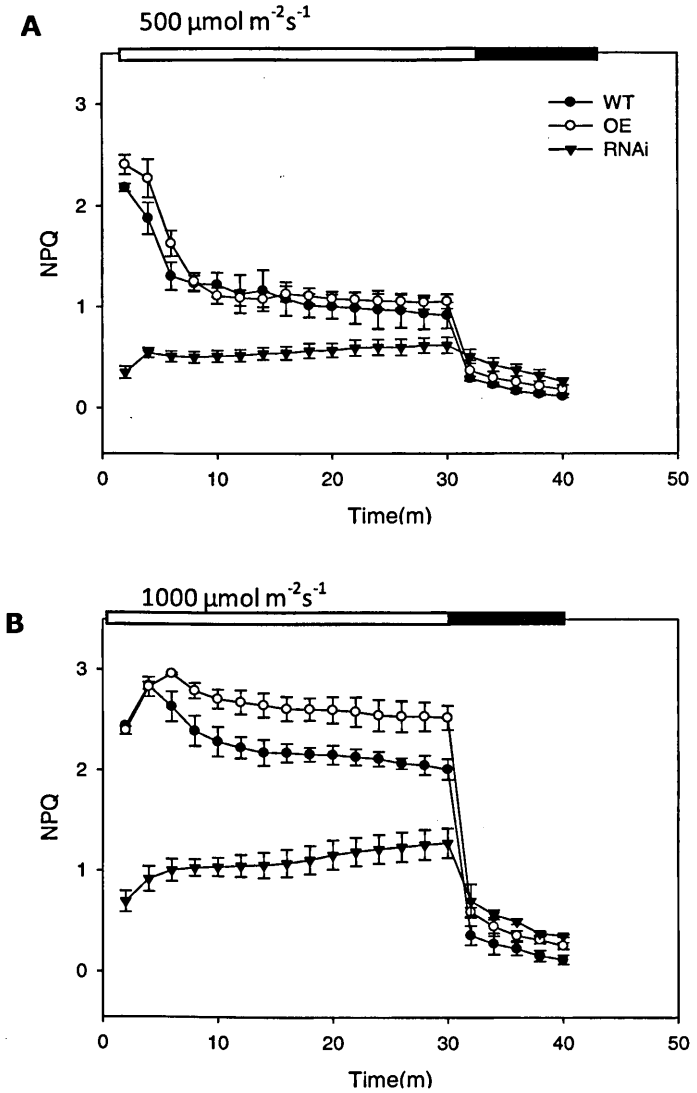

Figure 4. 1 Chlorophyll fluorescence analysis during NPQ induction from dark adaptation in wild type (WT), Overexpression (OE) and RNAi interference (RNAi) lines at a cuvette CO_2 concentration of 400µl L^{-1} and relative humidity of 60%. Actinic intensity is shown on figure. Leaves were dark adapted for 2h. Means ± SE (n = 4).

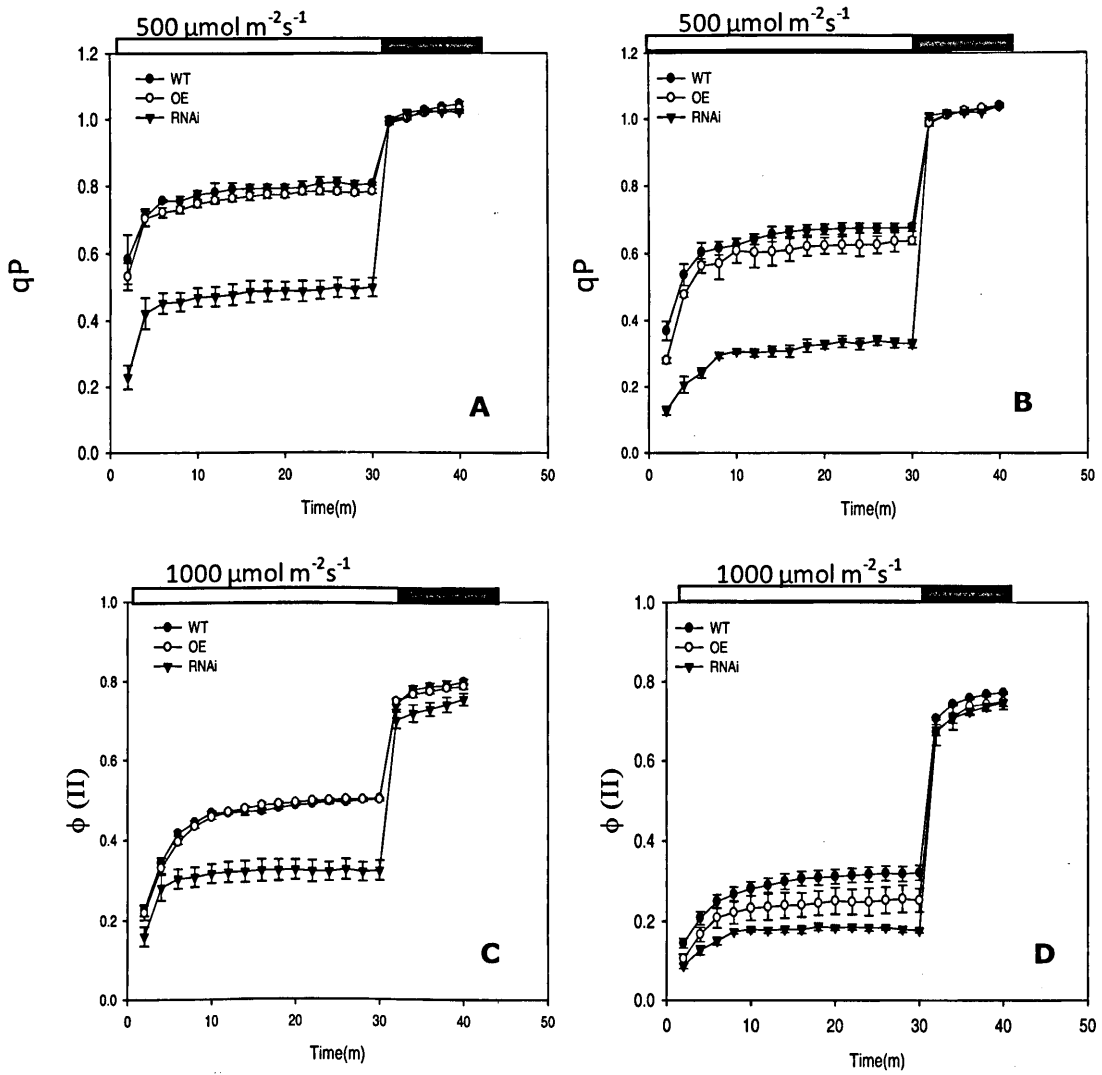

Figure 4. 2 (A&B) photochemical quenching (qP) and (C&D) quantum yield of photosystem II [ϕ(II)] during induction from darkness in wild type (WT), Overexpression (OE) and RNAi interference (RNAi) lines at a cuvette CO_2 concentration of 400µl L^{-1} and relative humidity of 60%. Actinic intensity is shown on figure. Leaves were dark adapted for 2h. Means ± SE (n = 4).

Following the switch off of the actinic light, a slow relaxation of NPQ in the dark was observed in RNAi 158 at light intensities of 500 and 1000 µmol $m^{-2}s^{-1}$ (Figure 4.1). The RNAi showed the slowest rate of relaxation compared to the OE and WT. Figure 4.3 shows the separation of the dark relaxation kinetics from Figure 4.1 into the fast (qE) and slow relaxing (qI) component of NPQ (Section 1.11; Maxwell and Johnson, 2000). qT was not discernable

and was considered to be part of qI. The lowest proportion of NPQ attributed to qI was observed in the WT and OE transgenic plants ranged between 9% -16% at both light intensities suggesting a high proportion of NPQ in these plants were of the qE-type. However about 41% of NPQ in RNAi 158 was attributed to qI, which increased to about 50% at 1000 µmol $m^{-2}s^{-1}$ suggesting that a large part of the quenching may be due to photoinhibition. This is expected since plants deficient in PGR5 protein show increased susceptibility to photoinhibition (Takahashi et al, 2009; Munekage et al, 2004). However it is inconsistent with data showing that growth room plants were not photoinhibited from measurements of Fv/Fm (Figure 3.4).

Figure 4.4 shows CO_2 assimilation rate in the WT and transgenic lines. In the presence of an actinic light intensity of 500 µmols $m-^2s^{-1}$, the rate of CO_2 assimilation in the RNAi was significantly lower ($P<0.05$) than observed in the WT at steady state (Figure 4.4A). With actinic light of 1000 µmols $m-^2s^{-1}$ (Figure 4.4B) , CO_2 assimilation rate was significantly lower ($P<0.05$) than observed in the WT ($P<0.05$) at induction and at steady state in agreement with previous studies (Munekage et al, 2008).

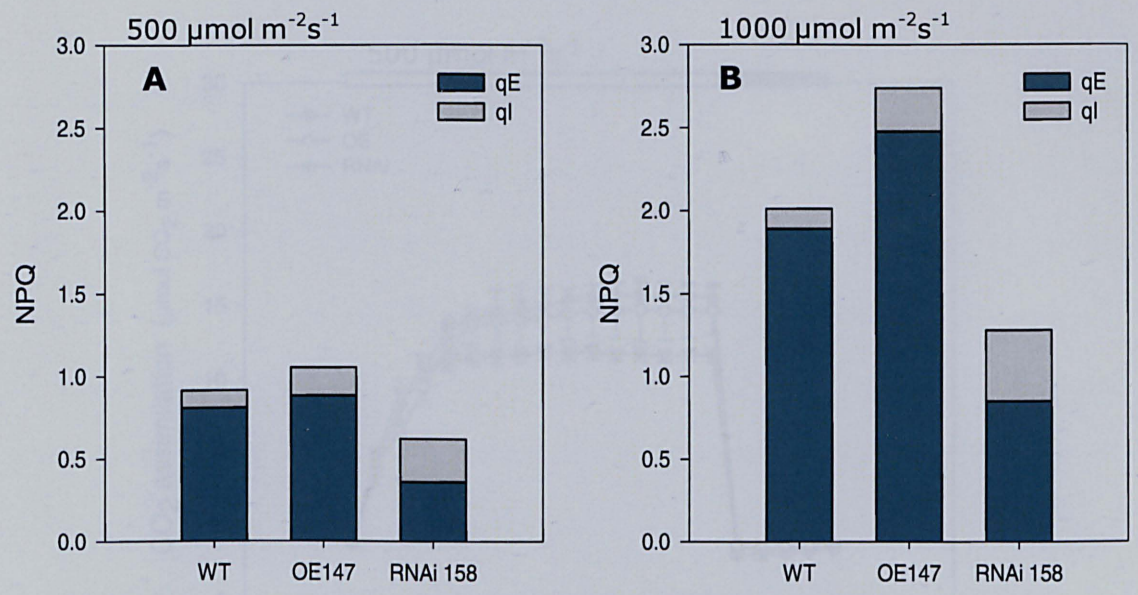

Figure 4. 3 Separation of qE and qI components of non-photochemical quenching (NPQ) in leaves of wild type (WT), Overexpressor (OE) and RNAi interference (RNAi) lines. qE and qI were calculated as described in section 1.11.3. Actinic intensity is shown on figure. Means (n = 4).

In the OE, the large NPQ transient observed within the first 10 min of induction coincided with reduced rate of CO_2 assimilation ($P>0.05$) within the same time period. At steady state under low light, there was no significant difference in the rate of CO_2 assimilation in the OE compared to the WT. However, at steady state under high actinic light intensity, significant reduction in CO_2 assimilation rate coincided with sustained slow-relaxing steady state NPQ (Figure 4.1A). These results suggest that the activity of the PGR5 protein is closely related to changes in the rate of rice leaf photosynthesis at induction and steady state photosynthesis and may play a role in maintaining balance of the redox state of the photosynthetic electron transport chain (PET).

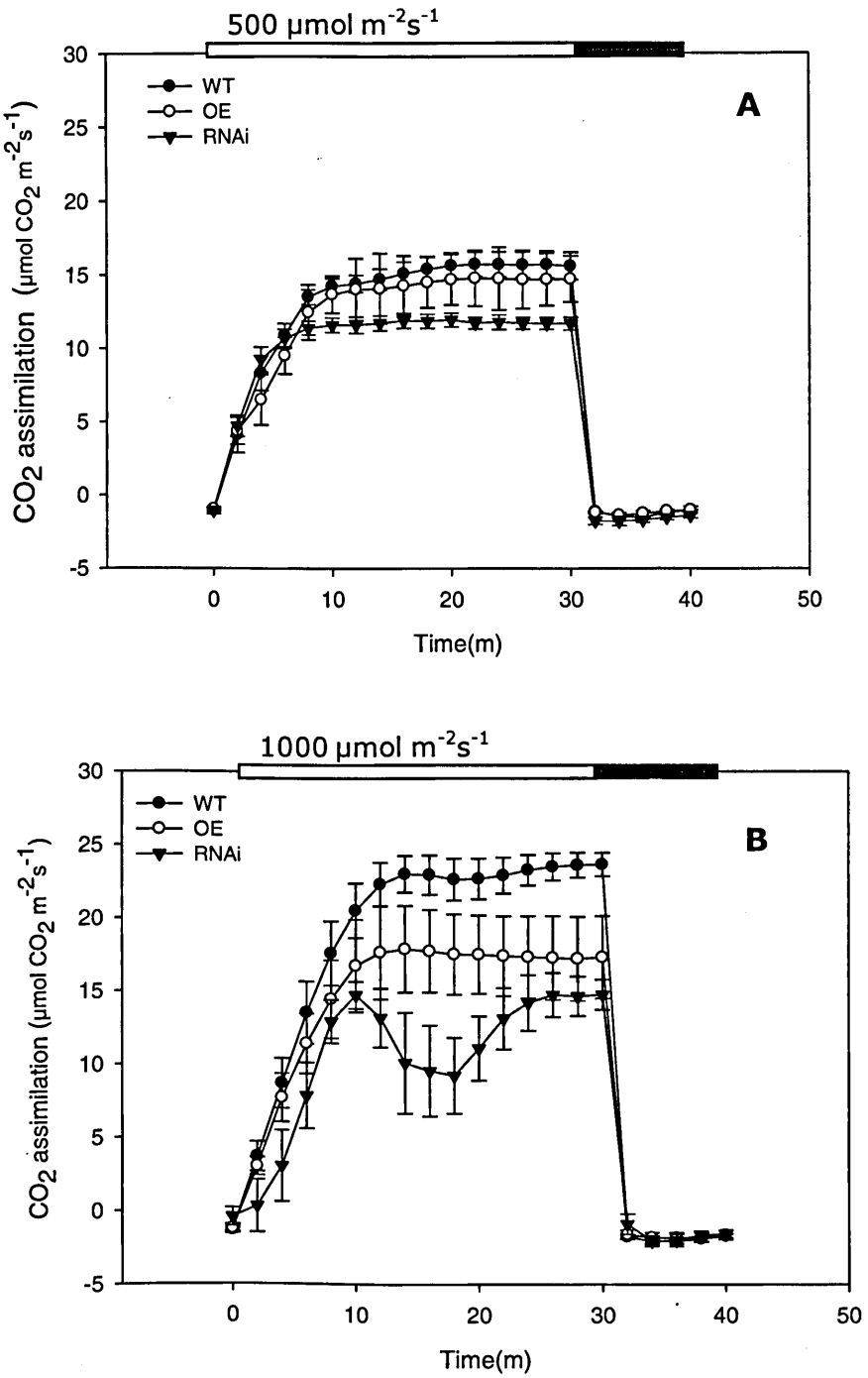

Figure 4. 4 Rate of CO_2 assimilation in wild type (WT), Overexpression (OE) and RNAi interference (RNAi) lines during induction from darkness at a cuvette CO_2 concentration of 400µl L^{-1} and relative humidity of 60%. Leaves were dark adapted for 2h. Actinic intensity is shown on figure. Means ± SE (n = 4).

4.4 NPQ induction and photosynthesis under high CO_2

To further investigate the development of high NPQ during the induction and steady state period of photosynthesis, an experiment was carried out with two cycles of illumination under high CO_2 simultaneously measuring gas exchange and chlorophyll fluorescence. *In vivo* increases in the activity of the enzyme ribulose-1,5-biphosphate carboxylase/oxygenase (Rubisco) after illumination can limit photosynthesis (Portis, 1992; Seeman et al, 1988) particularly in rice leaves (Hubbart et al, 2012; Makino et al, 2002). Thus, if Rubisco limitation is removed thereby increasing rate of CO_2 assimilation and further increasing leaf internal CO_2 concentrations for carboxylation, there should be a greatly reduced difference in the level of NPQ induced between WT and OE.

High CO_2 should reduce stomatal and Rubisco-associated limitations to photosynthesis during the initial phase of induction. To test this, at 1000 µl L^{-1} CO_2, dark adapted leaves were illuminated (1000 µmol m^{-2} s^{-1}) for 20mins to achieve steady state followed by a period of 10 min in the dark. Leaves were then re-illuminated for another 20 min at which point the leaves are "light activated", that is enzymes of Calvin cycle and other assimilatory processes are fully active than during first illumination. Figure 4.5 shows results from this experiment. After induction, WT NPQ did not relax but slightly increased throughout the course of illumination. However a large NPQ transient induced during the first 10 min of illumination in the OE was about 23% higher than peak NPQ in the WT at induction of photosynthesis. On re-illumination there was no difference in the level of induced transient in the WT and OE, which relaxed within 2 min of induction

to a steady state. At the end of 20 min induction (steady state) at first illumination, there was no difference in the level of NPQ in the WT and OE, a condition almost instantaneously reached at onset of second illumination since capacity for CO_2 assimilation may no longer be inhibited by Rubisco. Furthermore, at high CO_2 it is more likely that electron transport capacity will limit photosynthesis, rather than Rubisco and gs. In the RNAi, the transient was completely absent and NPQ was about 38% & 52% lower than the WT and OE respectively.

Photochemical quenching (qP) during the two cycles of illumination under high CO_2 are shown in Figure 4.6A. qP of about 0.6 was observed in the WT and OE. In the RNAi plant however, qP was about 30% lower ($P<0.05$) than the WT or OE at the end of each illumination cycle.

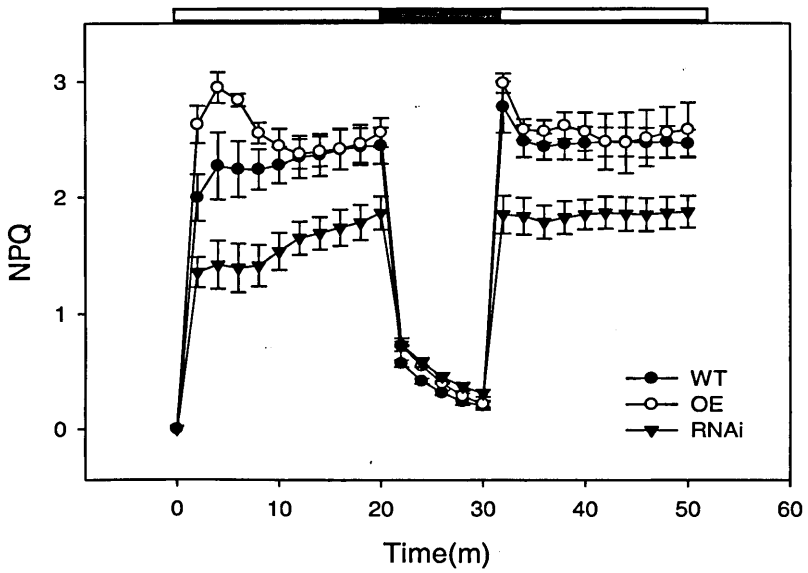

Figure 4. 5 NPQ induction at cuvette CO_2 concentration of 1000 µl L^{-1} during two cycles of 20 min actinic illumination at 1000 µmol m^{-2} s^{-1} and 10 min of dark relaxation in dark-adapted leaves of wild type (WT), Overexpression (OE) and RNAi interference (RNAi) lines. Means ± SE (*n* = 3-6).

In comparison with the WT, a 30% decrease in PSII quantum yield was observed in RNAi ($P<0.05$). Decrease in ϕPSII was diminished in the OE (6%) during induction although clearly not proportional to the size of transient observed (Figure 4.6B). The similarity between ϕPSII in OE and WT suggests some degree of 'photostasis' regulated by the differing NPQ and qP values.

Figure 4.7 shows CO_2 assimilation rate in the WT and transgenic lines. The rate of CO_2 assimilation in the RNAi was significantly lower ($P<0.05$) than that observed in the WT at induction and at steady state (Figure 4.7A) in agreement with previous studies (Munekage et al, 2008). In the OE, the large NPQ transient observed within the first 10 min of induction coincided with reduced rate of CO_2 assimilation ($P<0.05$; Figure 4.7B) within the

same time period due to a higher capacity for CET which relaxes completely as the Calvin-Benson cycle is fully activated. Thus, in the absence of stomatal and Rubisco associated limitations due to high rate of carboxylation, the Calvin-Benson cycle became an adequate sink for reducing equivalents of the PET chain.

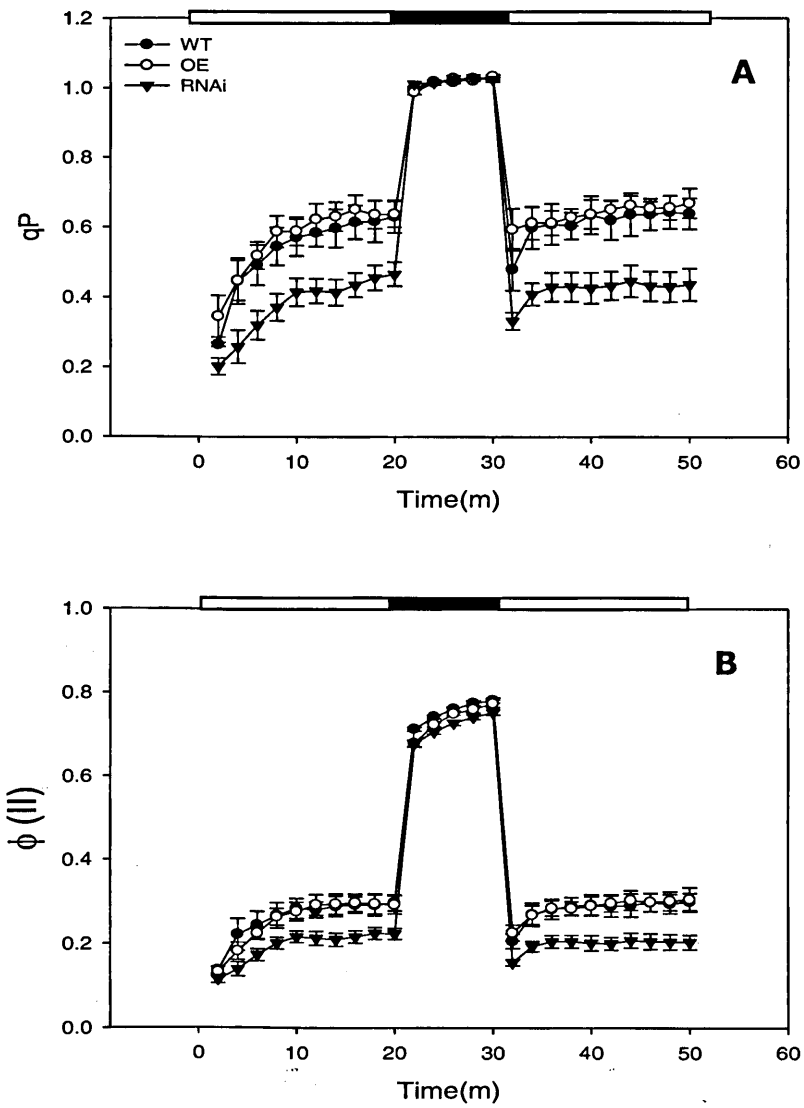

Figure 4. 6 (A) photochemical quenching (qP) (B) quantum yield of PSII [ϕ(II)] at cuvette CO_2 concentration of 1000µl L^{-1} during two cycles of 20 min actinic illumination at 1000 µmol m^{-2} s^{-1} and 10 min of dark relaxation in dark-adapted leaves of wild type (WT), Overexpression (OE) and RNAi interference (RNAi) lines. Means ± SE (n = 3-6).

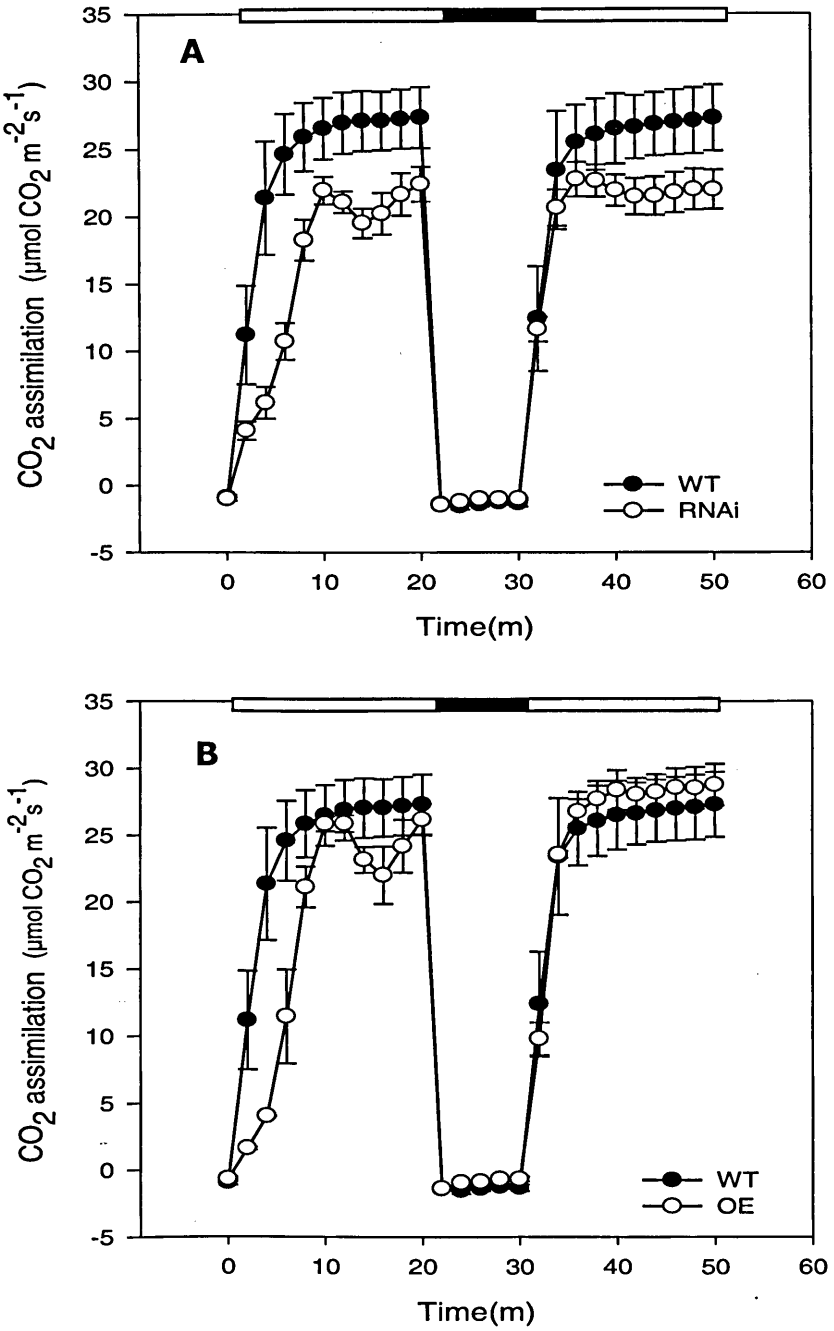

Figure 4. 7 Rate of CO_2 assimilation µmol CO_2 m^{-2} s^{-1} measured simultaneously with chlorophyll fluorescence at cuvette CO_2 concentration of 1000 µl L^{-1} during two cycles of 20 min actinic illumination at 1000 µmol m^{-2} s^{-1} and 10 min of dark relaxation in dark-adapted leaves of wild type (WT), Overexpression (OE) and RNAi interference (RNAi) lines. Means ± SE (n = 3-6).

4.5 NPQ induction and photosynthesis under low atmospheric moisture

Cyclic electron transport activities under stress conditions have been documented (see review Johnson, 2005). Rice is very sensitive to low moisture induced stress conditions (Hirasawa, 1999). Low moisture cause stomatal closure which restricts CO_2 uptake (Ci) by leaves inhibiting water potential for photosynthesis and growth (Flexas et al, 2004, 2006; Makino et al, 1997). A sensitive and most rapid response to stomatal closure in plants involves a significant reduction in rate of photosynthesis due to the low Ci which ultimately may result in photodamage and/or photoinhibition (Jaleel et al, 2009). The ability of a plant to respond rapidly to adverse reductions in rate of leaf photosynthesis by engaging photoprotective mechanisms will be beneficial for increased biomass.

As a quick way of manipulating stomatal conductance to reduce Ci in rice, we investigated the response of PGR5 transgenic plants to a steady decline in moisture level by simultaneous analysis of gas exchange and chlorophyll fluorescence analysis of PSII photochemistry under ambient CO_2 and actinic light intensity of 1000 μmol m^{-2} s^{-1}. From the dark-adapted state, actinic light was applied and steady state achieved (10 min) prior to application of saturating pulses. Saturating pulses were applied at 2 min intervals and during the course of induction while a stepwise decrease in cuvette relative humidity (RH%) was carried out every 10 min (Figure 4.8A). Leaf temperature was maintained between 27-29°C in all lines (Figure 4.8B). Clear phenotypes were observed.

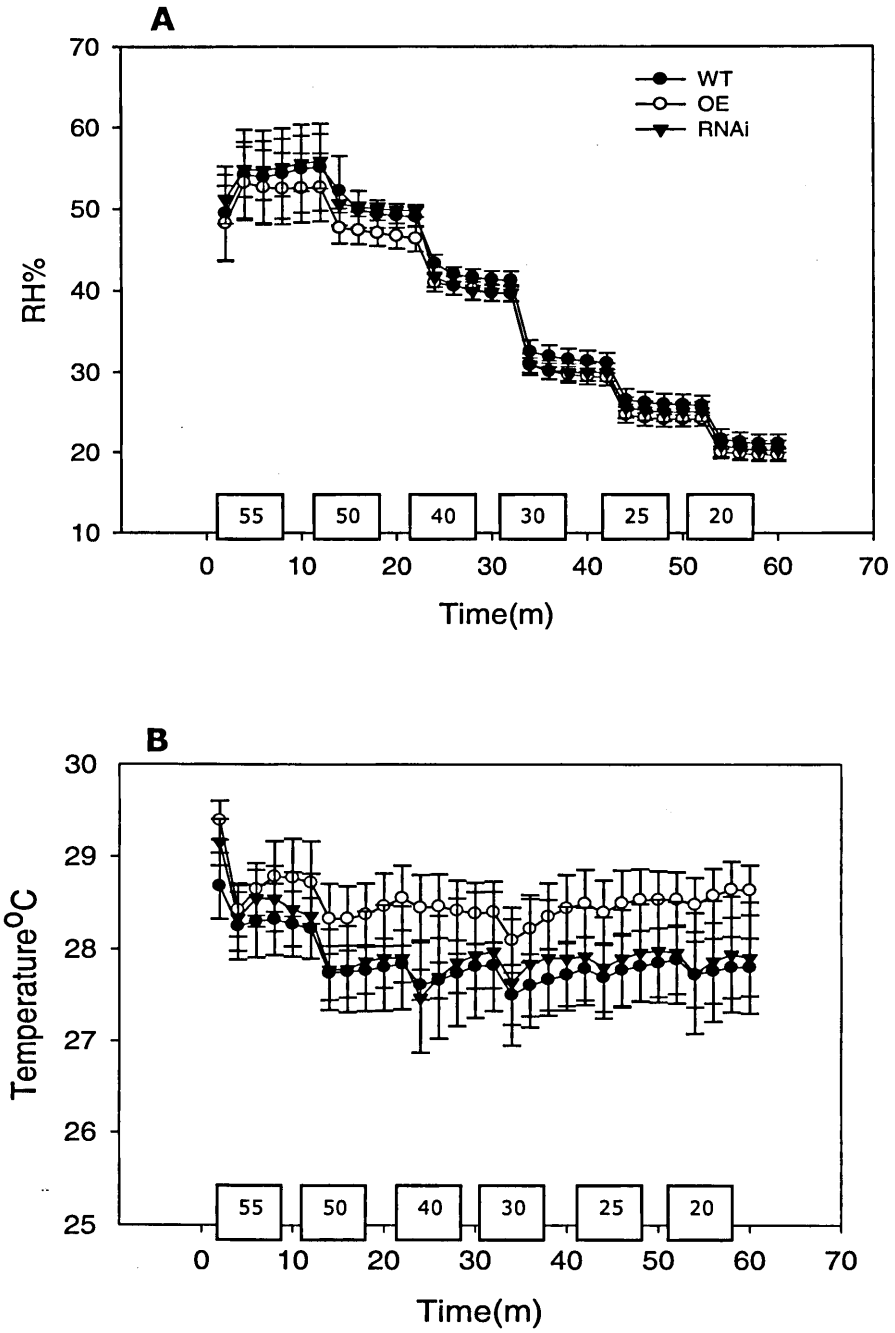

Figure 4. 8 (A) RH% (B) leaf temperature maintained in the cuvette during stepwise decrease in cuvette relative humidity (RH%) in dark-adapted leaves of wild type (WT), Overexpression (OE) and RNAi interference (RNAi) lines at a cuvette CO_2 concentration of 400µl L^{-1} and light intensity of 1000 µmols $m^{-2}s^{-1}$. Saturating light applied after 10 min light activation. Level of RH% maintained during a 10 min interval is indicated in boxes on X-axis. Means ± SE (n = 5).

The OE line induced and sustained high NPQ (20%, $P<0.05$) compared to the WT throughout 60 min period (Figure 4.9) while in the RNAi, NPQ was around 38% lower than the WT. Note that NPQ in the RNAi was steady within 20 min of induction despite gradual decline in moisture. WT NPQ reached a steady state at about 45 min. However, NPQ was still increasing steadily as moisture level decreased in OE transgenic rice plants indicating that plants overexpressing PGR5 protein can respond quickly to short term changes in moisture levels. The above observations suggest that the PGR5 is essential in the rapid photoprotective responses of rice plants under mild stress condition.

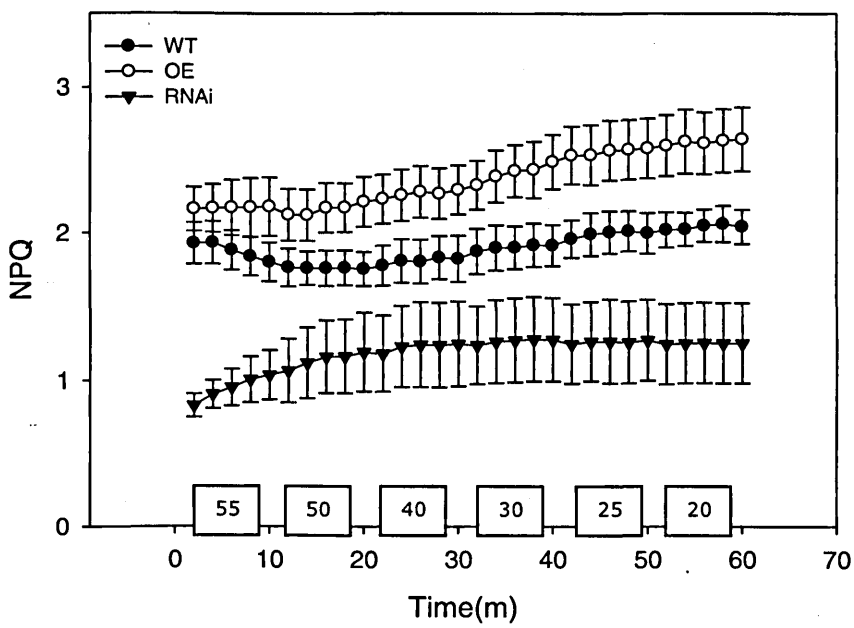

Figure 4. 9 Non-photochemical quenching measured simultaneously with gas exchange during stepwise decrease in cuvette relative humidity (RH%) in dark-adapted leaves of wild type (WT), Overexpression (OE) and RNAi interference (RNAi) lines at a cuvette CO_2 concentration of 400µl L^{-1} and light intensity of 1000 µmols $m^{-2}s^{-1}$. Saturating light applied after 10 min light activation. Level of RH% maintained during a 10 min interval is indicated in boxes on X-axis. Means ± SE (n = 5).

Figure 4.10A shows photochemical quenching (qP) measured during a stepwise decrease in moisture level. In the RNAi plants, qP was consistently lower than the WT and OE ($P<0.05$) decreasing by about 60% corresponding very closely to the low rate of ETR through PSII. qP in the OE was also slightly lower than the WT becoming significantly lower as moisture declined to about 20% indicating that as the decrease in moisture level became more severe, more electrons are returned to PSI, consistent with an increased CET. Furthermore, ϕPSII was down-regulated as indicated by the significant decline in PSII quantum yield (10%, $P<0.05$) consistent with the observed increase in their corresponding NPQ. ϕPSII was significantly lower in the RNAi (50%, $P<0.05$) compared with the WT or OE plants with decreasing moisture levels (Figure 4.10B).

The rate of CO_2 assimilation shown in Figure 4.11A gradually declined in the WT and transgenic rice plants as moisture level decreased. Again, the RNAi lines showed a significantly lower rate of CO_2 assimilation when compared with the WT and OE ($P<0.05$), consistent with observed down-regulation of ϕPSII. Reduction in rates of CO_2 assimilation as well as was also observed in OE plants compared with the WT in the final 50 min of measurement coinciding with the trend observed in NPQ (Figure 4.9). Low moisture is likely to increase the demand for ATP due to decrease in rate of photosynthesis, resulting in an imbalance in the ratio of ATP/NADPH. In addition, there was a small reduction in gs, and a relatively large change in Ci, indicating that photorespiration is involved here. Photorespiration consumes ATP - Is more ATP required for the photorespiratory pathway? Perhaps this is part of the reason. PGR5-dependent cyclic electron flow

responds to this imbalance in ATP/NADPH by increasing its activity thus increasing transthylakoid proton gradient (ΔpH) required for generation of NPQ and down-regulating LET (Johnson, 2003). This dynamic response mainly attributed to PGR5 in this study is clearly shown in Figure 4.11B displaying a strong but negative correlation between NPQ and rate of CO_2 assimilation in the WT and OE.

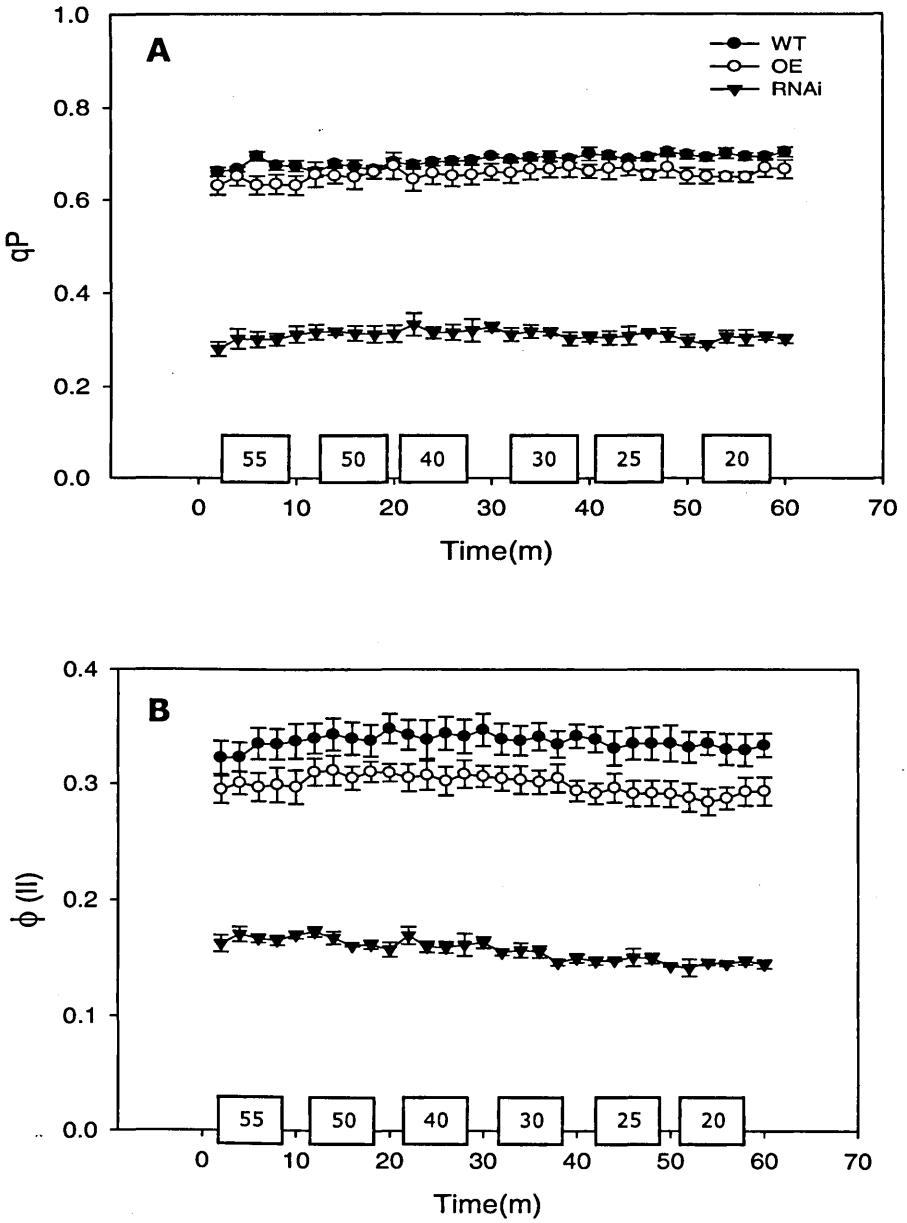

Figure 4. 10 (A) photochemical quenching [qP] (B) quantum yield of PSII [ϕ(II)] measured simultaneously with gas exchange during stepwise decrease in cuvette relative humidity (RH%) in dark-adapted leaves of wild type (WT), Overexpression(OE) and RNAi interference (RNAi) lines at a cuvette CO_2 concentration of 400µl L^{-1} and light intensity of 1000 µmols $m^{-2}s^{-1}$. (Saturating light applied after 10 min light activation. Level of RH% maintained during a 10 min interval is indicated in boxes on X-axis. Means ± SE (n = 5).

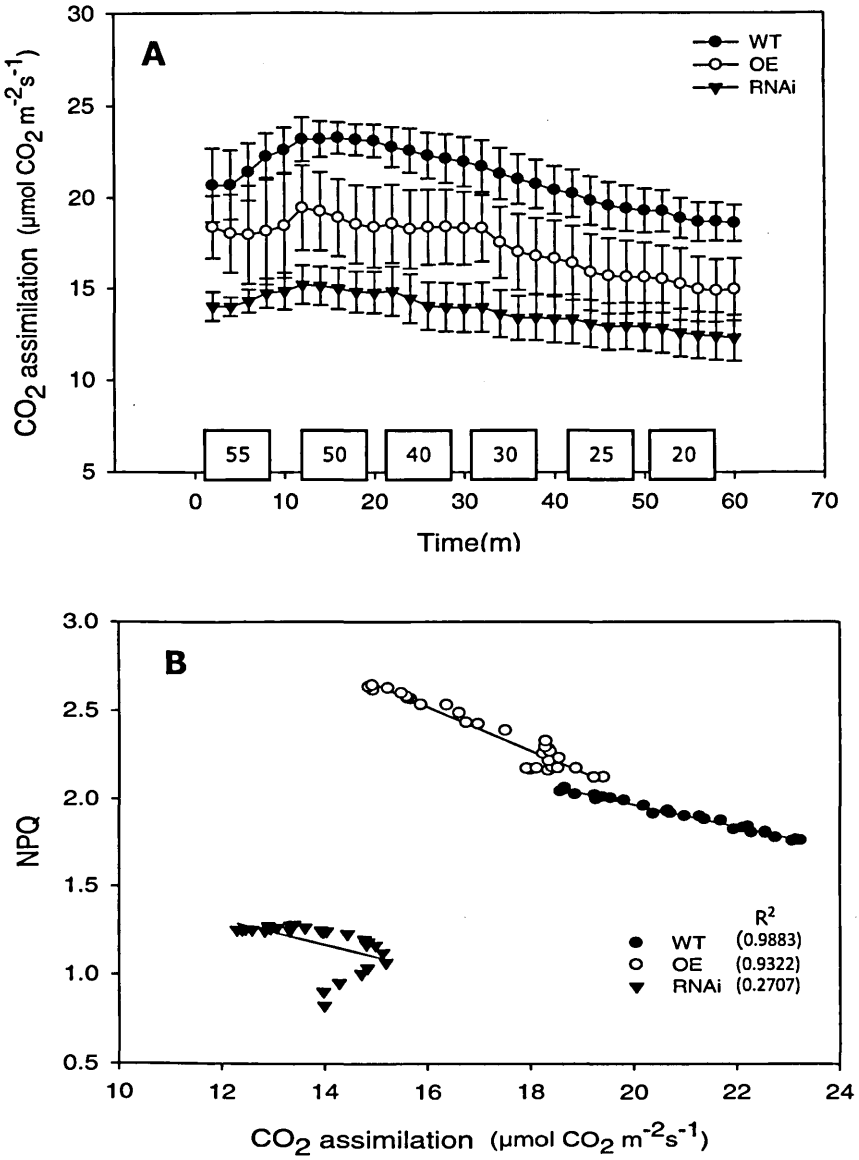

Figure 4. 11 (A) Rate of CO_2 assimilation (µmol CO_2 $m^{-2}s^{-1}$) measured during stepwise decrease in cuvette relative humidity (RH%) in dark-adapted leaves of wild type (WT), Overexpressor (OE) and RNAi interference (RNAi) lines at a cuvette CO_2 concentration of 400µl L^{-1} and light intensity of 1000 µmols $m^{-2}s^{-1}$. Saturating light applied after 10 min light activation. Level of RH% maintained during a 10 min interval shown in boxes on X-axis. Means ± SE (n = 5). (B) Non-photochemical quenching (NPQ) versus CO_2 assimilation. Each point represents a single measurement in Figures 4.9 & 4.11A. Lines shown are linear correlations for wild type (WT), Overexpression (OE) and RNA interference (RNAi) data.

Stomatal closure, a primary response of plants under mild to moderate drought stress is generally accepted as a major determinant for decreased photosynthesis (Medrano et al, 2002). This response minimizes water loss, lowering intercellular CO_2 concentration (Ci), causing stomatal or diffusional limitation to photosynthesis (Chaves et al, 2003) as a consequence of Rubisco's low affinity for CO_2. In this study, the OE line showed significant decrease in g_s and Ci ($P<0.05$, Figure 4.12) which suggests that stomatal limitations/closure may partly be a cause of decreased photosynthesis observed in rice plants over expressing the PGR5 protein although other non-stomatal limitations may also be present as seen in its Vcmax (Chapter 3, Figure 3.12B).

Stomatal conductance (g_s) was not significantly different in the RNAi plant compared to the WT (Figure 4.12B). This observation might indicate the existence of nonstomatal limitations impairing metabolic activities such as ATP synthesis, electron transfer and ribulose-1,5-biphosphate (RuBP) synthesis (Cossins & Chen, 1997). Thus, these results in the RNAi line suggest a reduction in the photosynthetic capacity as a result of lack of the PGR5 protein. Also intercellular CO_2 concentration was higher in the RNAi plant ($P<0.05$) compared to the WT indicating as suggested with g_s, a decrease in rate of CO_2 assimilation seen in its TPU and Amax (section 3.7).

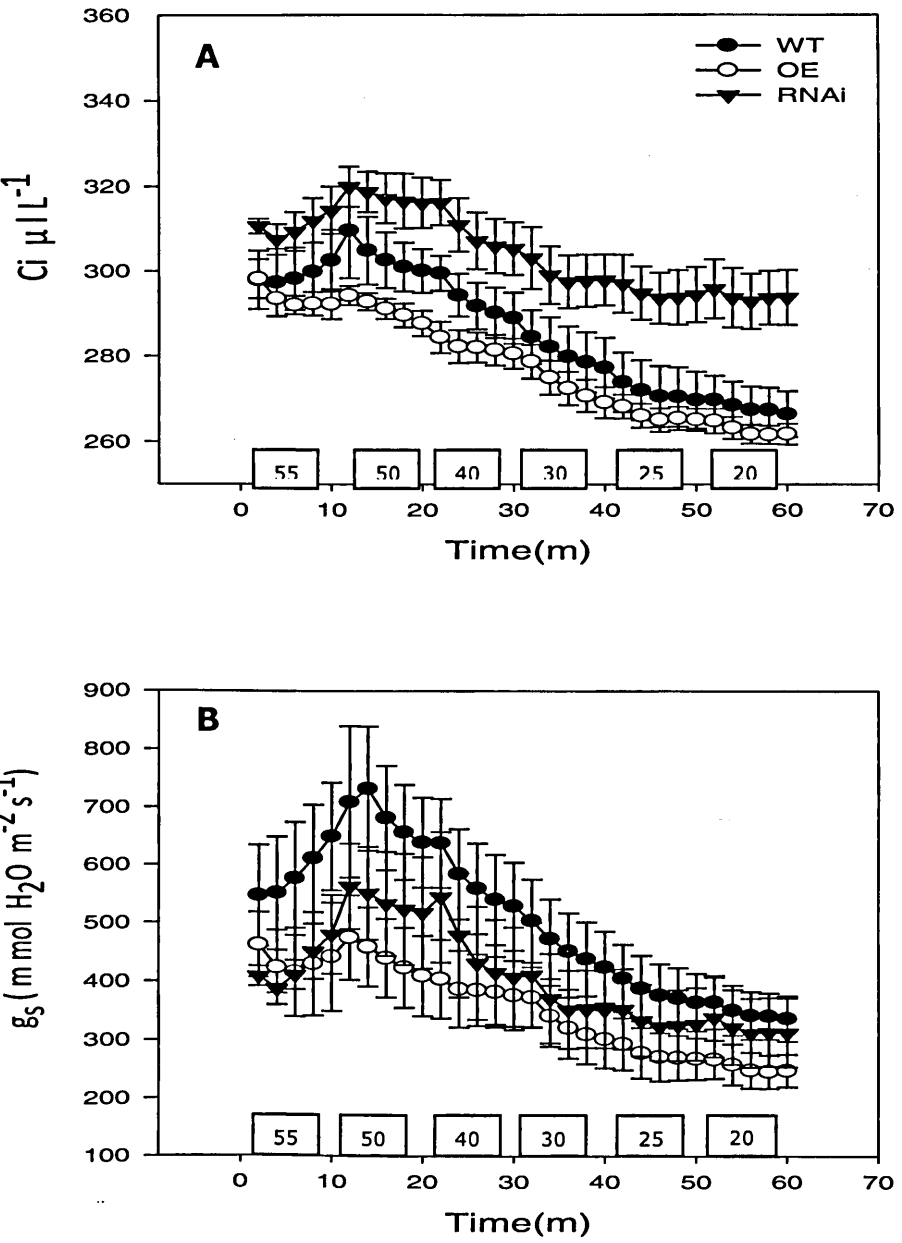

Figure 4. 12 Chlorophyll fluorescence analysis and gas exchange measured simultaneously during stepwise decrease in cuvette relative humidity (RH%) in dark-adapted leaves of wild type (WT), Overexpression (OE) and RNAi interference (RNAi) lines at a cuvette CO_2 concentration of 400µl L^{-1} and light intensity of 1000 µmols $m^{-2}s^{-1}$. (A) Intercellular CO_2 concentration, Ci (µl L^{-1}) (B) stomatal conductance (mmol H_2O $m^{-2}s^{-1}$). Saturating light applied after 10 min light activation. Level of RH% maintained during a 10 min interval shown in boxes on X-axis. Means ± SE (n = 5).

4.6 Discussion

A large NPQ transient was observed in rice during the induction of photosynthesis. The transient was absent in the RNAi and increased significantly in the OE line indicating that the PGR5 protein may influence the size of NPQ induced at onset of photosynthesis that is, following a shift from dark to light. A similar transient have been described in rice overexpressing the PsbS protein (Hubbart et al, 2012). In *A. thaliana,* a similar transient was reported under low light (Kalituho et al, 2007) and when the PGR5 protein over-accumulates *in vivo* (Okegawa et al, 2007). However, Makino et al, 2002 demonstrated that the water-water cycle may also function during induction of the NPQ transient at onset of photosynthesis in rice, although the contribution of this cycle could not be quantified in this study.

When compared to the WT during induction of photosynthesis, steady state levels of NPQ were significantly higher in the OE and lower in the RNAi after 30 minutes of illumination. The degree of NPQ observed in the PGR5 transgenic plants, in low and high light and under high CO_2, when stomata and Rubisco are no longer limiting, suggests that PGR5 may be required by rice for full expression of NPQ, indicating an essential role for cyclic electron transport during steady state photosynthesis. However, previous studies suggested that the PGR5 protein was not essential for cyclic flow in *Arabidopsis thaliana* pgr5 mutants (Nandha et al, 2007; Livingston et al, 2010). Similarly, from previous experiments with Arabidopsis plants overexpressing the PGR5 protein, Okegawa et al (2007) showed transient increase in NPQ at induction under low light. These differences may partly

be due to be variations in CET activity between species or conditions (Kramer et al., 2004).

Rapid relaxation of NPQ kinetics of the WT and OE in this study indicated that a qE-type of NPQ was predominant. In contrast, NPQ in the RNAi line was mostly due to photoinhibition with almost 40% showing characteristics of qI-type. The RNAi rice plants were earlier shown to be inhibited at the acceptor side of PSI (Section 3.7), likely to result in over-reduction of the PSI triggering PSI photoinhibition (Munekage et al, 2002) and ultimately inhibiting the generation of ΔpH important for qE development. In addition, the impairment of both CET and qE was shown to inhibit the de novo synthesis of the D1 protein, important for the repair of photodamaged PSII, under strong light. This in turn accelerates PSII photoinhibition observed as qI in this study.

Under mild water stress, rice is a drought-susceptible crop, due in part to its rapid stomatal closure (Hirasawa, 1999) which may reduce its capacity to assimilate carbon to result in photoinhibition under high light (Zhou et al, 2007). If rice is exposed to mild but fluctuating moisture stress, will the PGR5 protein enhance it's ability to engage photoprotective mechanisms, in response to rapid but adverse changes in rate of leaf photosynthesis in the long term? In this study, when PGR5 transgenic rice leaves were subjected a steady decline in atmospheric moisture level, significantly high NPQ was induced and sustained at steady state in OE lines. This suggests that there is a requirement for enhanced cyclic electron transport under such conditions in rice and that the PGR5 protein is implicated in stress

responses in plants both in the short and long-term probably as a result of an altered requirement for ATP (Section 6.6).

Low moisture results in stomatal closure in order to reduce transpiration rates, thereby limiting CO_2 uptake by leaves which in turn enhances Rubisco oxygenation and photorespiration (Flexas et al, 2006; Wingler et al, 1999). In addition, Bunce (1981) demonstrated that the rate of CO_2 assimilation decreased in leaves in response to a drop in air humidity under moderate leaf water deficits. In this study, stomatal conductance (g_s) and rate of intercellular CO_2 (Ci) were significantly lower in the OE transgenic rice plants compared with the WT, suggesting that in the low humidity experiments, low CO_2 assimilation observed in the OE lines may mostly be as a result of Rubisco/stomatal limitations as observed under non-photoinhibitory conditions (Chapter 3). Increase in rubisco oxygenation/ photorespiration in relation to CET is discussed in Section 6.5 & 6.6. However, photosynthesis is not only restricted by stomatal limitations but also by non-stomatal limitations that impair metabolic reactions such as RuBP synthesis, ATP synthesis and electron transfer (Cossins & Che, 1997). In the RNAi lines in this study, g_s was not significantly different when compared to the WT while the Ci was higher ($P<0.05$). This observation suggests a reduction in the photosynthetic capacity of the RNAi plants. Taken together, these observations suggest a direct role for PGR5 in the intrinsic photosynthetic capacity of rice plants.

CHAPTER FIVE:

RESPONSE OF PGR5 TRANSGENIC RICE TO FLUNCTUATING LIGHT AT CANOPY LEVEL

CHAPTER 5: RESPONSE OF PGR5 TRANSGENIC RICE TO FLUNCTUATING LIGHT AT CANOPY LEVEL

5.1 Introduction:

Photosynthesis is the most important biochemical process in nature, serving as energy source for most living organisms. It is driven solely by light energy and serves as the basis for all crop production practices (Evans, 1993). In the natural environment, plants are exposed to rapid fluctuations in solar radiation which may reach a peak on sunny days. Under such conditions, maximum energy utilization in photosynthetic processes is rarely achieved in crop plants such as rice (Murchie and Horton, 2007) partly as a result of delay in the dynamic adjustment of plants to rapid fluctuations in light (Schurr et al, 2006). This situation results in the absorption of excess light beyond photosynthetic capacity of leaves worsened further by the occurrence other stress conditions such as high nutrient deficiency, drought and temperature.

Plants possess series of photoprotective regulatory processes to harmlessly dissipate excess absorbed light energy as heat (NPQ), thus preventing damage to plant photosynthetic machineries which could limit photosynthesis and growth, ultimately reducing overall canopy photosynthesis and biomass production (Murchie et al, 1999). In rice, photoprotective regulatory processes have been identified by Horton et al (2001) as potential targets for improvement. The qE component of NPQ has been shown to affect plant fitness and productivity as well as protect plants from photoinhibition (Hubbart et al, 2012; Kasajima et al, 2011; Li et al,

2002). However in contrast, Frenkel et al. (2009) attributed a decline in PSII quantum yield of npq4 plant mutants lacking qE to diversion of assimilate towards defence mechanisms rather than growth. Thus, to enhance leaf photosynthesis, understanding the mechanisms of photoprotection is crucial for optimization of dynamic responses of plants to the environment.

In recent years, our understanding of regulatory processes of photosynthesis in particular qE has increased. Several studies were carried out mainly in Arabidopsis as well as in rice, which mostly involve monitoring single plants under controlled conditions in growth chambers (Hubbart et al, 2012; Sousa et al, 2012; DalCorso et al, 2008). Crop production however involves plants grown in a community, mutually interfering with one another forming crop canopy where most leaves experience fluctuating light. Such plants are able to respond to changing environmental conditions by altering their morphology and/or physiology (Navas and Garnier 2002; Sultan 1995). Knowledge of canopy light distribution and absorption is fundamental for understanding many aspects of crop growth and productivity. This is crucial for maximum photosynthetic efficiency while avoiding photoinhibition. In a comparison between *Arabidopsis* plants grown in the field and growth room, Mishra et al. (2012) reported variations in their morphological characteristics in response to prevailing environmental conditions. Rice plants grown under two different light intensities in the growth room have been described in chapter 3. Light conditions in the growth chamber however are rather low compared to the field where light intensity may reach 2000 μmol $m^{-2}s^{-1}$ on sunny days.

Therefore information on the performance of plants grown in the field will further enrich our understanding of molecular basis of photosynthesis in order to optimize crop yield.

Increase in photosynthetic efficiency in crop plants can be measured as an increase in crop biomass. In a recent review, Murchie et al. (2009) highlighted the potential for crop improvement by increasing production of crop biomass and grain yield through alterations of leaf photosynthesis. Therefore understanding the mechanisms and regulation of photoprotection is fundamental to a better understanding of plants growth and our ability to alter rate of biomass production. In this chapter, morphological and physiological characterisation of PGR5 antisense and overexpressing rice crops grown to canopy level in a crop glasshouse was carried out. This is aimed at investigating the potential impact of PGR5 cyclic electron transport on induction of NPQ, photosynthetic efficiency and growth performance of rice crops.

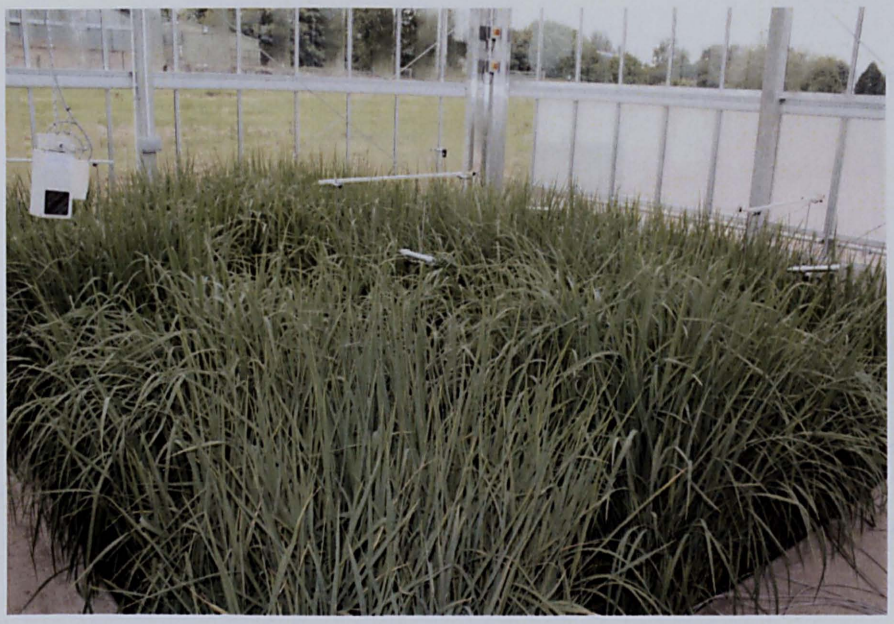

Figure 5. 1 Example of rice grown in the crop glasshouse

5.2 Results

Transgenic rice lines produced using OE construct (147) and RNAi construct (158) and WT (Kaybonnet variety) were grown in plots in the crop glasshouse (Figure 5.1). Plants were screened for NPQ level as described in 2.10 to allow selection of lines showing greatest divergence in their NPQ level from the WT. Figure 5.2 shows average NPQ levels of WT and transgenic plants. WT plants showed an average NPQ of 1.30, while RNAi and OE lines showed an average of 0.49 and 1.53 respectively. With the wild type intermediate between the transgenic lines, ten plants showing most extreme NPQ level (OE>1.5 and RNAi <0.5) were selected for further analysis.

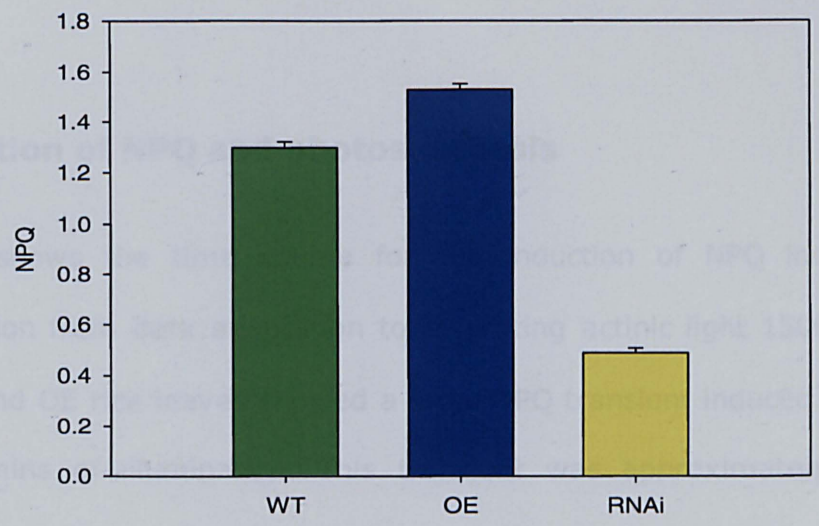

Figure 5. 2 Average NPQ measured on excised leaf segments after a 15-min actinic period in a chlorophyll fluorescence imager for wild type (WT), Overexpression (OE) and RNA interference (RNAi) lines. Means ± SE, n=30-80.

5.3 Continuous PAR and NPQ measurement.

Figure 5.3A shows 24 h time course of above the canopy average photosynthetically active radiation (PAR) readings. Six ceptometer were placed unattended at different locations within the experimental plots to automatically log PAR readings every 8 min. The six readings were averaged to get PAR for the whole experimental plots. PAR increased gradually through the day to reach a peak of about 490 µmols $m^{-2}s^{-1}$ at ~ 14 h, before gradually declining.

Figure 5.3B shows 24 h time course of NPQ at 10 min interval. NPQ was determined (section 1.10.2) from continuous chlorophyll fluorescence measurement (section 2.19). NPQ increased immediately after sunrise

following the same trend observed in PAR, with OE showing higher level than the WT.

5.4 Induction of NPQ and photosynthesis

Figure 5.4A shows the time course for the induction of NPQ induction during transition from dark adaptation to saturating actinic light 1500 μmol m^{-2} s^{-1}. WT and OE rice leaves showed a large NPQ transient induced during the first 5 mins of illumination. This transient was approximately 21% higher than NPQ level at steady state following 20 mins of illumination in both lines. Similar types of NPQ transient have been reported in rice lines overexpressing PsbS protein when grown at light intensity of 600 μmol m^{-2} s^{-1} (Hubbart et al, 2012) and in Arabidopsis when grown at very low light levels (Kalituho et al, 2007).

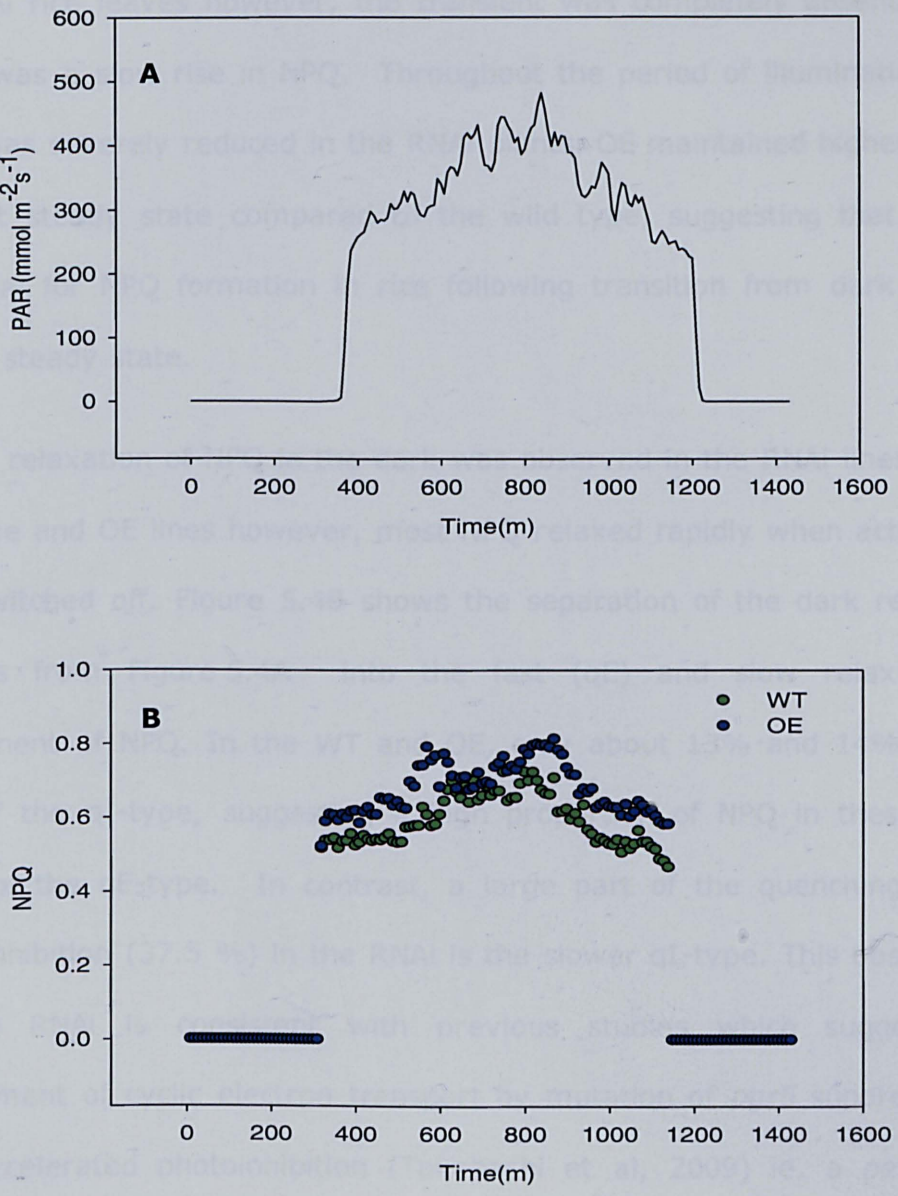

Figure 5. 3 24 h fluctuations in (A) photosynthetically active radiation (PAR) measured at interval of 8 min and (B) NPQ for wild type (WT) and Overexpressor (OE) line measured at 10 min interval. Each point corresponds to average readings across 7 consecutive days (6-12 June, 2012). Means, n=7.

In RNAi rice leaves however, the transient was completely absent instead there was a slow rise in NPQ. Throughout the period of illumination, NPQ level was severely reduced in the RNAi plants. OE maintained higher rate of NPQ at steady state compared to the wild type, suggesting that pgr5 is essential for NPQ formation in rice following transition from dark to light and at steady state.

A slow relaxation of NPQ in the dark was observed in the RNAi lines. In the wildtype and OE lines however, most NPQ relaxed rapidly when actinic light was switched off. Figure 5.4B shows the separation of the dark relaxation kinetics from Figure 5.4A into the fast (qE) and slow relaxing (qI) component of NPQ. In the WT and OE, only about 13% and 14% of NPQ was of the qI-type, suggesting a high proportion of NPQ in these plants were of the qE-type. In contrast, a large part of the quenching due to photoinhibition (37.5 %) in the RNAi is the slower qI-type. This observation in the RNAi is consistent with previous studies which suggest that impairment of cyclic electron transport by mutation of *pgr5* suppressed qE and accelerated photoinhibition (Takahashi et al, 2009) ie. a permanent closure of PSII reaction centers as a result of damage caused by excess light energy (Johnson & Ruban, 2010).

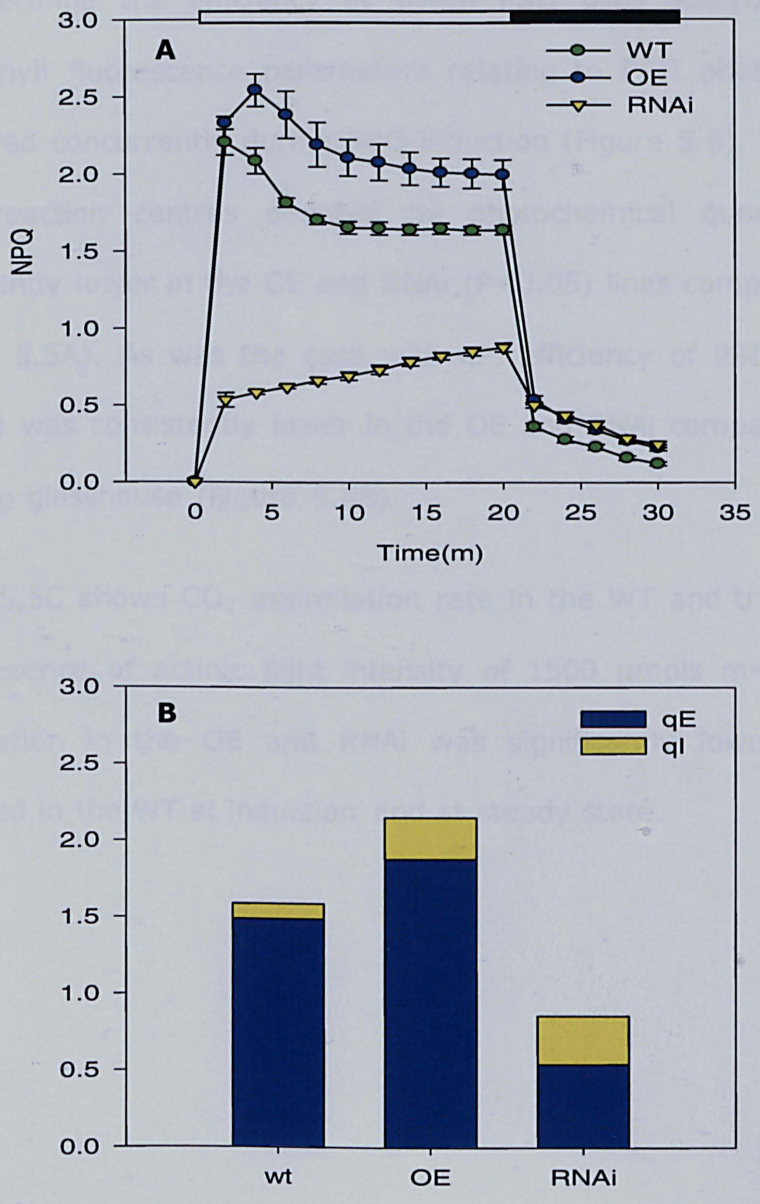

Figure 5. 4 Chlorophyll fluorescence analyses during induction from darkness. (A) Induction from darkness of non-photochemical quenching (NPQ) in wild type (WT), overexpression (OE) and RNA interference (RNAi) lines measure at an actinic light of 1500 µmol m^{-2} s^{-1}, a cuvette CO_2 concentration of 400 µl L^{-1} and relative humidity of 60%. Leaves were dark adapted for 2h. At 20 min the actinic light was switched off. Means ± SE (n = 4-8). (B) Separation of qE and qI components of nonphotochemical quenching in leaves of wild type (WT), OE and RNAi lines. qE and qI were calculated as described in section 1.11.3. Means (n = 4-8).

To determine the efficiency at which PSII uses absorbed light energy, chlorophyll fluorescence parameters relating to PSII photochemistry were measured concurrently during NPQ induction (Figure 5.5). The proportion of open reaction centres denoted by photochemical quenching (qP) was significantly lower in the OE and RNAi ($P<0.05$) lines compared with the WT (Figure 5.5A). As was the case with qP, efficiency of PSII photochemistry (ϕPSII) was consistently lower in the OE and RNAi compared to the WT in the crop glasshouse (Figure 5.5B).

Figure 5.5C shows CO_2 assimilation rate in the WT and transgenic lines. In the presence of actinic light intensity of 1500 µmols $m^{-2}s^{-1}$, rate of CO_2 assimilation in the OE and RNAi was significantly lower ($P<0.05$) than observed in the WT at induction and at steady state.

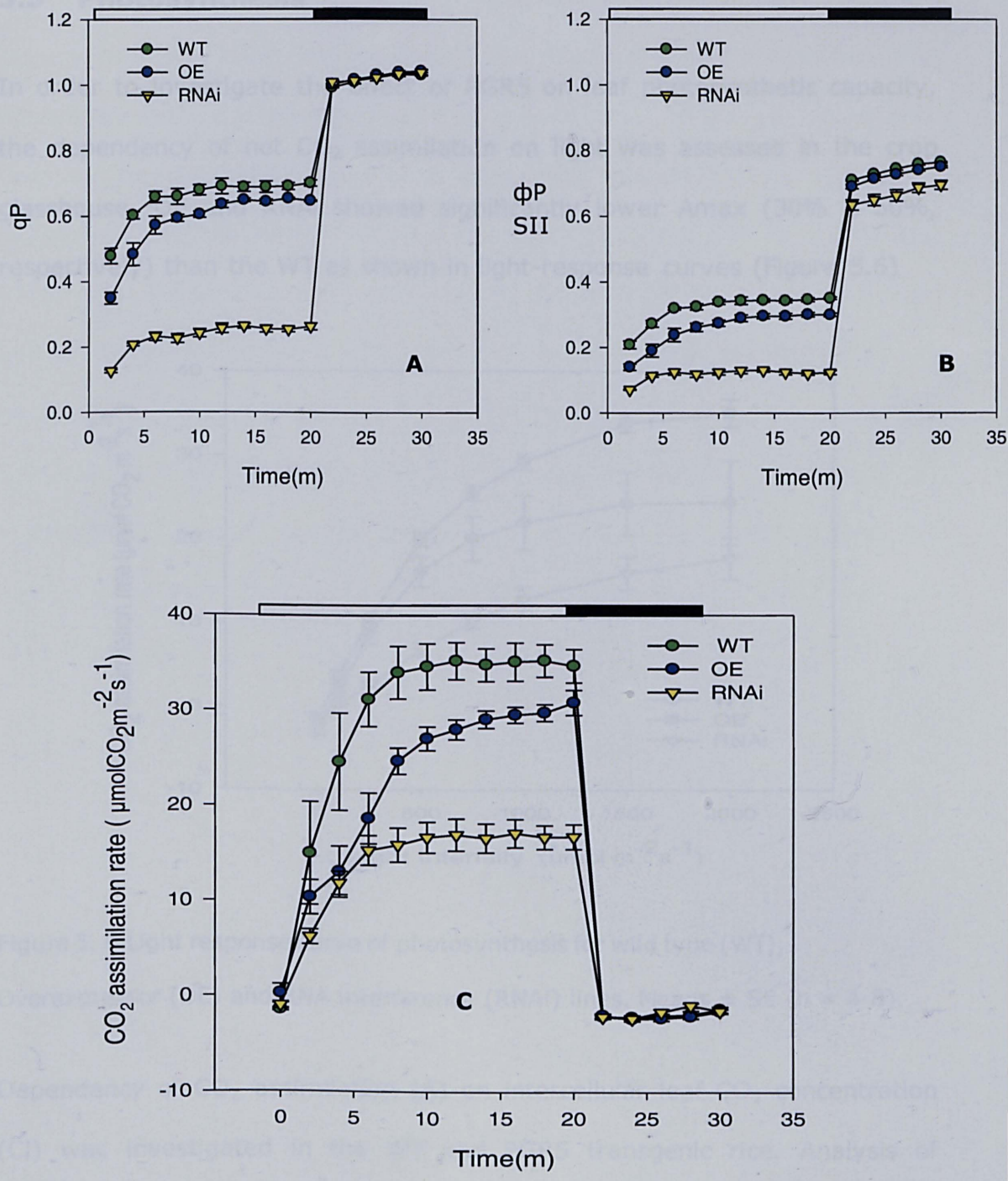

Figure 5. 5 (A) photochemical quenching (qP) and (B) quantum yield of PSII [ϕ(II)] (C) rate of CO_2 assimilation (µmol CO_2 $m^{-2}s^{-1}$) for wild type (WT), Overexpressor (OE) and RNA interference (RNAi) lines measured at an actinic light of 1500 µmol m^{-2} s^{-1}, a cuvette CO_2 concentration of 400 µl L^{-1} and relative humidity of 60%. Leaves were dark adapted for 2h. At 20 min the actinic light was switched off. Means ± SE (n = 4-8).

5.5 Photosynthesis

In order to investigate the effect of PGR5 on leaf photosynthetic capacity, the dependency of net CO_2 assimilation on light was assessed in the crop glasshouse. OE and RNAi showed significantly lower Amax (30% & 50%, respectively) than the WT as shown in light-response curves (Figure 5.6)

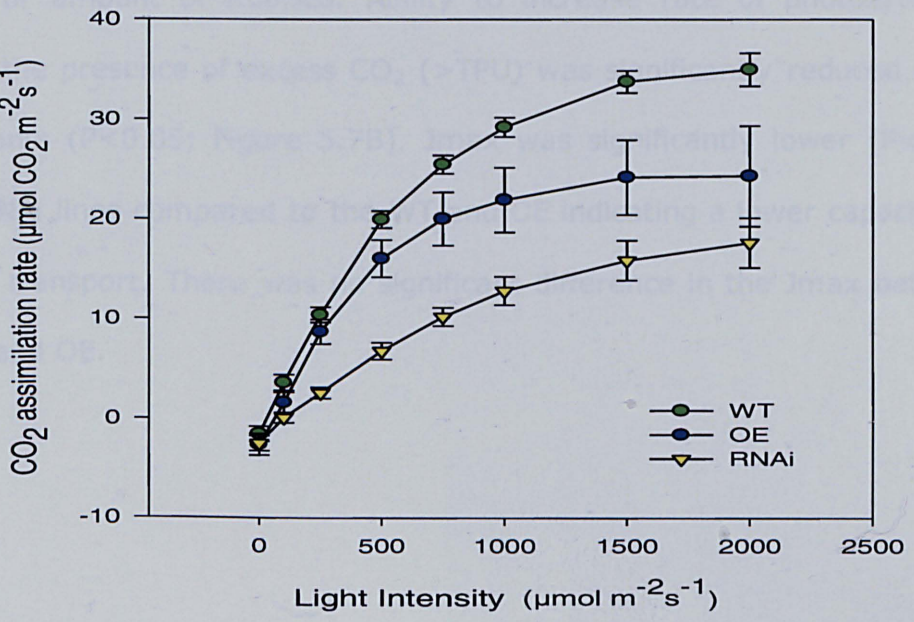

Figure 5. 6 Light response curve of photosynthesis for wild type (WT), Overexpressor (OE) and RNA interference (RNAi) lines. Means ± SE (n = 4-8).

Dependency of CO_2 assimilation (A) on intercellular leaf CO_2 concentration (Ci) was investigated in the WT and PGR5 transgenic rice. Analysis of assimilation-intercellular CO_2 concentration at light intensity of 1500 µmol $m^{-2}s^{-1}$ shown in Figure 5.7A was carried out to derive information on the maximum catalytic activity of Rubisco (Vcmax) a photosynthetic key enzyme catalyzing CO_2 fixation, maximum rate of electron transport activity (Jmax) and triose phosphate utilisation (TPU) (Von Caemmerer & Farquhar,

1981). Measurements were taken on cloudy days to minimize possible losses from the effect of photoinhibition, high rate of transpiration and decreased leaf stomatal conductance, which may singly or collectively decrease rate of leaf photosynthesis under high sunlight. Results are shown in Figure 5.7B. The Vcmax values were significantly reduced in the OE and RNAi lines compared to the WT ($P<0.05$; Figure 5.7B) indicative of limited activity or amount of Rubisco. Ability to increase rate of photosynthesis even in the presence of excess CO_2 (>TPU) was significantly reduced in the RNAi plants ($P<0.05$; Figure 5.7B). Jmax was significantly lower ($P<0.05$) in the RNAi lines compared to the WT and OE indicating a lower capacity for electron transport. There was no significant difference in the Jmax between the WT and OE.

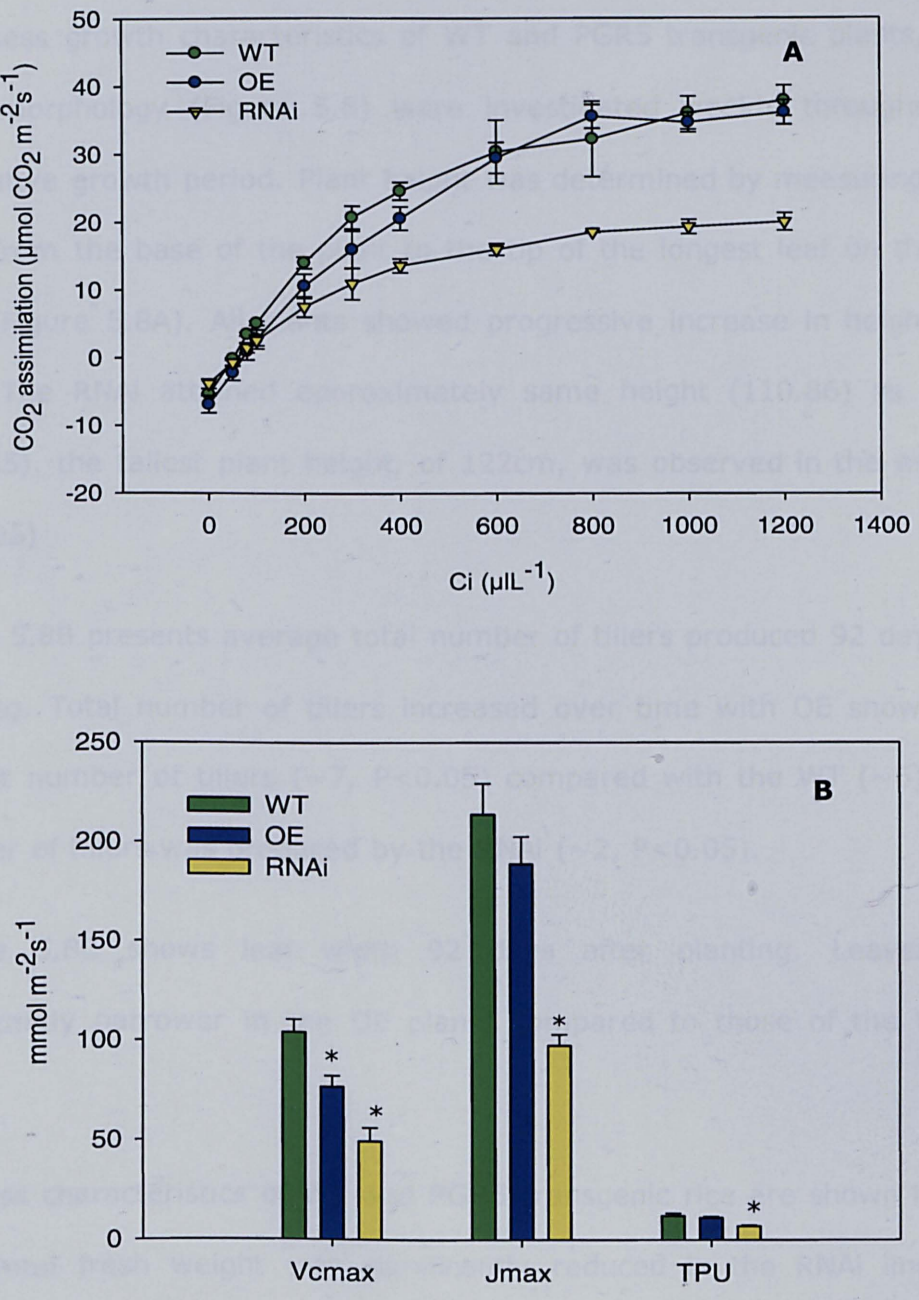

Figure 5. 7 Photosynthetic traits in the wild type (WT), Overexpressor (OE) and RNA interference (RNAi) lines (A) Intercellular CO_2 concentration (Ci) response of net CO_2 assimilation. (B) Calculated values from A-Ci analysis for the lines studied using the tool in Sharkey et al (2007) to compute values for maximum catalytic activity of Rubisco (Vcmax), maximum electron transport activity (Jmax) and triose phosphate utilization (TPU). Means ± SE (n = 5-7), *P<0.05.

5.6 Growth and biomass analysis

To assess growth characteristics of WT and PGR5 transgenic plants, whole plant morphology (Figure 5.8) were investigated weekly throughout the vegetative growth period. Plant height was determined by measuring with a ruler from the base of the plant to the tip of the longest leaf on the main tiller (Figure 5.8A). All plants showed progressive increase in height to 92 DAG. The RNAi attained approximately same height (110.86) as the OE (110.35). the tallest plant height, of 122cm, was observed in the wild type ($P<0.05$)

Figure 5.8B presents average total number of tillers produced 92 days after planting. Total number of tillers increased over time with OE showing the highest number of tillers (~7, $P<0.05$) compared with the WT (~6). Least number of tillers was produced by the RNAi (~2, $P<0.05$).

Figure 5.8C shows leaf width 92 days after planting. Leaves were significantly narrower in the OE plants compared to those of the WT and RNAi.

Biomass characteristics of WT and PGR5 transgenic rice are shown in Table 5.1. Total fresh weight was significantly reduced in the RNAi line while there was no significant difference between total fresh weight for the WT and OE lines. Similar trend were seen in the dry weight and total leaf area. The leaf area ratio (LAR) is the ratio of leaf area to total weight. LAR was significantly higher in OE and RNAi lines compared with the wild type while specific leaf area (SLA, leaf area per unit leaf dry weight), a measure of leaf

relative thickness (Evans & Poorter, 2001) was significantly higher in the OE line compared with the WT and RNAi.

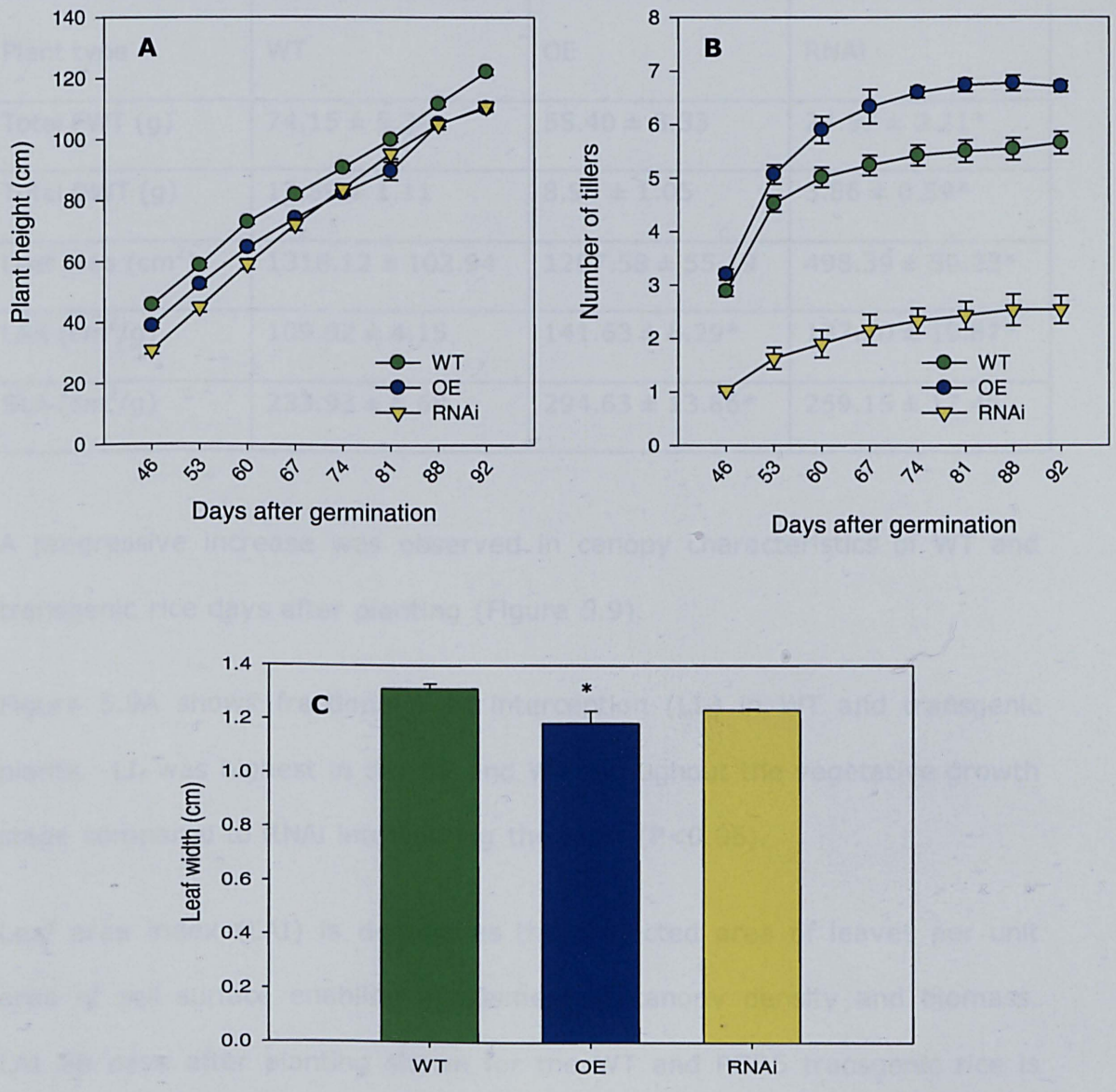

Figure 5. 8 Changes in (A) plant height (cm) and (B) average number of tillers by wildtype and PGR5 transgenic rice canopy on different dates. (C) Final leaf width (cm) 92 days after planting for wild type (WT), Overexpressor (OE) and RNA interference (RNAi) lines. Means ± SE, n=30-80, $P<0.05$.

Table 5. 1 Total fresh weight (FWT), total dry weight (DWT), leaf area ratio (LAR) and specific leaf area (SLA) of wildtype and PGR5 transgenic rice grown in the crop glasshouse 92 days after planting. Means ± SE, n=30-80. *P<0.05.

Plant type	WT	OE	RNAi
Total FWT (g)	74.15 ± 5.39	55.40 ± 3.33	24.57 ± 3.21*
Total DWT (g)	12.59 ± 1.11	8.95 ± 1.05	3.86 ± 0.59*
Leaf area (cm^2)	1318.12 ± 102.94	1207.58 ± 55.19	498.39 ± 50.23*
LAR (cm^2/g)	109.82 ± 4.15	141.63 ± 8.29*	137.20 ± 10.87*
SLA (cm^2/g)	233.93 ± 6.68	294.63 ± 13.86*	259.15 ± 17.45

A progressive increase was observed in canopy characteristics of WT and transgenic rice days after planting (Figure 5.9).

Figure 5.9A shows fractional light interception (LI_f) in WT and transgenic plants. LI_f was highest in the OE and WT throughout the vegetative growth stage compared to RNAi intercepting the least (P<0.05).

Leaf area index (LAI) is defined as the projected area of leaves per unit area of soil surface enabling assessment of canopy density and biomass. LAI 88 days after planting shown for the WT and PGR5 transgenic rice is presented in Figure 5.9B. LAI was significantly lower in the RNAi line compared to the OE and WT days after planting. There were no significant difference in the LAI of the WT and OE lines except between 74-88 days after planting were LAI for the OE increased sharply (P<0.05).

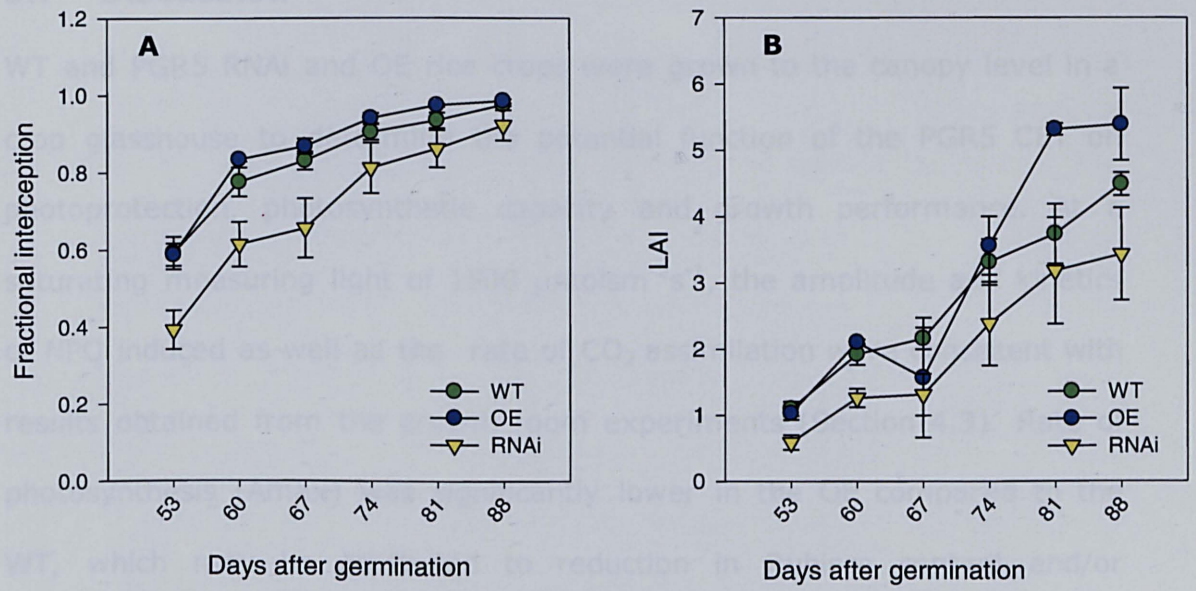

Figure 5. 9 Changes in the (A) fractional interception and (B) leaf area index (LAI) of solar radiation by wild type (WT), Overexpressor (OE) and RNA interference (RNAi) lines canopy on different dates. Means ± SE (n=5).

5.7 Discussion

WT and PGR5 RNAi and OE rice crops were grown to the canopy level in a crop glasshouse to determine the potential function of the PGR5 CET on photoprotection, photosynthetic capacity and growth performance. At a saturating measuring light of 1500 $\mu molsm^{-2}s^{-1}$, the amplitude and kinetics of NPQ induced as well as the rate of CO_2 assimilation were consistent with results obtained from the growth room experiments (Section 4.3). Rate of photosynthesis (Amax) was significantly lower in the OE compared to the WT, which may be attributed to reduction in Rubisco content and/or Rubisco activity and not RuBP regeneration (Section 6.5). This is consistent with findings under controlled growth chamber conditions.

The efficiency of solar radiation use by rice leaf canopy for CO_2 assimilation was investigated in this study. High LAI is important for efficient light interception and in rice has been reported to be in the range of 4–7 (Yoshida, 1972). Rapid increase in leaf area index (LAI) was observed in this study ranging between 0.59 – 5.4. Horie & Sakuratani (1985) found that when LAI is small in rice, there is a direct relationship between canopy CO_2 assimilation rate and LAI. In the WT and OE, a similar level of fractional light interception and utilization particularly at early stage of vegetative growth, may partly explain the non-significant difference in their biomass accumulation. However, LAI in OE reached a maximum level earlier than in the WT and RNAi.. This may be due to the high number of tillers produced by the OE which may increase leaf shading and reduce canopy photosynthesis (Evans & Poorter, 2001; Hayashi, 1972). High SLA

($P<0.05$) observed in the OE days after planting agrees with the possibility for leaf overlap/shading (Evans & Poorter, 2001; Hayashi, 1972).

Tiller number and plant height are major traits of agronomic importance which partly determines adaptability of a plant to cultivation, its harvest index and potential grain yield (Reinhardt and Kuhlemeier, 2002). In this study, numbers of tillers increased significantly in the OE throughout the experimental period in the glasshouse. Whether such tillers will be productive in terms of yield could not be determined within the duration of this experiment. However, excess tillers can cause high tiller mortality, small panicles, poor grain filling and consequently reducing grain yield (Peng et al. 1994). In rice, early tillering in the absence of late-tillers prompted higher partitioning of assimilates to panicle at crucial stages like booting and anthesis to enhance grain yield (Mohapatra & Kariali 2008). Van Quyen et al (2004) indicated that additional tillers become unproductive and lead to excessive LAI and vegetative growth, and a favorable environment for disease development resulting in a higher percentage of unfilled grains.

Plant height is affected by environmental conditions (Yoshida 1981). In the high-density rice field, individual plants prolong their culm to get light due to increasing competition for light (Van Quyen, et al, 2004). In the crop glasshouse experiment, plant height of OE and RNAi were lower than the WT. Light interception as well as biomass was significantly lower in the RNAi.

CHAPTER 6

GENERAL DISCUSSION

CHAPTER 6: GENERAL DISCUSSION

6.1 Introduction

Despite progress made in recent years in our understanding of PGR5-dependent photosystem I cyclic electron transport and its role in photosynthesis particularly in the model organism, Arabidopsis *thaliana*, little is known about the function of this protein in more resource demanding plant such as rice. Moreover the role of PGR5-dependent cyclic electron transport in photoprotection and its potential impact on photosynthesis is not yet well understood.

This work aimed to improve current knowledge of the regulation of cyclic electron transport with respect to leaf photosynthesis and specifically determine the role of the PGR5 protein in photoprotection and photosynthetic productivity in rice.

Chapter 3 was involved with physiological and morphological characterization of transgenic rice plants with manipulated levels of the PGR5 protein grown under non-photoinhibitory stress. The response of these transgenic rice plants to dynamic conditions was investigated in Chapter 4. In Chapter 5, the role of PGR5 in photoprotection, photosynthesis and growth performance in rice crop at the canopy level was explored.

This chapter considers the role of the PGR5 protein in steady and dynamic conditions and aims to enhance our understanding of the mechanism of

photoprotection, fundamental to a better understanding of crop photosynthesis and our ability to improve crop yield.

6.2 PGR5 is involved in CET in rice

Many previous studies have examined PGR5-dependent CET around PSI and have revealed its occurrence mainly under stress conditions such as high light, drought and low CO_2 (Nandha et al, 2007; Munekage et al, 2002). In this study CET was stimulated under ambient conditions in rice leaves overexpressing the PGR5 protein grown not only under high light, but also under non-saturating light intensity (Figure 3.8). To test for increased CET capacity, repetitive saturating-pulses for assessment of fluorescence and P700 absorbance changes was applied as described in section 2.16 to give an estimate of effective quantum yield of PSII [ϕ(II)] and PSI [ϕ(I)]. Involvement of CET should increase ϕ(I), with CET requiring excess of PSI turnover possibly to meet enhanced metabolic demand for ATP. Therefore, comparing the quantum yield of both photosystems, variations in the ratio of the effective quantum yield of PSII [ϕ(II)] to PSI [ϕ(I)] should give us an indication of the occurrence of CET. This study showed that PGR5-dependent CET, manifested as the decrease in ϕ(II):ϕ(I), was actively occurring in rice leaves grown under non-saturating light although it's rate increased significantly with overexpression of the PGR5 protein when the LET pathway is fully saturated (see Chapter 3). The negative correlation between ϕ(II):ϕ(I) and NPQ indicate that PGR5-dependent CET produced a pH gradient across the thylakoid membrane sufficient enough to drive NPQ and/or maintain it in

line with the view of Johnson (2004) that the maximum rate of cyclic flow was sufficient to support the ΔpH required to maintain NPQ.

6.3 PGR5 is essential for NPQ induction of photosynthesis

In this study, transient NPQ was observed in rice leaves during the induction period of photosynthesis i.e. dark to light transition, under steady as well as fluctuating light in ambient CO_2. The size of this NPQ transient was dependent upon the level of the PGR5 protein, which was absent in the RNAi but increased in the OE lines. This is supported by western blotting which show that PGR5 in thylakoid proteins accumulated in the OE but was absent in the RNAi lines. The appearance of transient NPQ can simply be explained by the rapid generation of transthylakoid pH gradient (ΔpH) upon sudden dark to light transition, probably related to a restriction of the LET chain, and its subsequent breakdown as reactions of the Calvin-Benson cycle and other assimilatory processes become fully active (Cardol et al, 2010; Horton, 1983). Indeed the large NPQ transient observed within the first 10 min of induction under high CO_2 concentration (Chapter 4) coincided with a reduced rate of CO_2 assimilation and yield of PSII within the same time period due to the requirement for light activation of enzymes and accumulation of metabolite pool sizes, which relaxes completely as CO_2 assimilation becomes fully activated at steady state.

Both CET and water-water cycle are thought to be involved in the generation of ΔpH across the thylakoid membrane for induction of NPQ (Finazzi et al, 2004) although recently CET has been associated with NPQ during induction of photosynthesis (Cardol et al, 2010; Nandha et al, 2007;

Munekage et al, 2002; Allen, 2002), particularly when the PGR5 protein over-accumulates *in vivo* (Okegawa et al, 2007). An increase in CET was seen in rice leaves overexpressing the PGR5 protein based on the $\phi(II):\phi(I)$ assay which was highly correlated with level of induced NPQ within the time period of 10 min, similar to the time previously reported in rice (Hubbart et al, 2012). In addition, the NPQ transient was consistently absent in the RNAi lines under the various conditions described in this study i.e. in plants grown under low or high constant light and those grown under fluctuating natural light. The water-water cycle may also contribute towards the induction of the NPQ transient as suggested by Makino et al (2002) although the contribution of this cycle could not be quantified in this study. The same authors concluded that CET can be a main starter of photosynthesis when the water-water cycle is suppressed.

However, the consistent occurrence of the NPQ transient in overexpressing lines and its absence in the RNAi lines under constant and fluctuating light condition in this study clearly suggests that the PGR5 protein is essential for cyclic electron flow in rice during induction period of photosynthesis.

6.4 PGR5 is essential for NPQ during steady-state photosynthesis

Many researchers have debated the occurrence of CET under steady state conditions (Golding et al, 2004; Makino et al, 2002; Joliot & Joliot, 2002; Joet et al, 2002; Harbinson & Foyer, 1991; Herbert et al, 1990). Munekage et al (2008) suggested that PGR5 may be more important during steady-state photosynthesis based on the inability of *A. thaliana* pgr5 mutant to

induce qE. A similar observation was made by Okegawa et al (2008) based on their experiment with ruptured chloroplasts of *A. thaliana* pgr5. In contrast, Okegawa et al (2007) showed that the overaccumulation of PGR5 enhanced qE induction transiently and not at steady state in fluctuating light. In fact, Livingston et al (2010) suggested that PGR5 was not essential for cyclic flow at steady-state. However, Heber et al (1978) pointed out that cyclic electron flow contributes to ATP synthesis for carbon assimilation, since this cyclic flow and CO_2 assimilation are sensitive to antimycin A.

Results in this study showed that at a light intensity of 500 µmol $m^{-2}s^{-1}$, steady-state levels of NPQ were almost the same in the OE lines and WT but significantly lower in the RNAi lines (Chapter 4) suggesting that PGR5 is essential for CET at steady state under non-saturating light intensities in rice. Furthermore, at higher light when transient NPQ relaxed in the WT, as the enzymes of the Calvin-Benson cycle are activated, the OE were able to maintain higher level of NPQ even after 30 min of illumination accompanied by down-regulation of LET. Also, the high NPQ phenotype was sustained at steady-state in PGR5 overexpressors under low moisture stress and when grown as a crop under fluctuating natural light in the glasshouse (see Chapter 5), indicating that the PGR5 protein is required for full expression of NPQ in rice at steady state photosynthesis under constant light, stress as well as in fluctuating natural light.

In addition the relaxation of NPQ at steady state in the WT indicates a progressive substitution of CET by LET as enzymatic reactions of photosynthesis are activated (Breyton et al, 2006). However, high NPQ

sustained at steady state in OE suggest a higher requirement for CET activity at saturating light due partly to significant reduction in the maximum rate of carboxylation as well as stomatal closure in rice which would in turn increase the demand for ATP possibly through photorespiration (see next section). Nevertheless, the activity of PSI CET is enhanced, releasing greater amounts of protons into the thylakoid lumen to build a high ΔpH for generation of NPQ, accompanied by down-regulation electron transport through PSII in saturating light.

These findings are consistent with those of Miyake et al (2004), who found that limitation of LET enhanced cyclic electron flow around PSI which in turn helps to dissipate excess light energy by driving NPQ in intact leaves of tobacco. The maximum rate of CET shown to be approximately two-thirds the maximum rate of LET (Golding & Johnson, 2004) was suggested sufficient to support the ΔpH required to maintain NPQ (Johnson 2004).

6.5 PGR5 impact on CO_2 assimilation

Apart from generating ΔpH for NPQ formation, CET is also suggested to function in supplementing the required amount of ATP needed for a balanced ATP/NADPH consumption of the Calvin-Benson cycle. The actual requirement for ATP/NADPH was outlined by Allen (2003). The Calvin-Benson cycle will require 3ATP:2NADPH per CO_2 assimilated under conditions where both CET and LET function. On the basis of the ATP synthase mechanism, 14 protons are required to synthesize three ATP (4.67 H^+/ATP; Seelert et al. 2000). However, the LET can only translocate 12 protons for every four electrons in the LET chain ($3H^+/e^-$). Thus, the

linear electron flow can generate 2.55ATP/2NADPH (12 protons × 3 ATP/14 protons) with a shortfall of about 0.45 ATP, likely to be met via CET synthesis of additional ATP. The CET translocates $2H^+/e^-$ to balance the shortfall of 2 protons (Allen, 2003).

The changes in the NPQ attributed to increased CET described above (6.4) can be linked to the rate of CO_2 assimilation in the leaves. This effect is seen as consistent reductions in rate of CO_2 assimilation at induction and at steady state assimilation rates in the OE lines (see Chapters 4 & 5). The lag in the rate of photosynthesis during induction is normally associated with slow activation of the Calvin-Benson cycle and other assimilatory processes. Thus the extra NPQ in the OE lines compared to the WT corresponds with lower assimilation rate.

At steady state under low light of 500 µmol $m^{-2}s^{-1}$, leaves are just emerging from induction, increasing activation of CO_2 assimilation will increase ATP utilization, reducing ΔpH and NPQ relaxes. In addition, LET out-compete CET, as rate of PSII excitation increases until a state of balance is reached within the electron transport system. However, under a high light intensity of 1000 µmol $m^{-2}s^{-1}$, rice leaves are saturated or at the point of saturation. A large fraction of P700 is also simultaneously oxidized under strong illumination increasing CET, reducing rate of LET (Joliot & Johnson, 2011; Ott et al, 1999). CO_2 assimilation rate becomes limited due partly to the down-regulation of LET.

The rate of photosynthesis can be limited via three basic biochemical processes (Vcmax, Jmax and TPU, see Chapter 3). The entry point of CO_2

into the Calvin-Benson cycle is through Rubisco while the primary CO_2 acceptor in the cycle is ribulose-1,5-biphosphate (RuBP). Based on Farquhar et al (1980) model of photosynthesis, Vcmax may be Rubisco or CO_2 limited while Jmax is RuBP regeneration or light limited.

In the OE lines, low Vcmax associated with lower Rubisco content and/or decreased Rubisco activities as well as low gs indicate that under ambient CO_2 conditions, CO_2 assimilation may be co-regulated in rice by Rubisco and stomatal resistance which partly explain the lower rate of PSII electron transport capacity in these plants (Chapter 3). This was confirmed by the increased CO_2 assimilation rate under high CO_2 concentrations (Chapter 4), which implies that under ambient CO_2, RuBP carboxylation by Rubisco (Vcmax) was inhibited, promoting Rubisco oxygenase activity and hence photorespiration. The oxygenase activity of Rubisco initiates photorespiration in plants (Tolbert et al, 1995). In addition, reductions in the total chlorophyll content were observed in some of these transgenic plants when compared to the WT (Chapter 3) which might indicate reductions in Rubisco leaf content (Quick et al, 1991).

The reduction in Vcmax in the transgenic OE lines that reduces capacity of CO_2 assimilation may have a 'knock-on' effect on results for both CET and LET. Reductions in CO_2 assimilation implies that PSI electron acceptor, ferredoxin (Fd), becomes increasingly reduced due to limitation of $NADP^+$ regeneration. Accumulation of reduced Fd is likely to promote CET by increasing plastoquinone reduction, subsequently increasing the Q cycle translocation of H+ into the lumen for ATP synthesis and NPQ thereby down-regulating LET (Heber and Walker, 1992). The low NPQ in the RNAi

lines in this study implies an inability to generate ΔpH required to drive ATP synthase for ATP synthesis consistent with pgr5 mutant phenotype described by Munekage et al (2008). ATP supply for photosynthesis cannot be met, leading to inhibition of CO_2 assimilation, since hydrolysis of ATP is required for Rubisco activation (Quick et al, 1991; Portis, 1990) which might suggest that PGR5 function supplying ATP for Rubisco activase partly explaining the low Vcmax in the RNAi lines.

The low rate of RuBP regeneration (Jmax) and CO_2 assimilation in the RNAi lines even at high CO_2, suggests that Rubisco-associated limitations is not the sole factor limiting photosynthesis in rice in the absence of the PGR5 protein but rather limitation partly lies in electron transport. Infiltration with MV showed PSI acceptor side limitation in the RNAi lines (Chapter 3) which may cause over-reduction of the stroma as well as photoinhibition/photodamage of PSI, leading to reduced LET (Munekage et al, 2002). In a recent study, Huang et al (2010) showed that PSII activity could not be recovered if PSI is severely photodamaged.

The Jmax and ϕPSII at high CO_2 allows a comparison of the linear electron transport capacity of the transgenic lines to that of the WT. According to Sharkey (1998), in conditions when RuBP regeneration is limited, increases in CO_2, which suppresses photorespiration, direct more RuBP and energy captured by the PET chain to carboxylation reactions without altering the limitation of RuBP regeneration. Quite reasonably, similar phenomena were also found in the transgenic lines in this study. Unlike under ambient CO_2 level, where ϕPSII in the OE was significantly lower than the WT both in the controlled growth environment and crop glasshouse, ϕPSII in the OE

was not significantly different from the WT under elevated CO_2. This may be due to increased carboxylation rate as photorespiration was suppressed. This is consistent with the Jmax in the OE lines, which was not different from the WT, clearly suggesting that in the OE transgenic rice lines under ambient conditions, the rate of photorespiration was higher, due to reductions in carboxylation rate, thereby reducing rate of LET to the Calvin cycle while increasing CET. This result thus fits with the reductions observed in the Vcmax of the OE lines. Taken together, the Vcmax, OE and ϕPSII results described above clearly show that photorespiration and Rubisco-associated limitations significantly influenced rate of CO_2 assimilation in rice plants overexpressing the PGR5 protein, likely increasing the demands of these lines for ATP. The reduction in ϕPSII of the RNAi under high CO2 could be attributed to possible photodamage/photoinhibition as suggested earlier.

6.6 Role of PGR5 in stress alleviation

In conditions of low atmospheric and soil moisture, plants tend to close their stomata to reduce transpiratory losses, restricting CO_2 uptake (Ci) by leaves (Flexas et al, 2004, 2006), thereby limiting Rubisco carboxylation. This process subsequently increases RuBP oxygenation, increasing photorespiration thereby reducing a plant's ability to efficiently utilize the reducing power of NADPH, the final product of linear electron transport. Similar reports have shown that mild drought stress in plants is accompanied by increased partitioning of electrons to photorespiration as a result of the increase in Rubisco oxygenase activity (Wingler et al, 1999) leading to an increased demand for ATP. Osmond (1981) showed the

importance of CET during photorespiration in supplying the additional required ATP. The shortfall may be worsened under stress conditions, where additional ATP is needed to drive other processes such as protein repair and transport.

In this study, the small reduction in gs, and a relatively large change in Ci observed under low moisture levels, indicates that photorespiration is involved, increasing the demand for ATP due to decrease in CO_2 assimilation to result in an imbalance in the ratio of ATP/NADPH. The 1.5 ratio of ATP/NADPH required by the Calvin-Benson to fix a molecule of CO_2 is reduced to about 1.42 when photorespiratory loses and nitrate assimilation is considered (Edwards & Walker, 1983). PGR5-dependent CET responds to this imbalance in ATP/NADPH by increasing its activity to meet the shortfall in ATP, thus increasing transthylakoid proton gradient (ΔpH) required for generation of NPQ and down-regulating LET as seen in reduced $\phi PSII$. This result is consistent with the findings of Golding & Johnson, 2003. This dynamic response mainly attributed to PGR5 in this study is seen in the strong but negative correlation between NPQ and rate of CO_2 assimilation in the WT. Indeed, the PGR5-CET pathway appears to be a flexible way by which plants maintain a balanced flow of electrons while meeting the required level of ATP.

The increase in electrons partitioned to the process of photorespiration under conditions limiting photosynthesis such as low moisture could prevent the over-reduction of the photosynthetic electron transport chain and photoinhibition by allowing metabolism to continue using the products of photosynthetic electron transport (Osmond and Grace, 1995) thereby

preventing over-reduction of the stroma. A reduced level of photoinhibition is seen as low qI component of NPQ in the OE lines in this study. However, results from this study raise the question of whether increase in the demand for ATP attributed to the photorespiratory process is directly linked to the overexpression of the PGR5 protein? If it does, how?

Photorespiration provides metabolites for other metabolic processes such as supplying glycine for the synthesis of glutathione, a component of the anti-oxidative system in plants involved in stress protection. Synthesis of glutathione was recently highlighted to be regulated by the photosynthetic electron transport system based on its requirement for ATP (Queval & Foyer, 2012). Thus under conditions limiting CO_2 assimilation rate, enhancing photorespiration, PGR5-dependent CET plays an important role in photoprotection of PSI and PSII. In this way the processes of photorespiration, oxidative stress and cyclic electron transport are linked.

Although the Calvin cycle is known to require more ATP than NADPH, photorespiration is a major contributory factor to increased ATP requirement in rice. This is in line with recent studies by Jung et al (2008). These workers on analysing light induced transcripts in rice revealed significant enrichment of the Biological category of GO Slim terms related to known light responses, including photosynthesis and photorespiration. Because photorespiration is a continuous light- dependent reaction under steady decline in moisture level, which is likely to worsen demand for ATP, PGR5-dependent CET activity is in continuous operation, seen as continuous increase in NPQ at steady-state photosynthesis in the OE lines in order to meet such demand, probably protecting thylakoid components

from potential damage. In addition, CET is likely to be sustained by the limitation to $NADP^+$ regeneration due to reduced ϕPSII as seen in the OE, while reduced ferredoxin accumulates to enhance CET. Indeed, as mentioned earlier, CET is suggested sufficient to support the ΔpH required to maintain NPQ (Johnson 2004). These results suggest that PGR5 function in stress alleviation both in the short- and long term and that the PGR5-CET is sensitive to changes in the redox state of the chloroplast stroma via ATP/NADPH ratio. This result implies that the ATP/NADPH modulates PGR5-dependent CET in rice, consistent with previous general views (Johnson, 2005; Bendall & Manasse, 1995).

Based on genetics and reverse-genetics approaches, the loss of either NDH or PGR5 pathways of CET were suggested to be compensated by each other in Arabidopsis (Munekage et al, 2002; Avenson et al, 2005). The findings here suggest otherwise in rice. The PGR5 RNAi rice lines showed a consistent phenotype under stress and non-stress conditions and under high CO_2. The differences in findings might not be unrelated to their contrasting physiology (Hubbart et al, 2012) in addition to differences in the two plants mentioned earlier (section 6.1). This is not surprising since the PGR5 gene showed high conservation within the monocot group (Chapter 3). Furthermore, the best documented cases of genome conservation are from the grass family, Poaceae (Devos & Gale, 2000) to which rice belongs. Adopting new approach of complete sequencing and annotation of bacterial artificial chromosome (BAC)-size clone to catch a glimpse of genome similarities at the micro-level, (Zhu et al, 2003; Liu et al, 2001), comparisons of Arabidopsis and rice led to the conclusion that

Arabidopsis may not be adequate as a model for the structure of grass genomes (Liu et al, 2001; Mayer et al, 2001; Devos et al, 1999).

6.7 Effect of PGR5 on growth and biomass in rice

In the controlled growth chambers, biomass accumulation in the lines studied followed the similar pattern based on CO_2 assimilation rate. This was not the case in the glasshouse experiment. Although Vcmax and Amax were significantly lower in the OE compared to the WT while its SLA was higher ($P<0.05$), there was no significant difference between their biomass. This may be due to the light use efficiency of their canopy.

A key prerequisite for enhanced crop growth and productivity through assimilate conversion into dry matter is to maximize the amount of intercepted radiation (Hopkins & Hüner, 2009; Squire, 1990; Monteith, 1977). The light environment in a crop canopy described as leaf area index (LAI), partly determines the efficiency of canopy radiation utilization (San-oh et al, 2004). In the glasshouse, LAI in the OE and WT was not different and this was reflected in their biomass. Horie & Sakuratani (1985) found that when LAI is small in rice, there is a direct relationship between canopy CO_2 assimilation rate and LAI. LAI in the present study (5.4) was within the range (4-7) proposed by Yoshida (1972). The rapid increase observed in LAI towards the end of growth in the OE, indicated the possibility of leaf shading, probably due in part to flat 'droopy' leaves (Figure 6.1). Increase in LAI late in the season is likely to reduce canopy photosynthesis (Evans & Poorter, 2001). Non reduction in biomass accumulation in the OE may be

due to early establishment advantage due to LAI during the early growth stage.

Tillering is closely related to panicle number per unit ground area and plays an important role in rice grain yield determination (Van Quyen, et al, 2004). Too few tillers result in too few panicles, but excess tillers cause high tiller mortality, small panicles, poor grain filling and consequently reducing grain yield (Peng et al. 1994). In modern rice varieties which tiller profusely, competing for resources under favorable conditions, about 50% of those tillers are productive (Van Quyen, et al, 2004). Numbers of tillers increased significantly in the OE throughout the experimental period in the glasshouse. Whether such tillers will be productive in terms of yield could not be determined within the duration of this experiment. However, Van Quyen et al (2004) indicated that additional tillers become unproductive and lead to excessive LAI and vegetative growth, and a favorable environment for disease development resulting in a higher percentage of unfilled grains. In contrast, Zhong et al. (2002) revealed that LAI and plant N status are two major factors that influence tiller production in rice crops. The same number of tillers was produced by the RNAi in the crop glasshouse and controlled growth chambers.

Plant height is affected by environmental conditions (Yoshida 1981). In the high-density rice field, individual plants prolong their culm to get light due to increasing competition for light (Van Quyen, et al, 2004). In the crop glasshouse experiment, plant height of OE and RNAi were lower than the WT. Light interception as well as biomass was significantly lower in the RNAi.

The cause of the differences observed in biomass between the glasshouse and controlled growth chamber plants is not known, but could be due to variations in light qualities and quantities.

Results from growth, biomass and canopy light use efficiency of WT and transgenic rice plants are consistent with our findings based on physiological characterization. Thus we conclude that the PGR5 protein is essential for efficient leaf photosynthesis, biomass accumulation and crop productivity in rice. However we could not identify any significant photosynthetic advantage due to overexpression of this protein except in photoprotection and regulation of the PET chain.

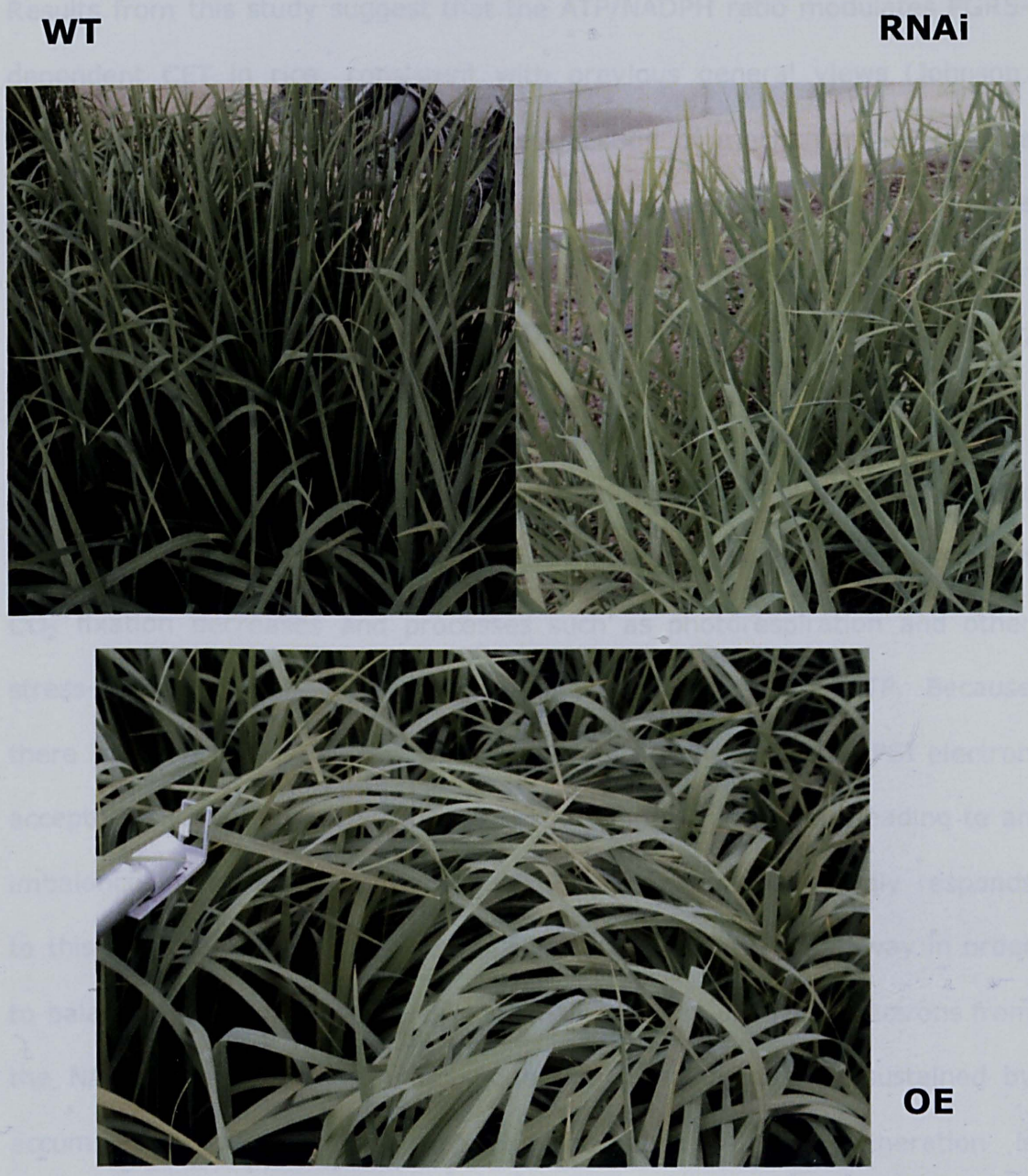

Figure 6. 1 Typical examples of the canopy of the wildtype (WT), RNA interference (RNAi) and overexpressor (OE) transgenic rice crops in the glasshouse.
Note how the OE transgenic line has 'droopy' leaves with lower leaves shaded.

6.8 Regulation of PGR5-CET

Results from this study suggest that the ATP/NADPH ratio modulates PGR5-dependent CET in rice, consistent with previous general views (Johnson, 2005; Bendall & Manasse, 1995). The question of mechanism arises. The mechanism implicated in regulating CEF is not known, but several plausible models were proposed including: via the redox state of NADPH/NADP+ (Munekage et al., 2004), stromal ADP or ATP levels (Joliot and Joliot, 2006), or the availability of PSI electron acceptors (Breyton et al., 2006).

However the present study suggests the following (Figure 6.2): Under conditions where photosynthesis is less efficient or inhibited, the rate of CO_2 fixation decreases and processes such as photorespiration and other stress-related damage imposes additional requirement for ATP. Because there is a deficit for ATP, the accumulation of NADPH and other PSI electron acceptors such as ferredoxin occurs in the chloroplast stroma leading to an imbalance in the ATP/NADPH ratio. PGR5-dependent CET rapidly responds to this cue by increasing the flux of electrons through the pathway in order to balance the redox state of the PET chain thereby diverting electrons from the NADPH pool to the plastoquinone pool. This process is sustained by accumulation of reduced ferredoxin because $NADP^+$ regeneration is inhibited by the slow rate of CO_2 assimilation. The increased rate of CET rapidly results in the formation of a ΔpH across the thylakoid membrane, which induces NPQ, as well as driving ATP synthase to produce ATP. Because of the high energy demand of photorespiration alongside CO_2 fixation, CET/NPQ level is induced and sustained until ATP demand

decrease. Thus the PGR5-dependent CET may be important in meeting demands for ATP in rice.

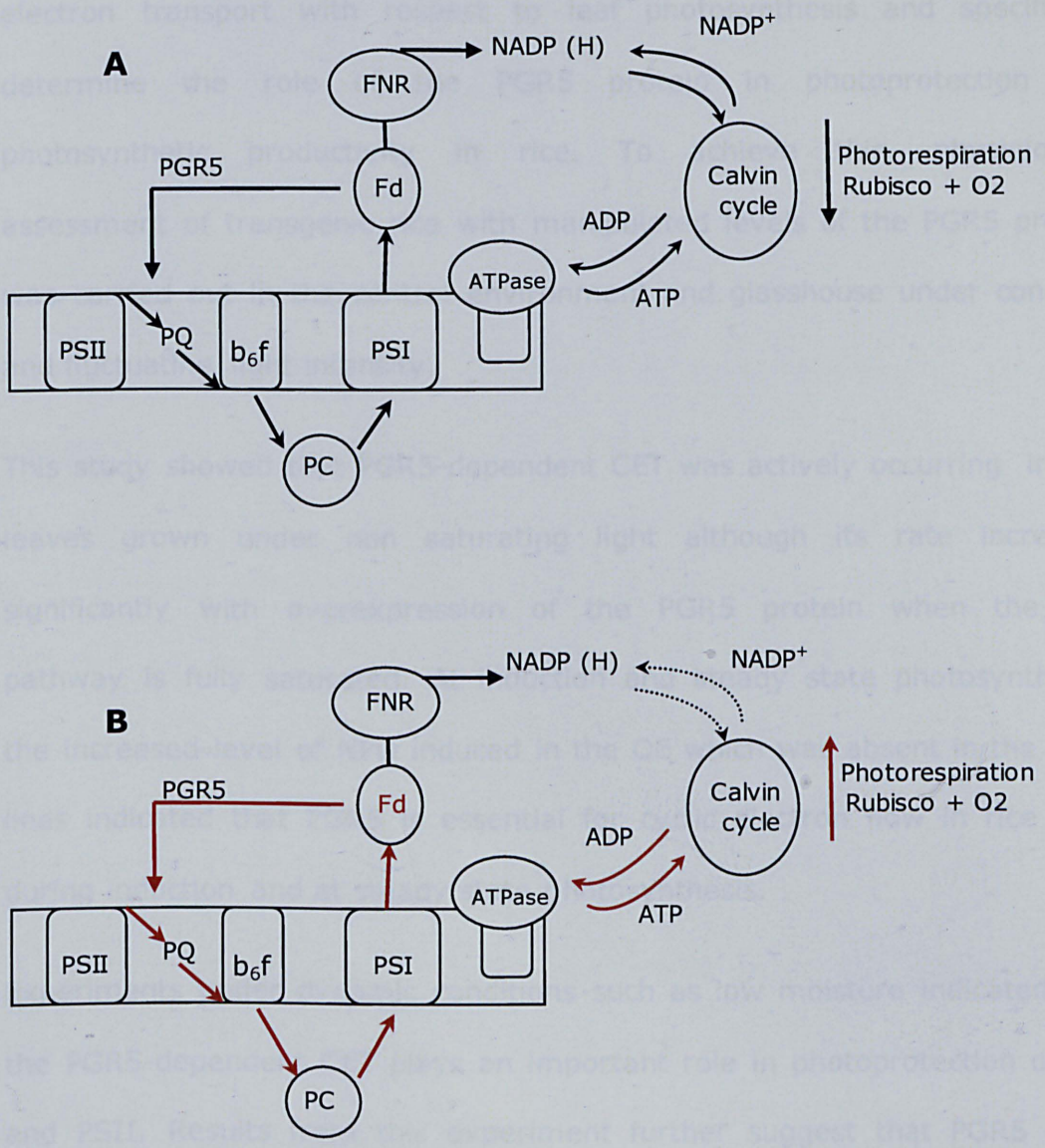

Figure 6. 2 Model of possible cyclic and linear electron transport pathways in rice in (A) ideal condition where ATP/NADPH ratio is in equilibrium (B) conditions causing imbalance in the ATP/NADPH ratio as rate of Rubisco oxygenase activity and photorespiration increase. Arrows in red depict increase in rate. Dash arrows indicate reduction in rate

6.9 Conclusions

This work aimed to improve current knowledge of the regulation of cyclic electron transport with respect to leaf photosynthesis and specifically determine the role of the PGR5 protein in photoprotection and photosynthetic productivity in rice. To achieve this, physiological assessment of transgenic rice with manipulated levels of the PGR5 protein was carried out in the control environment and glasshouse under constant and fluctuating light intensity.

This study showed that PGR5-dependent CET was actively occurring in rice leaves grown under non saturating light although its rate increased significantly with overexpression of the PGR5 protein when the LET pathway is fully saturated. At induction and steady state photosynthesis, the increased level of NPQ induced in the OE which was absent in the RNAi lines indicated that PGR5 is essential for cyclic electron flow in rice both during induction and at steady state photosynthesis.

Experiments under dynamic conditions such as low moisture indicated that the PGR5-dependent CET plays an important role in photoprotection of PSI and PSII. Results from this experiment further suggest that PGR5 could function efficiently in stress alleviation both in the short- and long term.

Considering leaf photosynthesis, growth biomass accumulation in the glasshouse and controlled environment studies, results showed that the PGR5 protein is important in rice leaf photosynthesis. However, in a biomass experiment we could not identify any significant photosynthetic

advantage which could be attributed to overexpression of PGR5 except in photoprotection and regulation of the PET chain.

In terms of regulation of the electron transport system, results indicate that the ATP/NADPH ratio modulates PGR5-dependent CET in rice, and may be important in meeting the demand for ATP in rice.

6.10 Future Work

This works aims to provide a broad and comprehensive physiological characterization of the function of the PGR5 protein in rice photoprotection and photosynthesis. Future work should focus on identifying the specific direct targets of PGR5 involved in these processes. An attempt to address this goal has begun by preliminary microarray analysis of the PGR5 RNAi and WT which will enable identification and validation of novel transcripts of interest with important role in optimizing photoprotection and photosynthesis in order to drive future crop improvement programs.

In addition, identification of some novel genes involved in plant signaling pathways which may influence biomass accumulation in rice and facilitate future manipulation of proteins of interest for further studies would be useful. In plants, proof of concept for this strategy has been demonstrated with the work of Frenkel et al (2009), which showed that photoprotection influences plant fitness, metabolism and gene expression most likely through signalling pathways similar to our findings in the gene expression studies mentioned above. The possibility of a link between PGR5 activity and gene expression and signalling pathways is intriguing and warrant further investigation.

It would be useful to evaluate the contribution of various Rubisco factors limiting CO_2 assimilation such as inhibition in Rubisco activity, reduction in the amount of Rubisco present in the leaf, reduction in Rubisco specificity for CO_2 or an increased affinity of this enzyme for O_2. This is based on the possibility of ΔpH, reduction state of PSI acceptor side and or the degree of thioredoxin pathway modulating the activity of Rubisco activase (Ruuska et al, 2000). Such may pave the way towards a clearer understanding of the regulatory mechanisms involved in the electron transport system in the chloroplast

The physiological function of the water-water cycle in the transgenic rice plants leaves should be determined.

REFERENCES

Ackerman SH, Tzagoloff A (2005) Function, structure, and biogenesis of mitochondrial ATP synthase. *Progress in Nucleic Acid Research & Molecular Biology* 80, 95-133.

Ahn TK, Avenson T, Ballottari M, Cheng YC, Niyogi KK, Bassi R, Fleming GR (2008) Architecture of a charge-transfer state regulating light harvesting in a plant antenna protein. *Science* 320, 794–797

Albertsson PÅ, Andreasson E, Svensson P (1990) The domain of the plant thylakoid membrane. *FEBS Letters* 273, 36-40

Alboresi A, Ballottari M, Hienerwadel R, Giacometti GM, Morosinotto T (2009). Antenna complexes protect Photosystem I from photoinhibition. *BMC Plant Biology* 9, 71

Allen JF (2002) Photosynthesis of ATP—electrons, proton pumps, rotors, and poise. *Cell* 110, 273-276

Allen JF (2004) Cytochrome b_6f: Structure for signalling and vectorial metabolism. *Trends in Plant Science* 9, 130–137.

Allen JF, Forsberg J (2001) Molecular recognition in thylakoid structure and function. *Trends in Plant Science* 6: 317–326

Amunts A, Nelson N (2009) Plant photosystem I design in the light of evolution. *Structure* 17, 637–650

Amunts A, Drory O, Nelson N (2007) The structure of a plant photosystem I supercomplex at 3.4A° resolution. *Nature* 447, 58–63

Anderson JM (1986) Photoregulation of the composition function, and structure of thylakoid membranes. *Annual Review of Plant Physiology* 37, 93-136

Andersson B, Aro EM (2001) Photodamage and D1 protein turnover in photosystem II. In: EM Aro, B Andersson, editors. Regulation of photosynthesis. *Kluwer Academic Publishers, Dordrecht, The Netherlands* 11, 377–393

Arnon DI, Allen MB, Whatley FR (1954) Photosynthesis by isolated chloroplasts. *Nature* 174, 394–396

Asada K (1999) The water-water cycle in chloroplasts: Scavenging of active oxygen and dissipation of excess photons. *Annual Review of Plant Physiology and Plant Molecular Biology* 50, 601-639

Avenson TJ, Kanazawa A, Cruz JA, Takizawa K, Ettinger WE, Kramer DM (2005) Integrating the proton circuit into photosynthesis: progress and challenges. *Plant, Cell & Environment* 28(1), 97–109

Bailey S, Thompson E, Nixon PJ, Horton P, Mullineaux CW, Robinson C, Mann NH (2002) A critical role for the Var2 FtsH homologue of Arabidopsis thaliana in the photosystem II repair cycle in vivo. *Journal of Biological Chemistry* 277, 2006–2011

Barber J, Nield N, Morris EP, Büchel (2000) Revealing the structure of the photosystem II chlorophyll binding proteins, CP43 and CP47. *Biochimica et Biophysica Acta* 1459, 239-247

Barber J, Nield N, Morris EP, Hankamer B (1999) Subunit positioning in photosystem II revisited. *Trends in Biochemical Science* 24, 43-45

Battisti DS, Naylor RL (2009) Historical warnings of future food insecurity with unprecedented seasonal heat. *Science* 323(5911), 240-244

Bellafiore S, Barneche F, Peltier G, Rochaix JD (2005) State transitions and light adaptation require chloroplast thylakoid protein kinase STN7. *Nature* 433, 892–895

Bendall DS, Manasse RS (1995) Cyclic photophosphorylation and electron transport. *Biochimica et Biophysica Acta (BBA) - Bioenergetics* 1229, 23–38

Björkman O, Demmig B (1987) Photon yield of O_2 evolution and chlorophyll fluorescence at 77K among vascular plants of diverse origins. *Planta* 170, 489-504

Blankenship RE ed. (2002) Molecular mechanisms of photosynthesis. *Blackwell Science Ltd. Oxford*

Boekema EJ, Hifney A, Yakushevska AE, Piotrowski M, Keegstra W, et al. (2001) A giant chlorophyll-protein complex induced by iron deficiency in cyanobacteria. *Nature* 412, 745–748

Boekema E, Wynn R, Malkin R (1990) The structure of spinach photosystem I studied by electron microscopy. *Biochimica et Biophysica Acta* 1017, 49–56.

Breyton C, Nandha B, Johnson GN, Joliot P, Finazzi G (2006) Redox modulation of cyclic electron flow around Photosystem I in C3 plants. *Biochemistry* 45, 13465-13475

Breyton C, Tribet C, Olive J, Dubacqi JP, Popot JL (1997) Dimer to monomer conversion of the cytochrome b_6f complex. *Journal Biological Chemistry* 272, 1892–21900

Bunce JA (1981) Comparative responses of leaf conductance to humidity in single attached leaves. *Journal of Experimental Botany* 32, 629-634

Burda K, Kruk J, Schmid GH, Strzalka K (2003) Inhibition of oxygen evolution in photosystem II by Cu (II) ions is associated with oxidation of cytochrome b(559). *Biochemical Journal* 371,597–601

Campbell GS (1986) Extinction coefficients for radiation in plant canopies calculated using an ellipsoidal inclination angle distribution. *Agricultural and Forest Meteorology* 36, 317–321

Cardol P, De Paepe R, Franck F, Forti G, Finazzi G (2010) The onset of NPQ and $\Delta\mu_H^+$ upon illumination of tobacco plants studied through the influence of mitochondrial electron transport. *Biochimica et Biophysica Acta* 1797(2), 177-88

Cassman KG, Liska AJ (2007) Food and fuel for all: Realistic or foolish? *Biofuels, Bioproducts and Biorefining* 1(1), 18–23

Chaves MM, Pereira JS, Maroco J (2003) Understanding plant response to drought – from genes to the whole plant. *Functional Plant Biology* 30, 239-265

Cook AC, Tissue DT, Roberts SW, Oechel WC (1998) Effects of long-term elevated CO2 from natural CO2 springs on *Nardus stricta*: photosynthesis, biochemistry, growth and phenology. *Plant, Cell and Environment* 21, 417–425

Cossins EA, Chen L (1997) Folates and one-carbon metabolism in plants and fungi. *Phytochemistry* 45, 437-452

Cramer WA, Zhang H (2006) Consequences of the structure of the cytochrome b_6f complex for its charge transfer pathways. *Biochimica et Biophysica Acta* 1757, 339–345

Croce R, Weiss S, Bassi R (1999) Carotenoid-binding sites of the major light-harvesting complex II of higher plants. *Journal of Biological Chemistry* 274, 29613-29623

Crookston RK & Moss DN (1974) Interveinal distance for carbohydrate transport in leaves of C_3 and C_4 grasses. *Crop Science* 14, 123-125

Crouchman S, Ruban A, Horton P (2006) PsbS enhances nonphotochemical fluorescence quenching in the absence of zeaxanthin. *FEBS Letters* 580, 2053–2058

DalCorso G, Pesaresi P, Masiero S, Aseeva E, Schunemann D, Finazzi G, Joliot P, Barbato R, Leister D (2008) A complex containing PGRL1 and PGR5 is involved in the switch between linear and cyclic electron flow in *Arabidopsis*. *Cell* 132, 273–28

Damkjaer JT, Kereïche S, Johnson MP, Kovacs L, Kiss AZ, Boekema EJ, Ruban AV, Horton P, Jansson S (2009) The photosystem II light-harvesting protein Lhcb3 affects the macrostructure of photosystem II and the rate of state transitions in Arabidopsis. *Plant Cell* 21, 3245–3256

Danielsson R, Albertsson PÅ, Mamedov F, Styring S (2004) Quantification of photosystem I and II in different parts of the thylakoid membrane from spinach. *Biochimica et Biophysica Acta* 1608, 53–61

Danielsson R, Suorsa M, Paakkarinen V, Albertsson PA, Styring S, Aro EM, Mamedov F (2006) Dimeric and monomeric organization of photosystem II. Distribution of five distinct complexes in the different domains of the thylakoid membrane. *Journal of Biological Chemistry* 281, 4241-14249

Daum B, Nicastro D, Austin JR, McIntosh JR, Kühlbrandt W (2010) Arrangement of photosystem II and ATP synthase in chloroplast membranes of spinach and pea. *The Plant Cell* 22, 1299-1312

De Las Rivas J, Balsera M, Barber J (2004) Evolution of oxygenic photosynthesis: genome-wide analysis of the OEC extrinsic proteins. *Trends in Plant Science* 9(1), 18-25

Dekker JP, Boekema EJ (2005) Supramolecular organization of thylakoid membrane proteins in green plants. *Biochimica et Biophysica Acta* 1706, 12-39

Demmig-Adams B (1990) Carotenoids and photoprotection: a role for the xanthophyll zeaxanthin. *Biochimica et Biophysica Acta* 1020,1-24

Demmig-Adams B, Adams W (1992) Photoprotection and other responses of plants to light stress. Annual *Review of Plant Physiology and Plant Molecular Biology 7*, 1–116

Demmig-Adams B, Winter K, Krüger A, Czygan FC (1989) Light response of CO_2 assimilation, dissipation of excess excitation energy, and zeaxanthin content of sun and shade leaves. *Plant Physiology* 90, 881–88

Devos KM, Beales J, Nagamura Y, Sasaki T (1999) Arabidopsis-rice: will colinearity allow gene prediction across the eudicot-monocot divide? *Genome Research* 9, 825–829

Devos KM, Gale MD (2000) Genome relationships: the grass model in current research. *Plant Cell* 12, 637–646

Eberhard S, Finnazi G, Wollman FA (2008) The dynamics of photosynthesis. *Annual Review of Genetics* 42, 463–515

Edwards G, Walker DA (1983) C3, C4: Mechanisms, cellular and environmental regulation of photosynthesis. *Oxford, Blackwell*

Endo T, Ishida S, Ishikawa N, Sato F (2008) Chloroplastic NAD(P)H dehydrogenase complex and cyclic electron transport around photosystem I. *Molecules and Cells* 25(2), 158-162

Endo T, Shikanai T, Takabayashi A, Asada K, Sato F (1999) The role of chloroplastic NAD(P)H dehydrogenase in photoprotection. *FEBS Letters* 457, 5–8

Evans JR, Poorter H (2001) Photosynthetic acclimation of plants to growth irradiance: the relative importance of specific leaf area and nitrogen partitioning in maximizing carbon gain. *Plant, Cell and Environment* 24, 755–767

Evans LT (1993) Processes, genes, and yield potential. In DR Buxton et al. (ed.) *International crop science. CSSA, Madison, WI687–696*

Fan DY, Nie Q, Hope AB, Hillier W, Pogson BJ, Chow WS (2007) Quantification of cyclic electron flow around photosystem I in spinach leaves during photosynthetic induction. *Photosynth Research* 94, 347–357

Farquhar GD, Von Caemmerer S and Berry JA (1980) A biochemical-model of photosynthetic CO_2 assimilation in leaves of C_3 species. *Planta* 149, 78–90

Finazzi G, Johnson GN, Dall"Osto L, Dallosto L, Joliot P, Wollman FA, Bassi R (2004) A zeaxanthin-independent nonphotochemical quenching mechanism localized in the photosystem II core complex.

Proceedings of the National Academy of Sciences of the United States of America 101(33), 12375-80

Finazzi G, Furia A, Barbagallo RP, Forti G (1999) State transition, cyclic and linear electron transport and photophosphorylation in *Chlamydomonas reinhardtii*. *Biochimica et Biophysica Acta* 1413, 117-129

Flexas J, Ribas-Carbó M, Bota J, Galmés J, Henkle M, Martínez-Cañellas S, Medrano H (2006) Decreased Rubisco activity during water stress is not induced by decreased relative water content but related to conditions of low stomatal conductance and chloroplast CO_2concentration. *New Phytologist* 172, 73-82

Flexas J, Bota J, Loreto F, Cornic G, Sharkey TD (2004) Diffusive and metabolic limitations to photosynthesis under drought and salinity in C3 plants. *Plant Biology* 6, 269–79

Foyer CH, Shigeoka S (2011) Understanding oxidative stress and antioxidant functions to enhance photosynthesis. *Plant Physiology* 155, 93–100

Frenkel M, Külheim C, Jänkänpää HJ, Skogström O, Dall'Osto L, Agren J, Bassi R, Moritz T, Moen J, Jansson S (2009) Improper excess light energy dissipation in Arabidopsis results in a metabolic reprogramming. *BMC Plant Biology* 9, 12

Gale MD, Devos KM (1998) Comparative genetics in the grasses. *Proceedings of National Academy of Science USA* 95(5), 1971–1974

Genty B, Briantais JM, Baker NR (1989) The relationship between the quantum yield of photosynthetic electron transport and quenching of chlorophyll fluorescence. *Biochimica et Biophysica Acta* 990, 87–92

Gilmore AM, Hazlett TL, Debrunner PG, Govindjee (1996) Comparative time-resolved photosystem II chlorophyll a fuorescence analyses reveal distinctive differences between photoinhibitory reaction centre damage and xanthophyll cycle-dependent energy dissipation. *Photochemistry and Photobiology* 64, 552-563

Goff SA, Ricke D, Lan TH, Presting G, Wang R, Dunn M, Glazebrook J, Sessions A, Oeller P, Varma H, Hadley D, Hutchison D, Martin C, Katagiri F, Lange BM, Moughamer T, Xia Y, Budworth P, Zhong J, Miguel T, Paszkowski U, Zhang S, Colbert M, Sun WL, Chen L, Cooper B, Park S, Wood TC, Mao L, Quail P, et al. (2002) A draft sequence of the rice genome (Oryza sativa L. ssp. japonica). *Science* 296, 92-100

Golding AJ, Finazzi G, Johnson GN (2004) Reduction of the thylakoid electron transport chain by stromal reductants--evidence for activation of cyclic electron transport upon dark adaptation or under drought. *Planta* 220(2), 356-363

Golding AJ, Johnson GN (2003) Down-regulation of linear and activation of cyclic electron transport during drought. *Planta* 218, 107–114

Groth G, Pohl E (2001) The structure of the chloroplast F1-ATPase at 3.2 Å resolution. *Journal of Biological Chemistry* 276, 1345–1352.

Groth G, Strotmann H, (1999) New results about structure, function and regulation of the chloroplast ATP synthase (CF0CF1). *Plant Physiology* 106, 142-148

Hald S, Pribil M, Leister D, Gallois P, Johnson GN (2008) Competition between linear and cyclic electron flow in plants deficient in Photosystem I. *Biochimica et Biophysica Acta* 1777, 1173–1183

Haldrup A, Jensen PE, Lunde C, Scheller HV (2001) Balance of power: A view of the mechanism of photosynthetic state transitions. *Trends in Plant Science* 6, 301–305

Halliwell B, Gutteridge JMC (1992) Free radicals, antioxidants and human diseases: where are we now? *Journal of Laboratory and Clinical Medicine* 119, 598-620

Hall TA (1999) BioEdit: a user-friendly biological sequence alignment editor and analysis program for Windows 95/98/NT. *Nucleic Acids Symposium Series* 41, 95-98

Hankamer B, Barber J, Boekema EJ (1997) Structure and membrane organization of photosystem II in green plants. *Annual Review of Plant Physiology and Plant Molecular Biology* 48, 641-671

Harbinson J, Foyer CH (1991) Relationships between the efficiencies of photosystems I and II and stromal redox state in CO_2-free air. *Plant Physiology* 97, 41–49

Havaux M (1988) Carotenoids as membrane stabilizers in chloroplasts. *Trends in Plant Science* 4, 147–151

Hayashi K (1972) Efficiencies of solar energy conversions in rice varieties. *Bulletin of the National Institute of Agricultural Sciences series D (plant physiology, genetics and crops in general)* 23, 1-68

Heber U, Walker D (1992) Concerning a dual function of coupled cyclic electron transport in leaves. *Plant Physiology 100*(4), 1621-1626

Heber U, Egneus H, Hanck U, Jensen M, Köster S (1978) Regulation of photosynthetic electron transport and photophosphorylation in intact chloroplasts and leaves of *Spinacia oleracea* L. *Planta* 143, 41–49

Henmi T, Miyao M, Yamamoto Y (2004) Release and reactive-oxygen-mediated damage of the oxygen-evolving complex subunits of PSII during photoinhibition. *Plant Cell Physiology* 45,243 –250

Herbert SK, Fork DC, Malkin S (1990) Photoaccoustic measurements *in vivo* of energy storage by cyclic electron flow in algae and higher plants. *Plant Physiology* 94, 926–934

Hirasawa T (1999) Physiological characterization of rice plant for tolerance of water deficit. In: O Ito, JC O'Toole, B Hardy, editors. Genetic improvement of rice for water-limited environments. *International Rice Research Institute (IRRI) Los Banos, Philippines* 89–98

Hibberd JM, Sheehy JE, Langdale JA (2008) Using C_4 photosynthesis to increase the yield of rice—rationale and feasibility. *Current Opinion in Plant Biology* 11, 228–231

Holt NE, Fleming GR, Niyogi KK (2004) Toward an understanding of the mechanism of nonphotochemical quenching in green plants. *Biochemistry* 43, 8281–8289

Hopkins WG, Hüner NPA (2009) *Introduction to Plant Physiology, 4th Edition, Wiley*

Horie T, Sakuratani T (1985) Studies on crop-weather relationship model in rice. (1) Relation between absorbed solar radiation by the crop and the dry matter production. *Journal of Agricultural Meteorology of Japan* 40, 331–34

Horton P, Johnson MP, Perez-Bueno ML, Kiss AZ, Ruban AV (2008) Photosynthetic acclimation: Does the dynamic structure and macro-organisation of photosystem II in higher plant grana membranes regulate light harvesting states? *FEBS Journal* 275, 1069–1079

Horton P, Murchie EH, Ruban AV, Walters RG (2001) Increasing rice photosynthesis by manipulation of the acclimation and adaptation to light. *Novartis Foundation symposium* 236, 117-134

Horton P, Ruvan AV, Walter RG (1996) Regulation of light harvesting in green plants. *Annual Review of Plant Physiology Plant Molecular Biology* 47, 655-684

Horton P (1983) Effects of changes in the capacity for photosynthetic electron transfer and photophosphorylation on the kinetics of fluorescence induction in isolated chloroplasts. *Biochimica et Biophysica Acta* 724, 404–410

Horvath EM, Peter SO, Joet T, Rumeau D, Cournac L, Horvath GV, Kavanagh TA, Schafer C, Peltier G, Medgyesy P (2000) Targeted inactivation of the plastid ndhB gene in tobacco results in an enhanced sensitivity of photosynthesis to moderate stomatal closure. *Plant Physiology* 123, 1337–1350.

Hoshikawa K (1989) The growing rice plant. An anatomical monograph. Published by; *Nosan gyosan bunka kyokai (nobunkyo) 7-6-1 Alasaka, Minatoku, Tokyo 107 Japan.*

Hsing YI, Chern CG, Fan MJ, Lu PC, Chen KT, Lo SF, Sun PK, Ho SL, Lee KW, Wang YC, *et al.* (2007) A rice gene activation/knockout mutant resource for high throughput functional genomics. *Plant Molecular Biology* 63, 351-364

Hubbart S, Ajigboye OO, Horton P, Murchie EH (2012) The photoprotective protein PsbS exerts control over CO_2 assimilation in fluctuating light in rice. *The Plant Journal* 71, 402-412

Hubbart S, Peng S, Horton P, Chen Y, Murchie EH (2007) Trends in leaf photosynthesis in historical rice varieties developed in the Philippines since 1966. *Journal of Experimental Botany 58*(12), 3429-3438

Ibaraki Y, Murakami J (2006) Distribution of chlorophyll fluorescence parameter Fv/Fm within individual plants under various stress conditions. *ISHS Acta Horticulturae 761, XXVII*

IRGSP (2005) The map-based sequence of the rice genome. *Nature* 436, 793–800

Ishida H, Nishimori Y, Sugisawa M, Makino A & Mae T (1997) The large subunit of ribulose-l,5-bisphosphate carboxylase/oxygenase into 37-kDa and 16-kDa polypeptides by active oxygen in the lysates of chloroplasts from primary leaves of wheat. *Plant and Cell Physiology 38*, 471- 479

Ishida H, Shimizu S, Makino A & Mae T (1998) Light-dependent fragmentation of the large subunit of ribulose-l,5-bisphosphate carboxylase/oxygenase in chloroplasts isolated from wheat leaves. *Planta* 204, 305-309

Ishikita H, Saenger W, Loll B, Biesiadka J, Knapp EW (2006) Energetics of a possible proton exits pathway for water oxidation in photosystem II. *Biochemistry* 45, 2063-2071

Jaleel CA, Riadh K, Gopi R, Manivannan P, Ines J, Al-Juburi HJ, Chang-Xing Z, (...), Panneerselvam R (2009) Antioxidant defense responses: Physiological plasticity in higher plants under abiotic constraints. *Acta Physiologiae Plantarum* 31(3), 427-436

Jensen PE, Bassi R, Boekema EJ, Dekker JP, Jansson S, Leister D, Robinson C, Scheller HV (2007) Structure, function and regulation of plant photosystem I. *Biochimica et Biophysica Acta* 1767, 335–352.

Jiang CD, Gao HY, Zou Q, Jiang GM, Li LH (2006) Leaf orientation, photorespiration and xanthophyll cycle protects young soybean leaves against high irradiance in field. *Environmental and Experimental Botany 55*(1-2), 87-96

Joët T, Holterman L, Stedman TT, Kocken CHM, van der wel A, Thomas AW, Krishna S (2002) Comparative characterization of hexose transporters of *Plasmodium knowlesi*, *Plasmodium yoelii* and *toxoplasma gondii* highlights functional differences within the apicomplexan family. *Biochemical Journal* 368, 923–929

Johnson GN (2011) Physiology of PSI cyclic electron transport in higher plants. *Biochimica et Biophysica Acta (BBA) – Bioenergetics* 1807, 906–911

Johnson GN (2005) Cyclic electron transport in C_3 plants: Fact or artefact? *Journal of Experimental Botany 6*(411), 407- 416

Johnson GN (2005) Controversy remains: regulation of pH gradient across the thylakoid membrane. TRENDS in Plant Science 9, 570-571

Johnson GN (2003) Thiol regulation of the thylakoid electron transport chain--a missing link in the regulation of photosynthesis? *Biochemistry* 42(10), 3040-3044

Johnson GN, Young AJ, Scholes JD, Horton P. 1993. The dissipation of excess excitation energy in British plant species. *Plant, Cell and Environment* 16, 673-679

Johnson MP, Ruban AV (2011) Restoration of rapidly-reversible photoprotective energy dissipation in the absence of PsbS protein by enhanced ΔpH. *Journal of Biological Chemistry* 286, 19973-19981

Johnson MP, Ruban AV (2010) Arabidopsis plants lacking PsbS protein possess photoprotective energy dissipation. *Plant J*ournal 61(2), 283-289

Joliot P, Johnson GN (2011) Regulation of Cyclic and Linear Electron Flow in Higher Plants. *Proceedings of the National Academy of Sciences USA* 108, 13317-13321

Joliot PA, Finazzi G (2010) Proton equilibration in the chloroplast modulates multiphasic kinetics of nonphotochemical quenching of fluorescence in plants. *Proceedings of the National Academy of Sciences USA* 107(28), 12728–12733

Joliot P, Joliot A. (2006) Cyclic Electron flow in C3 plants. *Biochimica et Biophysica Acta* 1757, 362–368

Joliot P, Joliot A (2002) Cyclic electron transfer in plant leaf. *Proceedings of National Academy of Science USA 99*(15), 10209-10214

Jordan DB, Ogren WL (1984) The CO2/O2 specificity of ribulose-1,5-bisphosphate carboxylase oxygenase - dependence on ribulose bisphosphate concentration, pH and temperature. *Planta* 161, 308–313

Jung KH, Dardick C, Bartley LE, Cao P, Phetsom J, Canlas P, Seo YS, Shultz M, Frank BC, Ly E, Zheng L, Jia, Y, Hsia AP, An K, Chou HH, Rocke D, Lee GC, Schnable PS, An G, Buell CR, Ronald PC (2008) Refinement of Light-Responsive Transcript Lists Using Rice Oligonucleotide Arrays: Evaluation of Gene-Redundancy. *PLoS ONE 3(10), e3337. doi:10.1371 / journal . pone. 0003337*

Kaiser WM (1979) Reversible inhibition of the Calvin cycle and activation of oxidative pentose phosphate cycle in isolated intact chloroplasts by hydrogen peroxide. *Planta* 145, 377–382

Kalituho L, Beran KC, Jahns P (2007) The transiently generated non-photochemical quenching of excitation energy in Arabidopsis leaves is modulated by zeaxanthin. *Plant Physiology* 143, 1861–1870

Kasajima I, Ebana K, Yamamoto T, Takahara K, Yano M, Yamada MK, Uchimiya H (2011) Molecular distinction in genetic regulation of

nonphotochemical quenching in rice. *Proceedings of the National Academy of Sciences USA* 108(33), 3835–13840

Kawamitsu Y, Hakoyama S, Agata W, Takeda T (1985) Leaf interveinal distances corresponding to anatomical types in grasses. *Plant Cell Physiology* 26(3), 589-593

Kirchhoff H, Schöttler MA, Maurer J, Weis E (2004) Plastocyanin redox kinetics in spinach chloroplasts: evidence for dis-equilibrium in the high potential chain. *Biochimica et Biophysica Acta* 1659, 63–72.

Kiss AZ, Ruban AV, Horton P (2008) The PsbS protein controls the organization of the photosystem II antenna in higher plant thylakoid membranes. *Journal of Biological Chemistry* 283, 3972–3978

Klughammer C, Schreiber U (1994) An improved method, using saturating light pulses, for the determination of photosystem I quantum yield via $P700^+$ absorbance changes at 830 nm. *Planta* 192, 261-268

Kok B, Forbush B, McGloin M (1970) Cooperation of charges in photosynthetic O_2 evolution-I, A linear four step mechanism. *Photochemistry and Photobiolology* 11(6), 457-475.

Kramer DM, Avenson TJ, Edwards GE (2004) Dynamic flexibility in the light reactions of photosynthesis governed by both electron and proton transfer reactions. *Trends in Plant Science* 9, 349–357

Krause GH, Weis E (1991) Chlorophyll fluorescence and photosynthesis: the basics. *Annual Review of Plant Physiology and Plant Molecular Biology* 42, 313-349

Külheim C, Ågren J, Jansson S (2002) Rapid regulation of light harvesting and plant fitness in the field. *Science* 297, 91–93

Kurisu G, Zhang H, Smith JL, Cramer WA (2003) Structure of the cytochrome *b6f* complex of oxygenic photosynthesis: Tuning the cavity. *Science* 302, 1009–1014.

Li XP, Gilmore AM, Caffarri S, Bassi R, Golan T, Kramer D, Niyogi KK (2004) Regulation of photosynthetic light harvesting involves intrathylakoid lumen pH sensing by the PsbS protein. *Journal of Biological Chemistry* 279: 22866–22874

Li XP, Muller-Moule P, Gilmore AM, Niyogi KK(2002) PsbS-dependent enhancement of feedback de-excitation protects photosystem II from photoinhibition. *Proceedings of the National Academy of Sciences USA* 99, 15222–15227

Liu H, Sachidanandam R, Stein L (2001) Comparative genomics between rice and *Arabidopsis* shows scant collinearity in gene order. *Genome Research* 11, 2020–2026

Livingston AK, Cruz JA, Kohzuma K, Dhingra A, Kramer DM (2010) An Arabidopsis mutant with high cyclic electron flow around photosystem I (hcef) involving the NADPH dehydrogenase complex. *Plant Cell* 22, 221–233

Lokstein H, Grimm B (2007) Chlorophyll-binding Proteins. *eLS*

Loll B, Kern J, Saenger W, Zouni A, Biesiadka J (2005) Towards complete cofactor arrangement in the 3.0 Å resolution structure of photosystem II. *Nature* 438, 1040–1044

Long SP, Zhu XG, Naidu SL, Ort DR (2006) Can improvement in photosynthesis increase crop yields? *Plant, Cell and Environment* 29, 315-330

Long TA, Okegawa Y, Shikanai T, Schmidt GW, Covert SF (2008) Conserved role of proton gradient regulation 5 in the regulation of PSI cyclic electron transport. *Planta* 228(6), 907-918

Lunde C, Jensen PE, Haldrup A, Knoetzel J, Scheller HV (2000) The PSI-H subunit of photosystem I is essential for state transitions in plant photosynthesis. *Nature* 408 613–615

Makino A, Miyake C, Yokota A (2002) Physiological functions of the water-water cycle (Mehler Reaction) and the cyclic electron flow in rice leaves. *Plant Cell Physiology* 43(9), 1017-1026

Makino A, Shimada T, Takumi S, Kaneko K, Matsuoka M, Shimamoto K, Nakano H, Miyao-Tokutomi M, Mae T, Yamamoto N (1997) Does decrease in ribulose-1,5-bisphosphate carboxylase by antisense *rbc*S lead to a higher N-use efficiency of photosynthesis under saturating CO_2 and light in rice plants? *Plant Physiology* 114, 483–491

Maxwell K, Johnson G (2000) Chlorophyll fluorescence – a practical guide. *Journal of Experimental Botany* 51(345), 659-668

Mayer K, Murphy G, Tarchini R, Wambutt R, Volckaert G, Pohl T, Dusterhoft A, Stiekema W, Entian KD, Terryn N et al (2001) Conservation of microstructure between a sequenced region of the genome of rice and multiple segments of the genome of *Arabidopsis thaliana*. *Genome Research* 11, 1167–1174

Medrano H, Escalona JM, Bota J, Gulías J, Flexas J (2002) Regulation of photosynthesis of C_3 plants in response to progressive drought: stomatal conductance as a reference parameter. *Annals of Botany* 89, 895-905

Melis A (1991) Dynamics of photosynthetic membrane composition and function. *Biochimica et Biophysica Acta* 1058, 87-106

Miki D, Shimamoto K (2004) Simple RNAi vectors for stable and transient suppression of gene function in rice. *Plant Cell Physiology* 45, 490–495.

Mishra Y, Jänkänpää HJ, Kiss AZ, Funk C, Schröder WP, Jansson S (2012) Arabidopsis plants grown in the field and climate chambers significantly differ in leaf morphology and photosystem components. *BMC Plant Biology* 12, 6

Mitchell PL, Sheehy JE (2006) Supercharging rice photosynthesis to increase yield. *New Phytologist* 171, 688-693

Miyake C (2010) Alternative electron flows (water–water cycle and cyclic electron flow around psi) in photosynthesis: molecular mechanisms and physiological functions. *Plant Cell Physiology* 51(12), 1951–1963

Miyake C, Horiguchi S, Makino A, Shinzaki Y, Yamamoto H, Tomizawa K (2005) Effects of light intensity on cyclic electron flow around PSI and its relationship to non-photochemical quenching of chlorophyll fluorescence in tobacco leaves. *Plant Cell Physiology 46*(11), 1819-1830

Miyake C, Shinzaki Y, Miyata M, Tomizawa K (2004) Enhancement of cyclic electron flow around PSI at high light and its contribution to the induction of non-photochemical quenching of chl fluorescence in intact leaves of tobacco plants. *Plant Cell Physiology* 45, 1426–1433

Miyata K, Noguchi K, Terashima I (2012) Cost and benefit of the repair of photodamaged photosystem II in spinach leaves: roles of acclimation to growth light. *Photosynthesis Research* 113, 165-180

Mlodzinska E (2009) Survey of Plant Pigments. Molecular environmental deteminants of plant colors. *Acta Biologica Cracovienna* 51, 7-16

Mohapatra PK, Kariali E (2008) Time of emergence determines the pattern of dominance of rice tillers. *Australian Journal of Crop Science* 1, 53–62

Monteith JL (1977) Climate and efficiency of crop production in Britain. *Philosophical Transactions of Royal Society London* 281, 277-294

Munekage Y, Eymery F, Rumeau D, Cuiné S, Oguri M, Nakamura N, Yokota A, Genty B, Peltier G (2010) Elevated expression of PGR5 and NDH-H in bundle sheath chloroplasts in C_4 *Flaveria* species. *Plant Cell Physiology* 51, 664-668

Munekage YN, Genty B, Peltier G (2008) Effect of *PGR5* impairement on photosynthesis and growth in *Arabidopsis thaliana*. *Plant Cell Physiology* 49(11), 1688-1689

Munekage Y, Hashimoto M, Miyaka C, Tomizawa KI, Tasaka M, Shikanai T (2004) Cyclic electron flow around photosystem I is essential for photosynthesis. *Nature* 429, 579-582

Munekage Y, Hojo M, Meurer J, Endo T, Tasaka M, Shikanai T (2002) PGR5 is involved in cyclic electron flow around photosystem I and is essential for photoprotection in Arabidopsis. *Cell* 110, 361–37

Munekage Y, Takeda S, Endo T, Jahns P, Hashimoto T, Shikanai T (2001) Cytochrome b(6)f mutation specifically affects thermal dissipation of absorbed light energy in Arabidopsis. *Plant Journal* 28, 351–359

Munné-Bosch S, Shikanai T, Asada K (2005) Enhanced ferredoxin-dependent cyclic electron flow around photosystem I and *a*-tocopherol quinone accumulation in water-stressed *ndhB*-inactivated tobacco mutants. *Planta* 222, 502–511

Murchie EH, Niyogi KK (2011) Manipulation of photoprotection to improve plant photosynthesis. *Plant Physiology* 155, 186-192

Murchie EH, Pinto M, Horton P (2009) Agriculture and the new challenges for photosynthesis research. *New Phytologist* 181,532-552

Murchie E, Horton P (2007) *Toward* C4 rice: learning from acclimation of photosynthesis in the C_3 leaf. *In* JE Sheehy, PL Mitchell, B Hardy editors. *Charting pathways to C_4 rice. Los Banos, Philippines: International Rice Research Institute, 333–350*

Murchie EH, Hubbart S, Peng S, Horton P (2005) Acclimation of photosynthesis to high irradiance in rice: gene expression and interactions with leaf development. *Journal of Experimental Botany* 56, 449-460

Murchie EH, Chen Y, Hubbart S, Peng S, Horton P (1999) Interactions between senescence and leaf orientation determine in situ patterns

of photosynthesis and photoinhibition in field-grown rice. *Plant Physiology* 119, 553-563

Müller P, Li X, Niyogi KK (2001) Non-photochemical quenching. A response to excess light energy. *Plant Physiology* 125, 1558-1566

Nandha B, Finazzi G, Joliot P, Hald S, Johnson GN (2007) The role of PGR5 in the redox poising of photosynthetic electron transport. *Biochimica et Biophysica Acta (BBA) – Bioenergetics* 1767, 1252-1259

Navas ML, Garnier E (2002) Plasticity of whole plant and leaf traits in Rubia peregrina in response to light, nutrient and water availability. *Acta Oecologica* 23, 375–38

Nelson N, Ben-Shem A (2004) The complex architecture of oxygenic photosynthesis. *Nature Review Molecular Cell Biology* 5, 971–982

Nelson N, Yocum CF (2006) The structure and function of photosystems I and II. *Annual Review of Plant Biology* 57, 521-565

Niyogi KK (1999) Photoprotection revisited: Genetic and molecular approaches. *Annual Review of Plant Physiology and Plant Molecular Biology 50*, 333-359

Norman JM (1979) Modeling the complete crop canopy. In BJ Barfield, J Gerber, editors. *Modification of the Aerial Environment of Crops. American Society of Agricultural Engineers* 249-277.

Notredame C, Higgins D, Heringa J (2000) T-Coffee: A novel method for multiple sequence alignment. *Journal of Molecular Biology* 302, 205-217

Nutrient Manager for Rice (2012) *International Rice Research Institute* (IRRI) www.irri.org/irrc/ssnm

Okegawa Y, Kagawa Y, Kobayashi Y, Shikanai T (2008) Characterization of factors affecting the activity of photosystem I cyclic electron transport in chloroplasts. *Plant Cell Physiology* 49, 825–834

Okegawa Y, Long TA, Iwano M, Takayama S, Kobayashi Y, Covert SF, Shikanai T (2007) A balanced PGR5 level is required for chloroplast development and optimum operation of cyclic electron transport around photosystem I. *Plant Cell Physiology* 48, 1462–1471

Ort DR, Zhu X, Melis A (2011) Optimizing antenna size to maximize photosynthetic efficiency. Plant Physiology 155, 79–85

Osmond CB, Grace SC (1995) Perspectives on photoinhibition and photorespiration in the field: quintessential inefficiencies of the light and dark reactions of photosynthesis? *Journal of Experimental Botany* 46, 1351–1362

Osmond CB (1981) Photorespiration and photoinhibition. Some implications for the energetics of photosynthesis. *Biochimica et Biophysica Acta* 639:77–98

Ott T, Clarke J, Birks K, Johnson GN (1999) Regulation of higher plant photosynthetic electron transport. *Planta* 209, 250-258

Palatnik JF, Carrillo N & Valle EM (1999) The role of photosynthetic electron transport in the oxidative degradation of chloroplastic glutamine synthetase. *Plant Physiology* 121, 471-478

Peng L, Shikanai T (2011) Supercomplex formation with photosystem I is required for the stabilization of the chloroplast NADH dehydrogenase-like complex in Arabidopsis. *Plant Physiology* 155, 1629-1639

Peng S, Khush GS, Cassman KG (1994) Evolution of the new plant ideotype for increased yield potential. In: KG Cassman, editors. Breaking the potential in favorable environments, *International Rice Research Institute (IRRI)* 5-20

Pfündel E, Klughammer C, Schreiber, U (2008) Monitoring the effects of reduced PS II antenna size on quantum yields of photosystems I and II using the Dual-PAM-100 measuring system. *PAM Application Notes* 1, 21-24

Porra RJ, Thompson WA, Kriedemann PE (1989) Determination of accurate extinction coefficients and simultaneous-equations for assaying chlorophyll-A and chlorophyll-B extracted with 4 different solvents—verification of the concentration of chlorophyll standards by atomic-absorption spectroscopy. *Biochemical et Biophysica Acta* 975 384–394

Portis AR (1992) Regulation of ribulose 1,5-bisphosphate carboxylase/oxygenase activity. *Annual Review of Plant Physiology and Plant Molecular Biology* 43, 415–437

Portis AR (1990) Rubisco activase. *Biochimica et Biophysica Acta* 1015(1), 15–28

Pospíšil P (2011) Enzymatic function of cytochrome b559 in photosystem II. *Journal of Photochemistry and Photobiology B: Biology* 104, 341–347

Queval G, Foyer CH (2012) Redox regulation of photosynthetic gene expression. *Philosophical Transactions of the Royal Society B: Biological Sciences* 367, 3475-3485

Quick WP, Horton P (1984) Studies on the induction of chlorophyll fluorescence in barley protoplasts. I. Factors affecting the observation of oscillations in the yield of chlorophyll fluorescence and the rate of oxygen evolution. *Proceedings of the Royal Society of London* 220, 361–370

Quick WP, Schurr U, Scheibe R, Schulze ER, Rodermel SR, Bogorad L, Stitt M (1991) Decreased ribulose-1,5-bisphosphate carboxylase-oxygenase in transgenic tobacco transformed with "antisense" *rbc*S.I. Impact on photosynthesis in ambient growth conditions. *Planta* 183, 542–554

Reinhardt D, Kuhlemeier C (2002) Plant architecture. *EMBO* Rep 3, 846-851

Rizhsky L, Liang H, Mittler R (2003) The water-water cycle is essential for chloroplast protection in the absence of stress. *Journal of Biological Chemistry* 278, 38921–38925

Roose JL, Wegener KM, Pakrasi HB (2007) The extrinsic proteins of photosystem II. *Photosynthesis Research* 92(3), 369-387

Ruban AV, Wentworth M, Horton P (2001) Kinetic analysis of non-photochemical quenching of chlorophyll fluorescence. I. Isolated chloroplasts. *Biochemistry* 40, 9896-9901

Rumeau D, Peltier G, Cournac L (2007) Chlororespiration and cyclic electron flow around PSI during photosynthesis and plant stress response. *Plant, Cell & Environment* 30(9), 1041-1051

Russell G, Jarvis PG, Monteith JL (1989) Absorption of radiation by canopies and stand growth. In: G Russell, B Marshall, PG Jarvis, editors. Plant canopies: their growth, form and function. *Cambridge University Press, Cambridge*, UK 21-39

Ruuska SA, Badger MR, Andrews TJ, von Caemmerer S (2000) Photosynthetic electron sinks in transgenic tobacco with reduced amounts of Rubisco: little evidence for significant Mehler reaction. *Journal of Experimental Botany* 51, 357–368.

Sage RF, Sharkey TD, Seemann JR (1989) Acclimation of photosynthesis to elevated CO2 in 5 C3 species. *Plant Physiology* 89, 590–596

Saitou N, Nei M (1987) The neighbor joining method: a new method for reconstructing phylogenetic trees. *Molecular Biology and Evolution* 4, 406-425

San-oh Y, Mano Y, Ookawa T, Hirasawa T (2004). Comparison of dry matter production and associated characteristics between direct-sown and transplanted rice plants in a submerged paddy field and relationships to planting patterns. *Field Crops Research* 87, 43–58

Sarvikas P, Hakala M, Pätsikka E, Tyystjärvi T, Tyystjärvi E (2006) Action of spectrum of photoinhibition in leaves of wild and *npq1-2* and *npq4-1* mutants of *Arabidopsis thaliana. Plant Cell Physiology* 49, 391-400

Sazanov LA, Burrows PA, Nixon PJ (1998) The plastid ndh genes code for an NADH-specific dehydrogenase: isolation of a complex I analogue from pea thylakoid membranes. *Proceedings of the National Academy of Sciences USA* 95, 1319–132

Schreiber U (2004) Pulse-Amplitude (PAM) fluorometry and saturation pulse method. In: G Papageorgiou, Go-vindjee, editors. Chlorophyll fluorescence: A signature of photosynthesis. *Kluwer Academic Publishers, Dordrecht, The Netherlands* 279-319

Schreiber U, Klughammer C, Neubauer C (1988) Measuring P700 absorbance changes around 830 nm with a new type of pulse modulation system. *Z Naturforsch* 43C, 686-698

Schurr U, Walter A, Rascher U (2006) Functional dynamics of plant growth and photosynthesis–from steady-state to dynamics–from homogeneity to heterogeneity. *Plant, Cell and Environment* 29, 340-352

Seelert H, Poetsch A, Dencher NA, Engel A, Stahlberg H, Müller DJ (2000) Structural biology: proton-powered turbine of a plant motor. *Nature* 405, 418–419

Seemann JR, Kirothouem MF, Sharkey TD, Pedray RW (1988) Regulation of ribulose-1,5-bisphosphate carboxylase activity in *Alocasia macrorrhiza* in response to step changes in irradiance. *Plant Physiology* 88, 148–152

Sharkey TD (1998) Photosynthetic carbon reduction. Chapter 8 In: AS Raghavendra, editor. Photosynthesis: A Comprehensive Treatise. *Cambridge University Press, Cambridge* 111-122

Sharkey TD, Bernacchi CJ, Farquhar GD, Singsaas EL (2007) Fitting photosynthetic carbon dioxide response curve for C3 leaves. *Plant, Cell & Environment* 30, 1035–1040

Shi LX, Schroder WP (2004) The low molecular mass subunits of the photosynthetic supracomplex, photosystem II. *Biochimica et Biophysica Acta 1608*(2-3), 75-96.

Shikanai T (2007) Cyclic electron transport around photosystem I: genetic approaches. *Annual Review of Plant Biology* 58, 199–217

Shinopoulos KE, Brudvig GW (2012) Cytochrome b_{559} and cyclic electron transfer within photosystem II. *Biochimica et Biophysica Acta* 1817(1), 66-75

Squire GR (1990) The physiology of tropical crop production. *CAB international, Wallingford* UK 236

Stitt M, Schultz D (1994) Does Rubisco control the rate of photosynthesis and plant growth? An exercise in molecular ecophysiology. *Plant, Cell & Environment* 17, 465-487

Strizh I (2008) The Mehler reaction as an essential link between environmental stresses and chloroplast redox signaling. In: JF Allen, E Gantt, JH Golbeck, B Osmond, editors. Photosynthesis. Energy from the sun. *Springer, Heidelberg* 1343-1346

Sultan SE (1995) Phenotypic plasticity and plant adaptation. *Acta botanica neerlandica* 44, 363–38

Suorsa M, Järvi S, Grieco M, Nurmi M, Pietrzykowska M, Rantala M, Kangasjärvi S, Paakkarinen V, Tikkanen M, Jansson S, Aro EM (2012) PGR5 is essential for proper acclimation of Arabidopsis photosystem I to naturally and artificially fluctuating light conditions. *Plant Cell* 24, 2934–2948

Szabó I, Bergantino E, Giacometti GM (2005) Light and oxygenic photosynthesis: energy dissipation as a protection mechanism against photo-oxidation. *European Molecular Biological Organization Reports 6*, 629-634

Taiz L, Zeiger E (2006) Plant Physiology. Fourth Edition. *Sinauer Associates*

Takahashi S, Milward SE, Fan D, Chow WS, Badger MR (2009) How does cyclic electron flow alleviate photoinhibition in Arabidopsis? *Plant Physiology* 149, 1560-1567

Takahashi S, Bauwe H, Badger MR (2007) Impairment of the photorespiratory pathway accelerates photoinhibition of photosystem II by suppression of repair process and not acceleration of damage process in *Arabidopsis thaliana. Plant Physiology* 144, 487-494

Tamura K, Peterson D, Peterson N, Stecher G, Nei M, Kumar S (2011) MEGA5: Molecular evolutionary genetics analysis using maximum likelihood, Evolutionary distance and maximum parsimony methods. *Molecular Biology and Evolution* 28, 2731-2739

Tang J, Chen X, Katsuyoshi S (2002) Varietal differences in photosynthetic characters and chlorophyll fluorescence induction kinetics parameters among intergeneric progeny derived from *Oryza x Sorghum*, its parents, and hybrid rice. *Journal of Zhejiang University* 3(1), 113-117

Tikkanen M, Grieco M, Kangasjärvi S, Aro E (2010) Thylakoid protein phosphorylation in higher plant chloroplasts optimizes electron transfer under fluctuating light. *Plant Physiology* 152, 723-735

Tikkanen M, Piippo M, Suorsa M, Sirpio S, Mulo P, Vainonen J, Vener AV, Allahverdiyeva Y, Aro EM (2006) State transitions revisited: a buffering system for dynamic low light acclimation of *Arabidopsis*. *Plant Molecular Biology* 62, 779–793

Tissue DT, Griffin KL Ball JT (1999) Photosynthetic adjustment in field-grown ponderosa pine trees after six years exposure to elevated CO_2. *Tree Physiology* 19, 221–228

Tolbert NE, Benker C, Beck E (1995) The oxygen and carbon dioxide compensation points of C3 plants: possible role in regulating atmospheric oxygen. *Proceedings of the National Academy of Sciences USA* 92, 11230-11233

Van Quyen N, Sy Tan P, Van Hach C, Van Du P, Zhong X (2004) Healthy rice canopy for optimal production and profitability. *Omonrice* 12, 69-74

von Caemmerer S, Farquhar GD (1981) Some relationships between the biochemistry of photosynthesis and the gas exchange of leaves. *Planta* 153, 376–387

Wang P, Duan W, Takabayashi A, Endo T, Shikanai T, Ye J-Y, Mi H (2006) Chloroplastic NAD(P)H dehydrogenase in tobacco leaves functions in alleviation of oxidative damage caused by temperature stress. *Plant Physiology* 141, 465–474

Wingler A, Lea PJ, Leegood RC (1999) Photorespiratory metabolism of glyoxylate and formate in glycine-accumulating mutants of barley and *Amaranthus edulis*. *Planta* 207, 518-526

Yoshida S (1981) Fundamentals of rice crop science. *International Rice Research Institute* (IRRI), Los Banős, Philippines

Yoshida S (1972) Physiological aspects of grain yield. *Annual Review of Plant Physiology 23, 437-464*

Zhang N, Kallis RP, Ewy RG, Portis AR (2002) Light modulation of Rubisco in *Arabidopsis* requires a capacity for redox regulation of the larger Rubisco activase isoform. *Proceedings of National Academy of Science, USA* 99, 3330–3334

Zhang L, Aro EM (2002) Synthesis, membrane insertion and assembly of the chloroplast-encoded D1 protein into photosystem II. *FEBS Letters* 512, 13–18

Zhang H, Whitelegge JP, Cramer WA (2001) Ferredoxin:$NADP^+$ oxidoreductase is a subunit of the chloroplast cytochrome b6f complex. *Journal of Biological Chemistry* 276, 38159-38165.

Zhou Y, Lam HM, Zhang J (2007) Inhibition of photosynthesis and energy dissipation induced by water and high light stresses in rice. *Journal of Experimental Botany* 58(5), 1207-1217

Zhu H, Kim D, Baek J, Choi H, Ellis L, Kuester H, McCombie WR, Peng H, Cook DR (2003) Syntenic relationships between *Medicago truncatula* and Arabidopsis reveal extensive divergence of genome organization. *Plant Physiology* 131, 1018–1026

Zuckerkandl E, Pauling L (1965) Evolutionary divergence and convergence in proteins. *New York, Academic Press*